

PhD PROCEEDINGS

ANNUAL ISSUES OF THE DOCTORAL SCHOOL

FACULTY OF INFORMATION TECHNOLOGY & BIONICS

2022

PhD PROCEEDINGS

ANNUAL ISSUES OF THE DOCTORAL SCHOOL

FACULTY OF INFORMATION TECHNOLOGY & BIONICS
PÁZMÁNY PÉTER CATHOLIC UNIVERSITY

PhD PROCEEDINGS

ANNUAL ISSUES OF THE DOCTORAL SCHOOL
FACULTY OF INFORMATION TECHNOLOGY & BIONICS
2022



PÁZMÁNY *1635*
— s i n c e

PÁZMÁNY UNIVERSITY *e*PRESS
BUDAPEST, 2022

© PPKE Információs Technológiai és Bionikai Kar, 2022

HU ISSN 2064-7271

Kiadja a Pázmány Egyetem eKiadó
Budapest, 2022

Felelős kiadó
Rev. Mons. Dr. Kuminetz Géza
a Pázmány Péter Katolikus Egyetem rektora

The publication of this volume was supported by
the New National Excellence Program of the Ministry for Innovation and Technology

Cover image by Katalin Schäffer: *A proposed wrist exosuit with four fabric pneumatic artificial muscles (fPAMs) as actuators, which are attached to the forearm and the hand through fabric structural elements.*

Contents

Introduction	9
PROGRAM 1: BIONICS, BIO-INSPIRED WAVE COMPUTERS, NEUROMORPHIC MODELS	10
The effect of artifact-rejection methods on the efficiency of neural networks	11
<i>András ADOLF</i>	
Quantitative analysis of the single cell trajectories	12
<i>Gréta Lilla BÁNYAI</i>	
Experimental and theoretical studies on the effects of chromosome missegregation	13
<i>Camilla CANCRINI</i>	
Investigating the robustness of biological oscillators	14
<i>Suchana CHAKRAVARTY</i>	
Surface Laplacian-based motor imagery EEG classification with deep learning	15
<i>Ward FADEL</i>	
Optimization of the expression and purification protocol of the GBR region of GKAP protein and initial NMR analysis	16
<i>Fanni FARKAS</i>	
Modelling the biochemical mechanisms underlying postsynaptic LTP in a CA1 pyramidal neuron spine head	17
<i>Gábor FARKAS</i>	
Understanding yeast colony growth	18
<i>Tünde Éva GAIZER</i>	
Continual learning on ACL abnormalities	19
<i>István HAJDU</i>	
Laser speckle contrast imaging of the rat brain	20
<i>Imre Gergely JÁNOKI</i>	
Prediction of the clinical outcome of COVID-19 from viral mutations using machine learning techniques	21
<i>Regina KALCSEVSZKI</i>	
Investigation of protein:protein interactions in the PSINDB from various aspects	22
<i>Zsófia Etelka KÁLMÁN</i>	
High-performance COVID pandemic simulator	23
<i>Bence Márk KEÖMLEY-HORVÁTH</i>	

Synchronization modes and factors in the septal network	24
<i>Barnabás KOCSIS</i>	
Drug absorption through psoriatic mouse skin	25
<i>Dorottya KOCSIS</i>	
Parameter space investigation for SVM-based Brain-Computer Interfaces	26
<i>Csaba Márton KÖLLÓD</i>	
Optical characterization of a flexible, transparent micro-ECoG device for multimodal neuroimaging	27
<i>Zsófia LANTOS</i>	
Examination of the distribution and structure of postsynaptic protein complexes by extended simulations	28
<i>Marcell MISKI</i>	
Closed neural spike sorting system using FPGA	29
<i>Obada MUHAMMAD</i>	
Isolation methods and storage stability of extracellular vesicles	30
<i>Afrodité NÉMETH</i>	
Link prediction in the protein-protein interaction network using generative adversarial networks	31
<i>Bence NÉMETH</i>	
Investigation of toxin producing yeast strains	32
<i>Biborka PILLÉR</i>	
Human movement analysis to improve control algorithms	33
<i>Balázs RADELECZKI</i>	
Mutations affecting the binding site of the Shank PDZ domain	34
<i>Anna SÁNTA</i>	
Thermal-based neuromodulation in a Penicillin-induced acute epilepsy model	35
<i>Ágnes SZABÓ</i>	
Examination of protein phase separation via experimental and computational methods	36
<i>András László SZABÓ</i>	
Prediction of Alzheimer’s disease using magnetic resonance imaging	37
<i>János SZALMA</i>	
Mechanisms of burst firing in hippocampal CA1 pyramidal cells	38
<i>Luca TAR</i>	
Qualitative analysis of generalized ribosome flows	39
<i>Mihály András VÁGHY</i>	
Structural characterization of the postsynaptic Drebrin protein	40
<i>Soma VARGA</i>	
Comparative evaluation of permeability properties of a human skin equivalent and ex vivo human skin tissue in skin-on-a-chip microfluidic device	41
<i>Zsófia VARGA-MEDVECZKY</i>	
Complexomic simulations of neurodegenerative diseases	42
<i>Áron WEBER</i>	

PROGRAM 2: COMPUTER TECHNOLOGY BASED ON MANY-CORE PROCESSOR CHIPS, VIRTUAL CELLULAR COMPUTERS, SENSORY AND MOTORIC ANALOG COMPUTERS	43
Fiber Photometry: a way to look inside the brain	44
<i>Boldizsár Zsolt BALOG</i>	
Tridsolver: a scalable building block for ADI applications	45
<i>Gábor Dániel BALOGH</i>	
Progress report on epidemic model inversion using feedback linearization	46
<i>Balázs CSUTAK</i>	
Approaches to OpenSet algorithms	47
<i>Lóránt Szabolcs DAUBNER</i>	
Recognition object to grasp by using a hybrid system	48
<i>Attila FEJÉR</i>	
HDR reconstruction techniques for light field images	49
<i>Mary GUINDY</i>	
Implementation of Memristor Cellular Nonlinear Network with non-linear template	50
<i>Dániel HAJTÓ</i>	
Improving the performance of Open-set Recognition with generated inner features	51
<i>András Pál HALÁSZ</i>	
Identifiability of delayed systems	52
<i>Gergely HORVÁTH</i>	
A new range-based breast cancer prediction model using the Bayes' theorem and Ensemble learning	53
<i>Sam KHOZAMA</i>	
Monitoring snoring in sleeping adults to detect respiratory disorders	54
<i>Ádám NAGY</i>	
Current results and challenges of wrist exoskeleton design	55
<i>Katalin SCHÄFFER</i>	
Achieving mixed precision computing with the help of domain specific libraries	56
<i>Bálint SIKLÓSI</i>	
The effects and mitigation of the object centering bias in common datasets	57
<i>Gergely SZABÓ</i>	
PROGRAM 3: FEASIBILITY OF ELECTRONIC AND OPTICAL DEVICES, MOLECULAR AND NANOTECHNOLOGIES, NANO-ARCHITECTURES, NANOBIONIC DIAGNOSTIC AND THERAPEUTIC TOOLS	58
An optimal retrodirective array	59
<i>András ESZES</i>	
Optimized implementations of neural networks	60
<i>András FÜLÖP</i>	
Design of oscillatory computing devices by machine learning	61
<i>Tamás RUDNER</i>	

Analysis of the effect of belief reconstruction on POMDP solving	62
<i>András Attila SÜLYÖK</i>	
Wireless-sensor-network-based wildfire monitoring with failure tolerant, event-driven multipath routing protocol	63
<i>Bálint Áron ÜVEGES</i>	
PROGRAM 4: HUMAN LANGUAGE TECHNOLOGIES, ARTIFICIAL UNDERSTANDING, TELEPRESENCE, COMMUNICATION	64
Question Answering System Based on Deep Learning Neural Networks for Azerbaijani language	65
<i>Kamran IBIYEV</i>	
Progress report on building a corpus for abstractive Arabic text summarization	66
<i>Mram KAHLA</i>	
PROGRAM 5: ON-BOARD ADVANCED DRIVER ASSISTANCE SYSTEMS	67
Data augmentation using saliency map	68
<i>Mohammad Jalal ALAFANDI</i>	
Analysis of ventricular function on echocardiographic recordings using deep neural networks	69
<i>Bálint MAGYAR</i>	
Vehicle pose tracking in lidar point cloud maps	70
<i>Örkény Ádám H. ZOVÁTHI</i>	
Appendix	71

Introduction

It is our pleasure to publish this Annual Proceedings again to demonstrate the genuine multidisciplinary research done at the Jedlik Laboratories by young talents working in the Roska Tamás Doctoral School of Sciences and Technology of the Faculty of Information Technology and Bionics at Pázmány Péter Catholic University. The scientific results of our PhD students outline the main recent research directions in which our faculty is engaged. We also appreciate the support of the supervisors and consultants, as well as that of the five collaborating National Research Laboratories of the Loránd Eötvös Research Network, Semmelweis University and the University of Pannonia. The collaborative work with the partner universities, especially Katolieke Universiteit Leuven, Politecnico di Torino, Technische Universität München, University of California at Berkeley, University of Notre Dame, Universidad de Sevilla, Università di Catania, Université de Bordeaux and Universidad Autónoma de Madrid is gratefully acknowledged.

We acknowledge the support of numerous institutes, organizations and companies:

- Loránd Eötvös Research Network (ELKH),
- National Research, Development and Innovation Office (NKFIH),
- Hungarian Academy of Sciences (MTA),
- UNKP Programme, Ministry for Innovation and Technology, Hungarian Government,
- KDP Programme, Ministry for Innovation, and Technology, Hungarian Government,
- Gedeon Richter Co.,
- Office of Naval Research (ONR) of the US,
- NVIDIA Ltd.,
- Verizon Computer Vision Group (Eutecus Inc.), Berkeley, CA,
- MorphoLogic Ltd., Budapest,
- Analogic Computers Ltd., Budapest,
- AnaFocus Ltd., Seville,

and several other companies and individuals.

Needless to say, the resources and support of the Pázmány Péter Catholic University are gratefully acknowledged.

Budapest, June 2022.

GÁBOR PRÓSZÉKY

Chairman of the Board of the Doctoral School

GÁBOR SZEDERKÉNYI

Head of the Doctoral School

PROGRAM 1

BIONICS, BIO-INSPIRED WAVE COMPUTERS, NEUROMORPHIC MODELS

Heads: Tamás FREUND, Zsolt LIPOSITS, Sándor PONGOR

The effect of artifact-rejection methods on the efficiency of neural networks

András ADOLF

(Supervisor: István ULBERT)

Pázmány Péter Catholic University, Faculty of Information Technology and Bionics

50/a Práter street, 1083 Budapest, Hungary

adolf.andras@itk.ppke.hu

Abstract—For a brain-computer interface system (BCI), the right classification of EEG signals is the most crucial part. EEG signals however can contain artifacts, which are the contamination of the electric signal of the brain, which can be caused by blinking or other muscle activity. There exist many algorithms to remove these components, for instance, the Fully Automated Statistical Thresholding for EEG artifact Rejection (FASTER). These methods however can filter out components that can be important during the classification process. In this work the previously implemented 2D and 3D Convolutional Neural Networks are examined: how the artifact rejection method influences classification accuracy in a 4 class scenario. The subjects I have tested my networks on consist of 105 patients from the Physionet database. As a result, it can be concluded, that the effect of the FASTER algorithm is highly subject dependent, as it resulted in an accuracy increase in many subjects, but a decrease in others.

Keywords-brain-computer interfaces; neural networks; artifact-rejection; 2D convolution, 3D convolution

I. SUMMARY

The research field of brain-computer interfaces (BCI) is rapidly evolving nowadays. However these devices could mean essential help to people with different serious disabilities, a reliable classification accuracy of EEG signals is essential.[1]

While recording the EEG signal, many artifacts can emerge and contaminate the raw brain signal, to be able to classify solely on the neural activity, it is needed to filter out the unwanted components. A well-known algorithm to perform this operation is the FASTER algorithm (Fully Automated Statistical Thresholding for EEG artifact Rejection).[2]

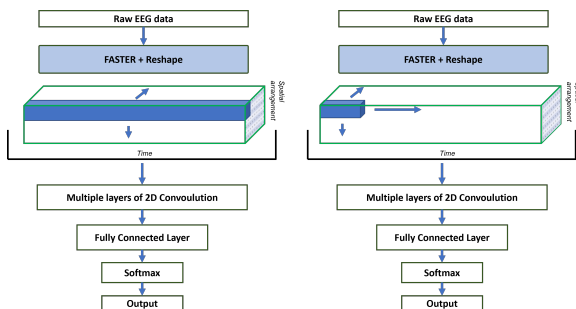


Fig. 1. Structure of the implemented neural networks

Two types of networks were implemented to perform the classification, one with 2D and the second with 3D convolution, both of them have an input of a 3D structured EEG time window. In this representation, 2 dimensions correspond to the spatial arrangement of the electrodes, while the third one is the time. The implemented structures can be observed in Figure 1.

To perform the classification and test the effect of artifact rejection, I tested the implemented convolutional neural network structures on the data of the Physionet database, which is a movement intention EEG dataset, collected by Schalk et al.. The database has 5 different labeled tasks, but by omitting the use of the 'both hands' class, the following tasks were classified: baseline activity, open and close the left hand, the right hand, and both legs. [3]

To compare the classification accuracy of networks trained on filtered and unfiltered data, I have examined both networks with both cases. I have also implemented the Transfer Learning method, by pre-training the neural networks on subjects that differ from the current patient we test the network on.

The results show that the effect of the FASTER algorithm is highly subject-dependent. The usage of the Artifact Rejection method resulted in an accuracy increase in many subjects, but a decrease in others. In the case of transfer learning the number of patients for which the AR method caused a decrease was increased in a serious manner.

ACKNOWLEDGEMENTS

I would like to express my sincere gratitude to my consultant, István ULBERT, who supported me during my work. I would also like to say thank you to the research group working on EEG classification with me, in particular, Csaba KÖLLÖD and Gergely MÁRTON. This work is prepared with the professional support of the Doctoral Student Scholarship Program of the Co-operative Doctoral Program of the Ministry of Innovation and Technology financed from the National Research, Development and Innovation Fund.

REFERENCES

- [1] J. R. Wolpaw, N. Birbaumer, W. J. Heetderks, D. J. McFarland, P. H. Peckham, G. Schalk, E. Donchin, L. A. Quatrano, C. J. Robinson, and T. M. Vaughan, "Brain-computer interface technology: a review of the first international meeting," *IEEE transactions on rehabilitation engineering*, vol. 8, no. 2, pp. 164–173, 2000.
- [2] H. Nolan, R. Whelan, and R. Reilly, "Faster: Fully automated statistical thresholding for eeg artifact rejection," *Journal of Neuroscience Methods*, vol. 192, no. 1, pp. 152–162, 2010.
- [3] A. L. Goldberger, L. A. N. Amaral, L. Glass, J. M. Hausdorff, P. C. Ivanov, R. G. Mark, J. E. Mietus, G. B. Moody, C.-K. Peng, and H. E. Stanley, "PhysioBank, PhysioToolkit, and PhysioNet: Components of a new research resource for complex physiologic signals," *Circulation*, vol. 101, no. 23, pp. e215–e220, 2000 (June 13). Circulation Electronic Pages: <http://circ.ahajournals.org/content/101/23/e215.full> PMID:1085218; doi: 10.1161/01.CIR.101.23.e215.

Quantitative analysis of the single cell trajectories

Gréta Lilla BÁNYAI

(Supervisor: Tamás Márton GARAY)

Pázmány Péter Catholic University, Faculty of Information Technology and Bionics

50/a Práter street, 1083 Budapest, Hungary

banyai.greta.lilla@itk.ppke.hu

Abstract—Importance of tumor cell migration from the primary tumor-site to another location to form metastasis has long been recognized. Thus, studying cell migration is essential to fully understand the process of metastasis and to seek possible treatments. Migration can be examined via videomicroscopy, for the analysis of the recordings cell tracking with image processing methods and migration parameter estimation have to be performed. These parameters may be affected differently by treatments. In this study we aim to investigate differences, stability and correlations between migration features.

Keywords—cell migration, videomicroscopy, displacement, traveled distance, mean velocity, directionality ratio

I. INTRODUCTION

Cell migration is involved in several biological processes, like in the formation of metastasis in cancer patients. Cancer is the leading cause of death worldwide, with metastasis accounting for 90% of the death of cancer patients. The ability of cancer cells to enter the bloodstream or lymphatic system and to form a metastasis is still not fully understood. [1] [2]. For survival of cancer patients, investigation of possible cell migration inhibitory substances plays a leading role in the research for treatment [3]. Several antitumor agents are available, aimed to prevent the development of metastases [4]. Commonly used instrument to monitor cell migration is time-lapse videomicroscopy, which produces a series of images on a microscope stage [5]. Samples are usually prepared in multiwell plates, where cells can be tracked either manually or with automated tracking algorithms. These programs use multiple images processing methods, beginning with pre-processing the images, detecting the cells in the recordings, determining their position in the examined area and tracking them over time. After the motion estimation, the features are extracted, and different migration parameters are calculated. Two major features are geometric features of the cells (cell area, volume) and parametric features of cell migration (speed, directionality, mean square displacement). There are more complex parameters, which can be detected in the videomicroscopic images, containing information relevant to various research, such as the rate of cell division. As a final step, data are analyzed, and different types of parameters are compared to each other [6].

II. ANALYZED DATA

The analysis of migration features was performed based on previous videomicroscopic images produced at Semmelweis University. More than two thousand manually analyzed recordings, and nearly three times as many videomicroscopy measurements, enabled to investigate the features of cancer cell migration.

III. FEATURES OF THE PROGRAM

Using the sets of coordinates of manually analyzed measurements, representing positions of the cells in the consecutive images, our program calculates several parameters, including displacement, traveled distance, mean velocity and directionality ratio. These parameters are calculated for each tracked cell individually, then their mean values are defined for each well. The average and standard deviation of replicates' parameters and their relative values to their corresponding control are also calculated.

IV. DISCUSSION

The treatments of the cancer cells exert a great variety of changes in the cellular behavior. Accordingly, treatments affect different migration parameters not equally. Some treatments can exert changes in different directions or may not have any influence on a given parameter at all. Our investigations have proven, that treatments can even have the opposite effect on the motion parameters, so an incomplete examination of the parameters may paint a false positive or negative picture of the treatment. Perfunctory evaluation in the context of clinical or preclinical research questions could lead to inappropriate treatments and worsening of patients' symptoms. Ultimate aim of our examination is to identify a parameter, which is the least sensitive to the differences to the various ways of changing cell migration with a compound. Such a parameter could be used universally to characterize the alteration of cell migration.

ACKNOWLEDGEMENTS

Videomicroscopy was performed at Semmelweis University. I would like to thank Márton Bese Naszlady for his help with the development of the program. This research was supported by the National Research, Development and Innovation Office through the grant TKP2021-EGA-42.

REFERENCES

- [1] C. Paul, P. Mistriotis, and K. Konstantopoulos, "Cancer cell motility: lessons from migration in confined spaces.," *Nat Rev Cancer*, vol. 17, p. 131–140, 2010.
- [2] C. Hayot, O. Debeir, P. V. Ham, M. V. Damme, R. Kiss, and C. Decaestecker, "Characterization of the activities of actin-affecting drugs on tumor cell migration.," vol. 211, no. 1, pp. 30–40, 2006.
- [3] J. Sleeman and P. S. Steeg, "Cancer metastasis as a therapeutic target," *European Journal of Cancer*, vol. 46, no. 7, pp. 1177–1180, 2010.
- [4] S. C. Gupta, B. Sung, S. Prasad, L. J. Webb, and B. B. Aggarwal, "Cancer drug discovery by repurposing: teaching new tricks to old dogs.," *Trends in Pharmacological Sciences*, vol. 34, no. 9, p. 508–517, 2013.
- [5] C. Terryn, A. Bonnomet, J. Cutrona, C. Coraux, J.-M. Tournier, B. Nawrocki-Raby, M. Polette, P. Birembaut, and J.-M. Zahm, "Videomicroscopic imaging of cell spatio-temporal dispersion and migration," *Critical Reviews in Oncology/Hematology*, vol. 69, no. 2, pp. 144–152, 2009.
- [6] P. Masuzzo, M. Van Troys, C. Ampe, and L. Martens, "Taking aim at moving targets in computational cell migration.," *Trends in Cell Biology*, vol. 26, no. 2, pp. 88–110, 2015.

Experimental and theoretical studies on the effects of chromosome missegregation

Camilla CANCRINI

(Supervisor: Andrea CILIBERTO)

Pázmány Péter Catholic University, Faculty of Information Technology and Bionics

50/a Práter street, 1083 Budapest, Hungary

cancrini.camilla@itk.ppke.hu

Abstract— My research plan is aimed at investigating chromosome segregation and how cells evolve when the latter is hindered, which is an effect typically achieved by anti-cancer drugs. To this aim, I am using budding yeast cells carrying a mutated allele of beta-tubulin, *tub2-401*. This is a cold-sensitive mutant of beta-tubulin that when grown at low temperature fails to polymerize microtubules. As a consequence, *tub2-401* cells grown at low temperature have a high chromosome missegregation rate. From previous studies, it emerged that if these cells are grown at the semi-permissive temperature (18 °C), they do manage to divide but with a substantial percentage of dead cells due to massive missegregation. After ~ 50 generations (we call it Gr, generation recovery), however, cells have partially recovered the ability to polymerize microtubules (see Fig. 1 (a).) Interestingly, at this stage different populations carry very few recurrent point mutations but they are all basically 100% disomic for chromosome VIII (see [1]). How cells transit in a relatively short time from the massive heterogeneity due to the increased missegregation rate into having only disomy of chromosome VIII is not clear. In order to investigate this aspect, I focused on understanding when the disomy first appears, if it is reproducible and its dependency on population size. In the future I aim to develop a mathematical model and experiments to rationalise how cells respond to increased chromosome missegregation.

I. INTRODUCTION

The process by which an incorrect number of chromosomes are segregated is called "missegregation" whereas the outcome of this process (i.e. a set of chromosome different from wild type cells) is referred to as aneuploidy. Missegregation can occur spontaneously, due to errors during cell division, or can be induced by external stimuli (such as drugs, high temperature, etc). Aneuploidy is known to be correlated to several human diseases such as Down's syndrome or cancer but also to stress and drug resistance. An increasing number of studies have indeed suggested aneuploidy to be a quick but transient solution in response to environmental stress conditions [5].

From previous studies [1] it emerged that if yeast cells carrying *tub2-401* mutations (cold-sensitive mutations that prevent microtubules from polymerizing properly) are grown at a semi-permissive temperature (18 °C), after ~ 50 generations (which we call Gr, generation recovery) they recover microtubule functionality and growth, though not at wild type level. At Gr different populations carry very few recurrent point mutations but they are all basically 100% disomic for chromosome VIII. Thus, chromosome VIII disomy seems to be involved in recovering the ability to correctly polymerize microtubules. How disomy of chromosome VIII is selected by cells is of primary interest to my project. In pursuit of this aim, I want to study the very early steps of evolution (from generation 0 to Gr).

I spent these first months conducting experiments aimed at defining a protocol that would allow the experiment to be repeated reproducibly regardless of the initial population size. Specifically, the question I sought to solve was: what is the range of *tub2-401* cells needed at time 0 (N_0 range) in order to have a recovery due to the appearance of chromosome VIII disomy after letting cells grow at 18 °C for about 50 generations? In other words, what is the range of initial population sizes that may be used to achieve the same outcome observed previously [1]? Furthermore, several studies suggest that the evolutionary pathway may be determined by the initial population size, meaning that the mechanism leading to resistance could be different depending on the initial population size [2]. This would imply that I may still observe population resistance if I choose the "wrong" N_0 , but through a different mechanism than chromosome VIII aneuploidy.

The experimental protocol was defined, and the results were found to be repeatable for N_0 values ranging from 10^6 to 10^4 . Initial populations smaller than 10^4 just have not been able to evolve. Initial populations with larger N_0 find different evolutionary trajectories.

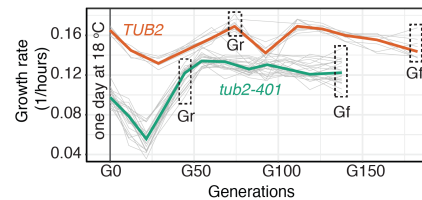


Fig. 1: This figure is taken from [1]. Scheme of the evolution experiment: from the clonal ancestor, 8 populations of *TUB2* cells (wild type) were produced, and 24 populations of *tub2-401* cells. The first measurement of growth rate was done after one day at 18 °C (generation 0 or G0). The last measurement was done at generation final (Gf). At Gr cells were analyzed by NGS. Every 3-4 days the growth rates (i.e net output between cell division and cell death) of the different populations were measured. *TUB2* cells are in orange whereas *tub2-401* ones in green. At Gr, *tub2-401* cells recover their growth even if it did not reach the one of the wild type. The population size at day 0 was 10^6 .

REFERENCES

- [1] PAVANI M, BONAIUTI P, CHIROLI E, ET AL., *Epistasis, aneuploidy, and functional mutations underlie evolution of resistance to induced microtubule depolymerization.*, EMBO J. (2021).
- [2] SCHENK, M.F., ZWART, M.P., HWANG, S. ET AL., *Population size mediates the contribution of high-rate and large-benefit mutations to parallel evolution.*, Nat Ecol Evol 6, 439–447 (2022).
- [3] ENRICO BENA, C., DEL GIUDICE, M., GROB, A. ET AL., *Initial cell density encodes proliferative potential in cancer cell populations.*, Sci Rep 11, 6101 (2021).
- [4] DI CRESCENZO A, PARAGGIO P., *Logistic Growth Described by Birth-Death and Diffusion Processes.*, Mathematics. 7(6):489 (2019).
- [5] GILCHRIST C, STELKENS R., *Aneuploidy in yeast: Segregation error or adaptation mechanism?*, Yeast. 2019;36(9):525-539 (2019).

Investigating the robustness of biological oscillators

Suchana CHAKRAVARTY

(Supervisor: Attila CSIKÁSZ-NAGY)

Pázmány Péter Catholic University, Faculty of Information Technology and Bionics

50/a Práter street, 1083 Budapest, Hungary

chakravarty.suchana@itk.ppke.hu

Abstract—Temperature compensation is one of the characteristics of a circadian clock. This characteristic enables the circadian pacemaker to maintain a constant period of oscillation in order to respond to any physiologic perturbations. The oscillations may arise as a result of a negative feedback effect on mRNA synthesis imposed by a nuclear period protein (PER). Many computational biologists were encouraged by Goodwin’s study to find the smallest network that may be responsible for oscillation formation. Additionally, positive feedback can cause oscillations. In this section, we will show the temperature compensation property and robustness of four distinct types of oscillatory systems: cyanobacterial model, positive feedback model, basic negative feedback loop model, and a single molecule model with both positive and negative feedback loops.

Keywords-biological oscillator; negative feedback; cyanobacterial oscillator; positive feedback; temperature compensation.

DISCUSSION

Oscillatory networks arise in living organisms. These biological oscillations are one of the organism’s distinguishing characteristics, allowing it to cope with any type of environmental variation. Calcium oscillations and circadian rhythms are two examples of oscillatory networks. Previous research has shown that in order to generate oscillatory behavior, the system must have a negative feedback loop. Furthermore, the existence of both a positive and a negative feedback loop might increase the likelihood of producing oscillations without sacrificing the magnitude of the oscillation.

Goodwin’s model [1] is a typical example of an oscillatory network. Many theorists are currently interested in determining the smallest network motif that can be accountable for oscillation. Rosa D. Hernansaiz-Ballesteros et.al [2] suggest a minimum network architecture necessary for oscillation in prokaryotic cyanobacteria. This model is a combination of positive and negative feedback loops. A substrate depletion model with positive auto-catalytic feedback, on the other hand, is known to display prolonged oscillation. Another oscillatory network that can create oscillations is presented by Rust et al. This more complex model drives the oscillation of a three-protein circadian clock [4].

Our goal is to find the most robust oscillatory network. We would want to concentrate on four distinct types of network motifs for this purpose: negative feedback oscillator, cyanobacterial oscillator, positive feedback oscillator, and mix of positive and negative feedback loop model. We applied the temperature sensitivity co-efficient Q_{10} to the dynamical equations of the networks in order to establish a temperature compensated [3] biological clock. Without any temperature disturbance, these systems exhibit a comparable length of period of oscillation (Fig1). Investigating the robustness of the oscillatory system might aid in the development of a synthetic oscillator.

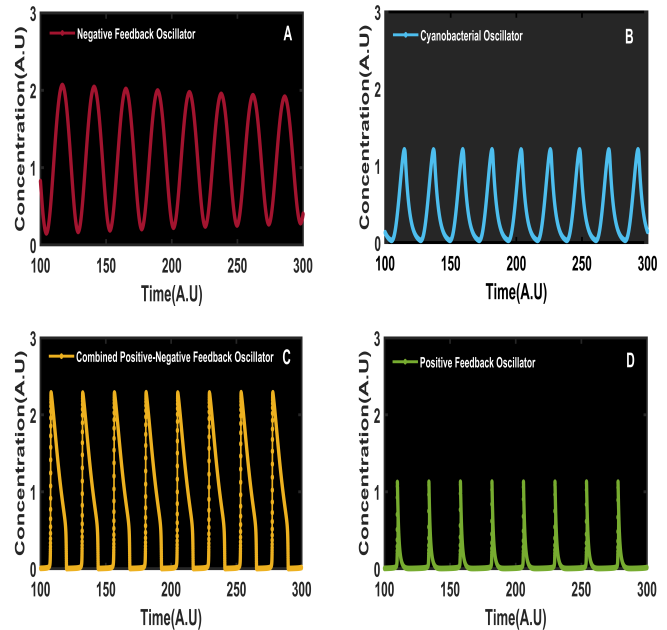


Fig. 1. The time course oscillatory behavior of four different examples is given here: negative feedback oscillator (A), cyanobacterial oscillator (B), combined positive-negative feedback oscillator (C), and positive feedback oscillator (D).

REFERENCES

- [1] D. Gonze and P. Ruoff, “The Goodwin Oscillator and its Legacy.”, *Acta Biotheor.*, 2020.
- [2] R. D. Hernansaiz-Ballesteros, L. Cardelli, and A. Csikász-Nagy, “Single molecules can operate as primitive biological sensors, switches and oscillators.”, *BMC Syst. Biol.*, vol. 12, no. 1, pp. 1-14, 2018.
- [3] C. H. Johnson and Martin Egly, “Metabolic Compensation and Circadian Resilience in Prokaryotic Cyanobacteria.”, *Annu Rev Biochem.*, vol. 83, pp. 221-247, 2014.
- [4] Rust MJ, Markson JS, Lane WS, Fisher DS, O’Shea EK, “Ordered phosphorylation governs oscillation of a three-protein circadian clock.”, *Science.*, vol. 318,5851, pp. 809-12, 2007.

Surface Laplacian Based Motor Imagery EEG classification with Deep Learning

Ward FADEL

(Supervisor: Firstname SURNAME) or

(Supervisors: István ULBERT, Lucia WITTNER)

Pázmány Péter Catholic University, Faculty of Information Technology and Bionics

50/a Práter street, 1083 Budapest, Hungary

fadel.ward@itk.ppke.hu

Abstract—Classification of EEG signals is the main part of the Motor-Imagery (MI) based Brain Computer Interface (BCI) systems. EEG signals differ from one subject to another and even for the same subject among different trials, and this is why designing a general classification model is still debated. Deep learning is dominant in so many fields like computer vision and natural language processing but it is still under investigation for EEG signals classification. We followed a new trend in EEG signals classification in which these signals are transformed into images, and so classifying such signals become an image classification problem where Deep learning can work well. The Physionet dataset for EEG motor movement/imagery tasks was used which consists of 109 subjects and the motor imagery EEG signals for three frequency bands (Mu [8-13 Hz], and Beta [13-30 Hz], Gamma[30-45]) was transformed into 3-channel images (one channel for each band) using the Azimuthal equidistant projection and Clough-Tocher algorithm for interpolation. These 2-D images represent the input data to our model which consists of Deep Convolutional Neural Network (DCNN) to extract the spatial and frequency then finally to be classified into 4 different motor imagery classes. Our results were promising (68 % average accuracy) and 3.5% better than the results of Support Vector Machine (SVM) method over the same dataset. Using Surface Laplacian Transform increased the classification accuracy significantly.

Keywords-Brain-Computer Interface (BCI); Surface Laplacian; Classification; Motor Imagery; Convolutional Neural Networks (CNN).

I. SUMMARY

Classification of the EEG features is the main part of BCI systems. The classification of motor imagery activity is a challenging task due to the low signal-to-noise ratio of EEG signals and their non-stationary nature for the same subject and among subjects, the high sensitivity for artifacts, the limited number of training data, and the low reliability of current BCI systems. Therefore, classification algorithms mainly aim to overcome one or more of the previously mentioned challenges. The goal in [1] was to classify memory/cognitive load. The EEG data gathered from 64 electrodes was transformed into colored images using 3 frequency bands, and these images were fed to a CNN followed by LSTM in order to keep the spatial, frequency and temporal features of the EEG signals. We used a similar approach for MI-EEG classification. In our approach, we used CNN followed by LSTM and we used Physionet dataset with 109 subjects taken from 64 electrodes and by transforming the MI-EEG signals into images that preserve the spatial-frequency dimensions of the signals. LSTM was used to extract the temporal information between consecutive images that were classified into 5 different classes. the motor imagery EEG signals activity is mainly dominant in two bands; Mu [8-13 Hz] and Beta [13-30 Hz], so for the first scenario, the

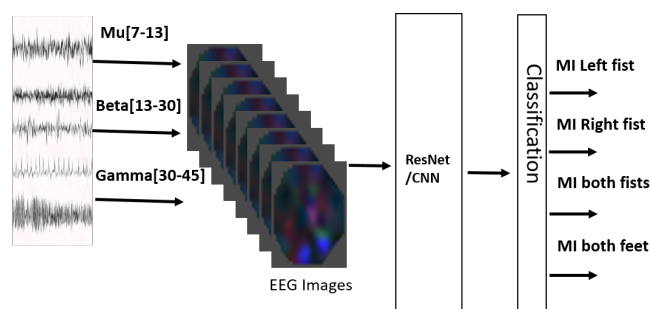


Fig. 1. Single Trial Motor Imagery Classification Approach.

signals for each subject were bandpass filtered into two bands. Then, for the second scenario, we also band pass filtered Gamma band [30-45 Hz] to add another option to the selected bands for feature extraction. Next, we applied Fast Fourier Transform (FFT) on 4 seconds trials 1 for every electrode, and then the sum of the squared absolute values was calculated for each band, then the measurements for 64 electrodes were transformed into 2-D images, and thus the problem of EEG signal classification becomes an image classification task. In order to project the 3-D electrodes space into a 2-D plane, we applied the Azimuthal Equidistant Projection (AEP) and then Clough-Tocher interpolation was applied over 32 x 32 mesh and thus we got the 2-D topology-preserving unicolor images for each band (red refers to Delta, green refers to Mu and blue refers to Beta) which represents the average activity for motor imagery EEG signals over the scalp for 4 seconds, then we added the resulting images for each band together to form either 2-channel images for the 2 band scenario or 3-channel images for the 3 bands scenario. After Applying the Surface Laplacian, the average classification accuracy is 68% after adding Gamma band to the image generation process, which is usually ignored in MI-EEG signals classification approaches, and this is 3.5% improvement compared to SVM.

REFERENCES

- [1] Pouya Bashivan, Irina Rish, Mohammed Yeasin, Noel Codella, *Learning Representations from EEG with Deep Recurrent-Convolutional Neural Networks*, ICLR Conference, 2016.
- [2] Reza Abiri et al, *A comprehensive review of EEG-based brain-computer interface paradigms*, *J. Neural Eng.* 2019, 16, 011001.
- [3] F Lotte1, L Bougrain, A Cichocki, M Clerc, M Congedo, A Rakotomamonjy and F Yger, *A review of classification algorithms for EEG-based brain-computer interfaces: a 10 year update*, *J. Neural Eng.* 2018, 15, 031005.

Optimization of the expression and purification protocol of the GBR region of GKAP protein and initial NMR analysis

Fanni FARKAS

(Supervisor: Zoltán GÁSPÁRI)

Pázmány Péter Catholic University, Faculty of Information Technology and Bionics

50/a Práter street, 1083 Budapest, Hungary

farkas.fanni@itk.ppke.hu

Abstract—Beneath the postsynaptic membrane, there is an elaborate protein network called the postsynaptic density (PSD). The protein GKAP is one of the most important components of the PSD. This protein establishes interactions with PSD-95 and Shank and thereby forms the core structure of PSD network. Mutations in these proteins are associated with a number of neurodegenerative diseases. The aim of my studies is the detailed structure-function characterization of the intrinsically disordered GK-binding segment of GKAP using NMR spectroscopy.

Keywords—PSD; GKAP; GBR1-3; NMR; interaction

I. INTRODUCTION

The postsynaptic density (PSD) is located under the postsynaptic membrane of the neurons. It is a large protein complex with thousands of interactions. These proteins participate, among others, in learning processes and memory formation [1]. To understand the mechanism of action of this dynamic structure and its role in neural processes, detailed structural investigation of its constituent proteins and their interactions are needed. NMR spectroscopy is one of the major techniques to investigate the three-dimensional structure and dynamics of proteins to decipher their function at atomic level. To investigate intrinsically disordered protein segments, NMR is the method of choice, but it requires special conditions, such as highly concentrated protein sample, low pH, and low amount of buffer components [2]. GKAP is one of the most abundant scaffold proteins in the PSD. Its mutations have been linked to OCD or schizophrenia. Two of its most important interaction partners are the GK domain of PSD-95 and the PDZ domain of Shank proteins. Its interaction with the GK protein is phosphorylation-dependent [3]. My goal was to prepare constructs spanning the GK-binding region of GKAP that are suitable for NMR investigation.

II. METHOD

Recombinant GBR1-3 protein production was performed in competent BL21 *E. coli* cells. Cells were grown in minimal media and ^{15}N labelled variant was produced as well. After emulsiflex the protein was purified with immobilized metal affinity chromatography (IMAC) on a manual column, and to render it suitable for suitable NMR, a dialysis, and a size exclusion chromatography (SEC) was made. To check the results, SDS-PAGE was used. From the ^{15}N labelled GBR1-3, NMR measurements were performed on a Bruker Avance III HD 800 MHz NMR spectrometer and the obtained HSQC spectra was analyzed with Sparky and CCPNMR. To improve

sample stability, a number of buffers and additives were tested, and a heat treatment was also performed.

III. RESULTS

Optimization of GBR1-3 expression and purification protocols were accomplished successfully. The stability of GBR1-3 was seemed sufficient when using NaPi, DTT, EDTA at pH 8. ^{15}N GBR1-3 was produced for NMR, HSQC spectra was successfully acquired, which proved its disordered nature. The number of peaks is less than expected based on the sequence, but the simple explanation for this is severe peak overlap which is expected to be resolved during resonance assignment.

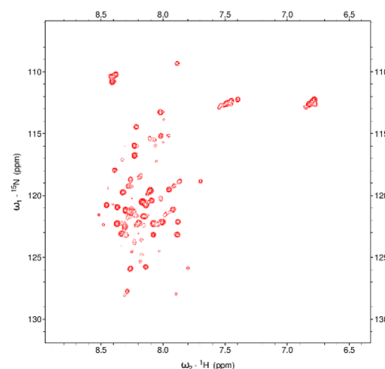


Fig. 1. ^1H - ^{15}N HSQC spectrum of GBR1-3.

ACKNOWLEDGEMENTS

I would like to thank Dr. Perttu Permi for the opportunity to work in his Jyväskylä research group, Dr. Bálint Péterfia and Dr. Chandan Thapa for all the help in the laboratory work in Budapest and in Jyväskylä, respectively, and the Erasmus+ organization for the opportunity to spend 5 months in Jyväskylä, Finland. This research was also supported by the National Research, Development and Innovation Office through the grant TKP2021-EGA-42.

REFERENCES

- [1] C.-Y. Zheng, G. K. Seabold, M. Horak, and R. S. Petralia, “Maguks, synaptic development, and synaptic plasticity,” *The Neuroscientist*, vol. 17, no. 5, pp. 493–512, 2011.
- [2] L.-Y. Lian and G. Roberts, *Protein NMR spectroscopy: practical techniques and applications*. John Wiley & Sons, 2011.
- [3] J. Zhu, Q. Zhou, Y. Shang, H. Li, M. Peng, X. Ke, Z. Weng, R. Zhang, X. Huang, S. S. Li, *et al.*, “Synaptic targeting and function of sapaps mediated by phosphorylation-dependent binding to psd-95 maguks,” *Cell reports*, vol. 21, no. 13, pp. 3781–3793, 2017.

Modelling the biochemical mechanisms underlying postsynaptic LTP in a CA1 pyramidal neuron spine head

Gábor FARKAS

(Supervisor: Szabolcs KÁLI)

Pázmány Péter Catholic University, Faculty of Information Technology and Bionics

50/a Práter street, 1083 Budapest, Hungary

farkas.gabor@itk.ppke.hu

Abstract—The persistent, activity-driven changes in the efficacy of synaptic transmission is referred to as synaptic plasticity that is believed to be the basis of information storage in the brain. A sophisticated system of intracellular signaling pathways in the spine heads of postsynaptic dendrites remarkably takes part in shaping synaptic plasticity. Modelling such a system of biochemical cascades can help to understand the underlying molecular mechanisms of synaptic plasticity.

Keywords—CA1 pyramidal cell, synaptic plasticity, LTP, intracellular signaling

I. INTRODUCTION

Synaptic plasticity is believed to be the underlying mechanism of cellular learning and memory storage. Besides the biophysical features of neurons, intracellular biochemical signaling pathways also contribute to the formation of complex neuronal functions such as activity-dependent synaptic plasticity. Long-lasting increase in the strength of synaptic communication is referred to as long-term potentiation (LTP) which is a result of interactions between sophisticated subcellular signaling cascades.

II. METHODS

Computational methods allow the quantitative modelling of network of signaling pathways that – combined with experimental investigations – helps to understand the underlying mechanisms of synaptic plasticity. A computational model of the related intracellular signaling pathways was created based on the model described in [1]. The model is located in a dendritic spine head of a CA1 pyramidal neuron and contains the main signaling pathways that were reported to take part in the formation, maintenance, and expression of hippocampal LTP: the CaMKII, the PKA and the PKC cascades. The model was used to fit experimental data gathered from papers in which the effects of the inhibition of the mentioned kinases were investigated. The Optimizer optimization software tool [2] was applied to optimize the model parameters. Such optimizations require powerful computational resources, so the Neuroscience Gateway (NSG) [3] – a portal for computational neuroscience – was used.

III. RESULTS

Figure 1 illustrates the results of model fittings to distinct experimental data in which the CaMKII, PKA and PKC kinases were inhibited. It seems that the fitted models describe these experimental results well, so they can be used for the further investigation of the mechanisms of synaptic plasticity.

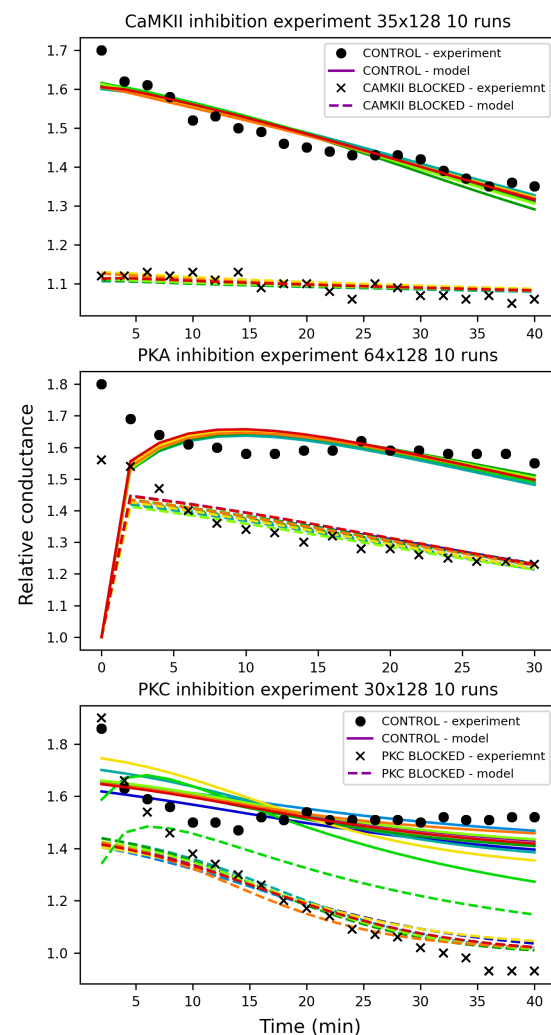


Fig. 1. Results of model fittings to experimental data.

REFERENCES

- [1] T. Mäki-Marttunen, N. Iannella, A. Edwards, G. Einevoll, and K. Blackwell, "A unified computational model for cortical post-synaptic plasticity," *eLife*, vol. 9, p. e55714, 07 2020.
- [2] P. Friedrich, M. Vella, A. I. Gulyás, T. F. Freund, and S. Káli, "A flexible, interactive software tool for fitting the parameters of neuronal models," *Frontiers in Neuroinformatics*, vol. 8, 2014. [Online]. Available: <https://www.frontiersin.org/article/10.3389/fninf.2014.00063>
- [3] S. Sivagnanam, A. Majumdar, K. Yoshimoto, V. Astakhov, A. Bandrowski, M. Martone, and N. Carnevale, "Introducing the neuroscience gateway," *CEUR Workshop Proceedings*, vol. 993, 01 2013.

Understanding yeast colony growth

Tünde GAIZER

(Supervisor: Attila CSIKÁSZ-NAGY)

Pázmány Péter Catholic University, Faculty of Information Technology and Bionics

50/a Práter street, 1083 Budapest, Hungary

gaizer.tunde.eva@itk.ppke.hu

Abstract—Yeast has been researched for a long time and applied in many areas in food and biotechnology industries, however these seemingly simple unicellular eukaryotes still leave us with many open questions. In this paper I am aiming to address some of these questions regarding colony formation. Our research group aims to understand the changes in colony development by combining experimental and computational tools. Preliminary results of multiple investigations are presented here that aim to establish good experimental protocols to support building and parametrizing a realistic computational model for modelling colony growth.

Keywords—yeast; colony growth; giant colony; systems biology

I. INTRODUCTION

Colony growth and factors effecting it were studied for a long time in *S. cerevisiae* [1]. The biphasic characteristic of yeast colony growth was shown by Meunier and Choder, demonstrating that initial rapid growth phase is followed by a sharp transition to a slower growth phase [2]. This slowing down is accompanied by cells in the center going into stationary phase and growth being driven by peripheral cells dominantly. Recent research with improved techniques allowed a better insight into this phenomenon characterizing the molecular differences as well. Ageing of the colony leads to a scarce of nutrients and oxygen inside the colony, that in addition is also unbalanced, leading to increased communication and differentiation in these colonies [3]. Differentiation within colony was also described by transcriptional profiling by Traven et al. [4]. Their study also showed that outer layer is in an actively, fermentatively growing state while cell in the inner areas are in a resting state, as well as the restructuring in cell wall functions, namely the enrichment of cell wall biosynthesis enzymes and cell wall proteins, while the inside cells express cell wall degrading enzymes [4].

An important area of colony research is biofilm formation. Biofilm forming yeast, *C. albicans* can cause serious hospital infections that is due to the structural changes and differentiation within the colony. Development of colony and biofilm structures are also described in wild and domesticated *S. cerevisiae* colonies by the Palkova group [3]. Advances in research techniques, especially in high-throughput and omics technologies aim to scale up these investigations. These efforts have revealed many important mechanisms in colony structure and dynamics, nevertheless many details are yet to be understood especially in the fields of communication and interactions [5].

II. DISCUSSION

In this project my aim is to further our understanding of the growth of *S. cerevisiae* colonies. These biotechnologically and industrially important yeast are capable of showing a diverse range of morphology. Morphological and growth differences

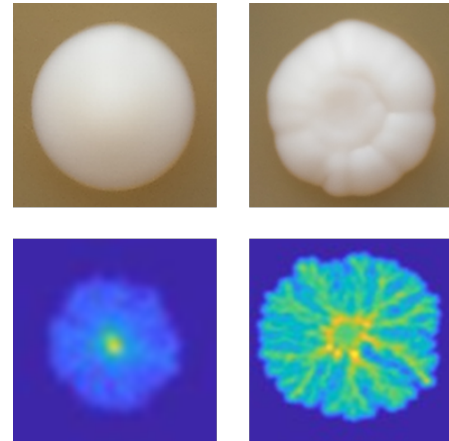


Fig. 1. Single cell colony and colony of approx. 100 cells of Sgu421 both experimentally and simulation

were shown in this paper, as well as the capabilities of our agent-based model was illustrated in couple of examples. Our current focus is to improve these experimental protocols towards high-throughput methods to be able to include multiple strains and environmental factors. Based on experimental results and the predictions of the agent-based model, colonies of mixed strains will be measured to identify interactions between strains.

ACKNOWLEDGEMENTS

Experimental work described was carried out together with Bíborka Pillér, Luca Dávid, Zsófia Béltéki. Model was developed by János Juhász and Bence Makove.

The research has been supported by the Hungarian National Research, Development and Innovation Office (NKFI/NRDI) through the Hungarian Scientific Research Fund (OTKA-K20-134489) and the Thematic Excellence Programme (TKP2020-NKA-11).

REFERENCES

- [1] R. S. Kamath and H. R. Bungay, "Growth of Yeast Colonies on Solid Media," *Microbiology*, vol. 134, pp. 3061–3069, 11 1988.
- [2] J.-R. Meunier and M. Choder, "Saccharomyces cerevisiae colony growth and ageing: biphasic growth accompanied by changes in gene expression," *Yeast*, vol. 15, pp. 1159–1169, 9 1999.
- [3] V. Plocek, L. Váchová, V. Štoviček, and Z. Palková, "Cell Distribution within Yeast Colonies and Colony Biofilms: How Structure Develops," *International Journal of Molecular Sciences*, vol. 21, p. 3873, 5 2020.
- [4] A. Traven, A. Jänicke, P. Harrison, A. Swaminathan, T. Seemann, and T. H. Beilharz, "Transcriptional Profiling of a Yeast Colony Provides New Insight into the Heterogeneity of Multicellular Fungal Communities," *PLoS ONE*, vol. 7, p. e46243, 9 2012.
- [5] Z. Palková and L. Váchová, "Spatially structured yeast communities: Understanding structure formation and regulation with omics tools," *Computational and Structural Biotechnology Journal*, vol. 19, pp. 5613–5621, 2021.

Continual learning on ACL abnormalities

István HAJDU

(Supervisors: Andor Viktor GÁL, Zoltán VIDNYÁNSZKY)

Pázmány Péter Catholic University, Faculty of Information Technology and Bionics

50/a Práter street, 1083 Budapest, Hungary

hajdu.istvan@itk.ppke.hu

Abstract—Continual learning (CL) in medical applications is a challenging not only because of mathematical and engineering adversities, but because of the scrutiny required in clinical validations prior to production release. I aim to investigate several CL methods on a medical dataset containing 7300 anterior cruciate ligament (ACL) specimens.

Keywords—continual learning; medical imaging; anterior cruciate ligament, ACL

I. INTRODUCTION

Catastrophic forgetting (CF) is a major pitfall affecting continual learning ambitions in machine learning, especially deep learning. CF occurs when a previously learned information or behaviour is overwritten when learning in a new task. This loss of competence occurs not because of insufficient model capacity, but of lacking a mechanism to retain information. Mammalian brains overcome this obstacle by mechanisms that rely on two assets: metaplasticity and complementary learning systems. In deep learning, these mechanisms are simulated, resulting in several methods.

In this work, three metaplasticity-based algorithms, two complementary learning system based, and a mixed approach is evaluated on a class-incremental and task-incremental learning scenario on medical images.

II. DATA

A private set of 7300 knee MR studies, annotated by expert radiologists was used for our methods. The ACL abnormalities were categories to 4 classes: healthy, degeneration or partial tear, total tear, and ACL graft. See Table I for dataset composition. To assess the CL frameworks, I constructed a task-incremental (Task-IL) and a class-incremental learning (Class-IL) scenario: the convolutional networks were first trained to identify the first two categories. Then, while applying the different CL methods, they were trained solely on the second two categories. In Class-IL, the network is expected to be able to distinguish between all classes seen so far, while in Task-IL, the network needs only to do so for class pairs it has actually been trained on.

TABLE I
DATASET COMPOSITION.

Category	Training set	Test set
Healthy	4111	1823
Degeneration/Partial tear	277	102
Total tear	500	189
Graft	180	61

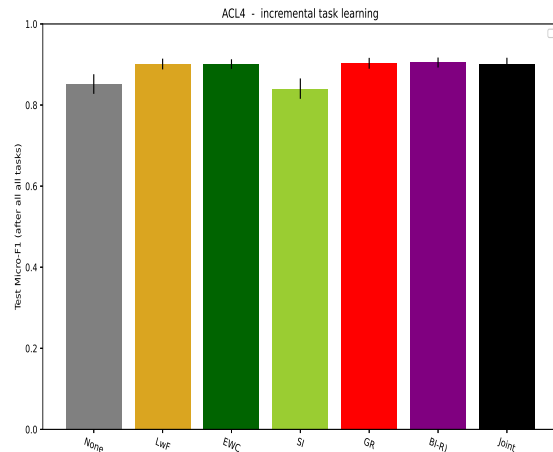


Fig. 1. Test micro-F1 score for various CL methods in a Task-IL scenario.

III. METHODS

The metaplasticity-based approaches are Learning without Forgetting (LwF), Synaptic Intelligence, and Elastic Weight Consolidation. Complementary learning systems (CLS) [1] theory inspired approaches include Generative Replay (GR), Brain-Inspired Generative Replay (BI-GR), and BI-GR with SI. The Class-IL challenge is known to disrupt metaplasticity-based approaches, while complementary learning inspired methods tackle this problem well. In this abstract, we report the results on the Task-IL scenario, where all CL methods are expected to mitigate catastrophic forgetting. [2]

IV. RESULTS

As we can see in Fig 1, all CL methods succeeded but Synaptic Intelligence on the Task-IL learning scenario.

REFERENCES

- [1] Kumaran D, Hassabis D, McClelland JL. What Learning Systems do Intelligent Agents Need? Complementary Learning Systems Theory Updated. *Trends Cogn Sci*. 2016 Jul;20(7):512-534.
- [2] van de Ven, G.M., Siegelmann, H.T., and Tolias, A.S. Brain-inspired replay for continual learning with artificial neural networks. *Nat Commun* 11, 4069 (2020).

Laser speckle contrast imaging of the rat brain

Imre Gergely JÁNOKI

(Supervisor: Péter FÖLDESZ)

Pázmány Péter Catholic University, Faculty of Information Technology and Bionics

50/a Práter street, 1083 Budapest, Hungary

janoki.imre.gergely@itk.ppke.hu

Abstract—Laser speckle contrast imaging is heavily researched in recent years. It is an optical technique that utilizes laser speckle effect which is the salt-and-pepper-like intensity pattern picked up by a camera, generated by the superposition of scattered coherent light (laser light). As scatterers move during exposure time, the pattern changes creating a blurring effect, hence movement can be mapped as a contrast map. It is a valuable tool in flowmetry that can be used to monitor the blood flow on the surface of a rat brain during surgery situations. During my research, I developed and implemented techniques to improve laser speckle contrast imaging of the rat brain.

Keywords—laser speckle contrast imaging; LSCI; rat brain; surgery; flowmetry

I. INTRODUCTION

Laser speckle contrast imaging (LSCI) maps the movement of dynamic scatterers to a contrast map utilizing the changing pattern of the speckle effect during the exposure time of the camera. The speed of movement (or flowrate) is inversely proportional to the decorrelation time, but the contrast and decorrelation time has a complex relation, and its description is still heavily researched and being improved [1], [2]. Measurements heavily depend on hardware setup and have a number of restrictions. In my work, I research LSCI to improve the contrast map for mapping the relative flow rates.

II. METHODS

First we developed a method to increase the otherwise low dynamic range of the traditional LSCI. Instead of using constant level illumination, we gradually decrease the illumination level during a single exposure. The practical implementation of this technique uses fixed intensity short laser pulses, where the frequency modulation mimics the change of light intensity. This way a higher range of blood flowrates - from arteries to capillaries - can be correctly mapped at once during the LSCI of the rat brain. [3]

Granularity - a frozen pattern on the contrast map - introduced by the static scatterers, causes false measurements at areas where static scatterers are abundant. To address this issue, we utilize ensemble averaging, during which we use one fixed and one rotating diffuser. The slow rotation of the diffuser ensures an interframe decorrelated illumination, essentially forcing the pattern to be a statistical error that we eliminate by averaging the set of consecutive frames. This results in the smoothing of said frozen pattern over the ensemble averaged final contrast map. [4]

We have created an online feedback-based measurement system using a Raspberry Pi 4. It implements gradient-based and latin hypercube sampling based optimization of exposure time and pulse frequency decay parameters based on the feedback of continual measurements of the subject. The Pi controls the camera and the laser pulse as well, then

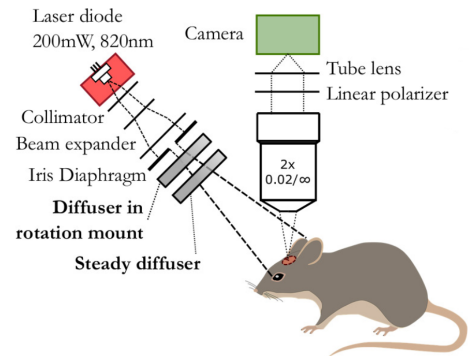


Fig. 1. Experimental arrangement using double diffusers for LSCI of the rat brain. [4]

calculates the contrast map and adjusts parameters accordingly. Measurement protocols and implementation was done for the following paradigms: contrast setpoint control, dynamic range maximization, sensitivity maximization. Both traditional and our new, high dynamic range method were implemented.

Finally, we created a method to compensate the saturation of the cameras during LSCI measurements extending the maximum illumination level that can be used. The method extrapolates based on the saturated pixel ratio and the changed contrast. As a result, the measurement results depend less on the precise illumination setting and imaging of darker areas become easier with better quality.

ACKNOWLEDGEMENTS

The author would like to express gratitude to Péter FÖLDESZ and Máté SIKET, with whom the presented research was done in close cooperation.

REFERENCES

- [1] J. W. Goodman, *Speckle Phenomena in Optics: Theory and Applications*. Roberts & Company, 1 ed., 2006.
- [2] D. D. Postnov, J. Tang, S. E. Erdener, K. Kılıç, and D. A. Boas, “Dynamic light scattering imaging,” *Science Advances*, vol. 6, no. 45, p. eabc4628, 2020.
- [3] M. Siket, I. Jánoki, K. Demeter, M. Szabó, and P. Földeszy, “Time varied illumination laser speckle contrast imaging,” *Optics Letters*, vol. 46, pp. 713–716, Feb 2021.
- [4] P. Földeszy, M. Siket, I. Jánoki, K. Demeter, and Ádám Nagy, “Ensemble averaging laser speckle contrast imaging: statistical model of improvement as function of static scatterers,” *Opt. Express*, vol. 29, pp. 29366–29377, Aug 2021.

Prediction of the clinical outcome of COVID-19 from viral mutations using machine learning techniques

Regina KALCSEVSZKI

(Supervisor: Sándor PONGOR)

Pázmány Péter Catholic University, Faculty of Information Technology and Bionics

50/a Práter street, 1083 Budapest, Hungary

kalcsevszki.regina@itk.ppke.hu

Abstract—Several studies shown the connection between the outcome of COVID-19 and the general health condition of the patient, like their other diseases and age. It is also clear that the outcome of the disease changes with the variants of the virus. Our aim in this study was to build a machine learning model that can predict the outcome of the diseases (mild or severe) based on the mutations found in the genome of the virus. The model training pipeline is shown in Figure 1.

We downloaded more than 65 thousands of SARS-CoV-2 viral genome that had outcome data from GISAID database and analysed the genomes and the metadata [1]. Using MUMmer we generated a fast multiple alignment to compare the genomes to the reference genome [3]. After sorting out the bad quality genomes based on the MUMmer alignment, we determined the SNVs, deletions and insertions compared to the Wuhan reference genome with a new high-quality multiple alignment of the samples and the reference genome using MAFFT [4]. We annotated the found mutations with SnpEff [5].

We found, that the ratio of severe and mild samples as well as the mutations in the genome varied by the time period the samples were taken. We stratified the samples by the quarter of the year the samples were taken, so we would compare samples from the same time period.

We selected the most prevalent mutations and used JADBio automatic machine learning tool to build machine learning model to classify the samples to mild and diseased groups using the found mutations and the patient age [2]. The model reached 0.883 ROC AUC with 0.826 ACC.

We also analysed the selected features to check whether they are significant out of the training set. We also found selected mutations that also appeared in the WHO Variant of Concerns, like NS3a Q57H in Gamma variant or Spike S371L in Omicron variant.

The generated machine learning model is able to classify the severe and mild samples with high accuracy. The pipeline we implemented makes it easy to complete the model with new samples containing new mutations and variants that may appear in the future.

Keywords-COVID-19; viral mutations; automatic machine learning

ACKNOWLEDGEMENT

I would like to offer my special thanks to Balázs Ligeti, who guided me through my whole work. Assistance provided by Sándor Pongor was greatly appreciated.

REFERENCES

- [1] Khare, S. et al *GISAID's Role in Pandemic Response*, China CDC Weekly 2021.
- [2] Tsamardinos, I. et al *ust Add Data: Automated Predictive Modeling and BioSignature Discovery*, BioRxiv 2020.
- [3] Marçais, G. et al *MUMmer4: A fast and versatile genome alignment system*, PLoS Computational Biology 2018.

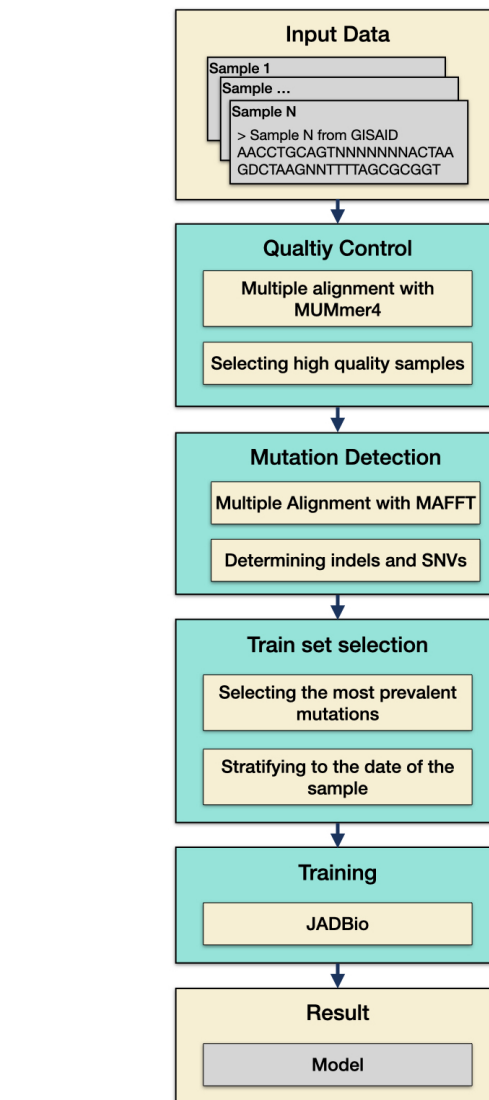


Fig. 1. Training pipeline of the disease outcome (severe vs mild) classification model from SARS-CoV-2 virus genomes.

- [4] Katoh, K. et al *MAFFT multiple sequence alignment software version 7: Improvements in performance and usability*, Molecular Biology and Evolution 2013.
- [5] Cingolani, P. et al *A program for annotating and predicting the effects of single nucleotide polymorphisms, SnpEff: SNPs in the genome of Drosophila melanogaster strain w1118; iso-2; iso-3*, Fly 2012.

Investigation of protein:protein interactions in the PSINDB from various aspects

Zsófia KÁLMÁN

(Supervisor: Zoltán GÁSPÁRI)

Pázmány Péter Catholic University, Faculty of Information Technology and Bionics

50/a Práter street, 1083 Budapest, Hungary

kalman.zsafia.etelka@itk.ppke.hu

Abstract—The postsynapse is an important participant of the neuronal signaling machine. Although postsynapse is highly studied, many aspects of its attribute and function are still to be unrevealed. In the past several years experimentally verified binary protein-protein interactions were unrevealed for proteins located in the PS. Last year we established a unique postsynapse specific database (PSINDB) that includes a wide variety of data from interactions to diseases. We believe that the understanding of the complexity in the nervous system requires an integrated approach using different sources of biological data. Particular combination and analysis of relevant information might shed line previously unknown connections.

Keywords-postsynapse; protein-protein interactions; disease

I. INTRODUCTION

Human brain is the most complex organ in the body containing billions of synapses formed by presynaptic and postsynaptic neurons. The postsynaptic site is responsible for taking the released neurotransmitter from the synaptic cleft where neurotransmitters (NT) are released by exocytosis from the presynapse [1]. The postsynaptic site of dendrites can be distinguished to three main parts: the postsynaptic density, the postsynaptic cytoskeleton and the postsynaptic membrane [2]. The most interesting one is the postsynaptic density, a protein dense organelle, where proteins form a mesh-like structure to serve as a skeleton for protein-protein interaction formation. Despite extensive research the exact composition of the PSD is still unknown. According to the prevailing view 1500 individual proteins are abundant here and many of them are found in multiple copies. The estimation is that altogether 1 gigaDalton worth of mass is formed which equals 10 000 proteins [3], [4], [5], [6]. Postsynaptic density consists of an elaborate network of proteins. Much of the information about it is binary protein-protein interactions. Although now it is clear that most proteins are forming complexes and supercomplexes they are extremely hard to determine because of experimental difficulties such as PSD purification. An additional aggravating factor is that these complexes are highly dynamic and differ in composition in distant brain regions [1]. An important role of the postsynapse is suggested in basic neural processes such as learning and memory [3], [7]. The importance of the postsynapse is also supported by the fact that more than 100 diseases were linked to its proteins, including major psychiatric and neurodevelopmental diseases such as Alzheimer, Parkinson and schizophrenia [4], [8]. Although more and more information is emerging from the scientific results on the postsynapse most of the pieces from the puzzle are still not in place.

II. SUMMARY

Last year we established the postsynaptic protein-protein interaction database (PSINDB). PSINDB contains the following data: PS localization of proteins, binary interactions, prediction of structural and unstructural segments, GeneOntology and DiseaseOntology annotation of the interacting partners of PS proteins (Figure 1). The focus of my research this year was preliminary calculations combining different data from PSINDB to determine some possible perspectives for further more detailed research.

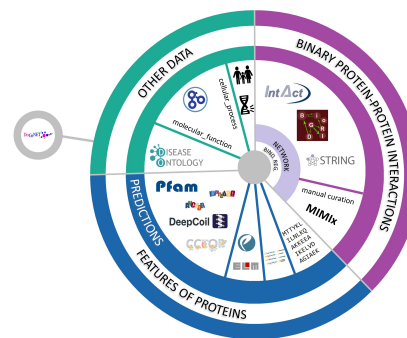


Fig. 1. The data on which the analysis is based - for the most part from the PostSynapticInteractionDataBase (PSINDB)

ACKNOWLEDGEMENTS

This research was supported by the NRDI Office through the grant TKP2021-EGA-42.

REFERENCES

- [1] Grant, Seth GN. "Synapse molecular complexity and the plasticity behaviour problem." *Brain and Neuroscience Advances* 2: 2398212818810685. 2018
- [2] Koopmans, Frank, et al. "SynGO: an evidence-based, expert-curated knowledge base for the synapse." *Neuron* 103.2: 217-234 2019.
- [3] Borczyk, Malgorzata, Kasia Radwanska, and K. Peter Giese. "The importance of ultrastructural analysis of memory." *Brain Research Bulletin* 173: 28-36. 2021
- [4] Sheng, Morgan, and Eunjoon Kim. "The postsynaptic organization of synapses." *Cold Spring Harbor perspectives in biology* 3.12: a005678. 2011
- [5] Wilkinson, Brent, and Marcelo P. Coba. "Molecular architecture of postsynaptic Interactomes." *Cellular Signalling* 76: 109782. 2020
- [6] Kaizuka, Takeshi, and Toru Takumi. "Postsynaptic density proteins and their involvement in neurodevelopmental disorders." *The Journal of Biochemistry* 163.6: 447-455. 2018
- [7] Abraham, Wickliffe C., Owen D. Jones, and David L. Glanzman. "Is plasticity of synapses the mechanism of long-term memory storage??" *NPJ science of learning* 4.1: 1-10. 2019
- [8] Bayés, Alex, et al. "Characterization of the proteome, diseases and evolution of the human postsynaptic density." *Nature neuroscience* 14.1: 19-21. 2011

High-performance COVID pandemic simulator

Bence KEÖMLEY-HORVÁTH

Supervisors: István REGULY, Attila CSIKÁSZ-NAGY

Pázmány Péter Catholic University, Faculty of Information Technology and Bionics

50/a Práter street, 1083 Budapest, Hungary

keomley-horvath.bence.mark@itk.ppke.hu

Abstract—There are many approaches to simulate the COVID-19 pandemic. In our approach we wanted to have more detailed control thus we use an agent based approach, where we simulate every person and location separately. The algorithm uses Thrust library extensively to accelerate the algorithm on both CPU and GPU.

I. INTRODUCTION

There are many papers when they applied a deterministic model for the current COVID pandemic. Röst et al. proposed a system control model that can modify the constants in runtime in the differential equations to achieve different goals. [1]

The deterministic models are driven by differential equations. There are some limitations of the deterministic approaches. It is not feasible to include that many parameters as in a direct agent-based model, which leads to less detailed control possibilities. Also, realistically many events are not continuous, like getting infected, being in lockdown or hospital and travelling between locations.

Another limitation of deterministic models is that they can not predict situations that might have a small chance, but they can significantly change the simulation's output. With stochastic models, if we run the simulations multiple times, we can have a good chance of catching these behaviours.

A. Related works

There are many agent-based models created for this pandemic, with different level of accuracies and runtime performance.

Bicher et al. [2] propose a decision tree to handle the possible events for the agents. They do not consider different locations. The only possible movement is emigration when the agents leave the simulation. They implemented the model in Python3, which does not provide high-performance, but for the simplified event handling and reduced agent number, they can archive reasonable runtime.

Epidemics simulations are not a new challenge. It just became more important due to the current COVID pandemic. There has already been an existing agent-based model, which they used to specialise for this pandemic. For Australia there is a pre-existing model [3], where agents have a specific schedule and corresponding movement pattern on a highly detailed location graph. They improved and specialised that model for the COVID-19 pandemic [4]. Using the HPC cluster (Artemis at the University of Sydney), with 4264 computing cores to simulate entire Australia for 180 days, it takes 42 minutes.

B. Goals

Our goal is to simulate every person directly, considering every aspect of life relevant to the virus's spreading with agent-based modelling. We have to follow their movements because this defines where they can be infected and transmit

the virus. Another critical aspect is those data that can affect their response to the virus; therefore, we must consider the agent's age and precondition.

When an agent got infected, there are multiple paths where the course of the disease can lead. We can describe it with a weighted directed graph where the nodes are the possible states, and the edges are the possible progressions from that state. The sum of the weights of edges starting from a node has to be one because it represents chances. There are multiple models to describe this disease; therefore, it will be an input for the simulation. There are three groups of states. The first group mainly only contains a susceptible state. The second which varies the most is the infected state. Here we have to model everything from being infected and not having any symptoms to the disease's seriousness. The last group is the outcome of the infection, which can be either recovering or death.

The purpose of this simulation is to predict the effect of different scenarios. These can be governmental regulations like obligatory mask-wearing, closing various institutions and lockdowns. Different testing policies define when an agent gets tested and the effect of a positive test. We have to handle all these events in a way that some can dynamically change throughout the simulation.

Many of the use cases require good runtime from the simulation. Before we can give any predictions, we have to fit some parameters to mimic real-life data. We have to evaluate the function, which is an entire simulation run, many dozens of times for all parameter fitting algorithms. When we want to predict the progression of the pandemic, we still need multiple runs due to the stochastic nature of the simulation. The same pertains to different scenario testing.

ACKNOWLEDGEMENTS

Thank you for István Reguly for his help in planning and implementing the algorithms. Kálmán Tornai and his team for the input data. And for the whole COVID simulation team for the work.

REFERENCES

- [1] T. Péni, B. Csutak, G. Szederkényi, and G. Röst, "Nonlinear model predictive control with logic constraints for covid-19 management," *Nonlinear Dynamics*, vol. 102, p. 1965–1986, Dec 2020.
- [2] M. Bicher, C. Urach, and N. Popper, "Gepoc abm: A generic agent-based population model for austria," in *2018 Winter Simulation Conference (WSC)*, IEEE, Dec 2018.
- [3] O. M. Cliff, N. Harding, M. Piraveenan, E. Y. Erten, M. Gambhir, and M. Prokopenko, "Investigating spatiotemporal dynamics and synchrony of influenza epidemics in australia: An agent-based modelling approach," *Simulation Modelling Practice and Theory*, vol. 87, p. 412–431, Sep 2018.
- [4] S. L. Chang, N. Harding, C. Zachreson, O. M. Cliff, and M. Prokopenko, "Modelling transmission and control of the covid-19 pandemic in australia," *Nature Communications*, vol. 11, Nov 2020.

Synchronization modes and factors in the septal network

Barnabás KOCSIS

(Supervisor: István ULBERT)

Pázmány Péter Catholic University, Faculty of Information Technology and Bionics

50/a Práter street, 1083 Budapest, Hungary

kocsis.barnabas@itk.ppke.hu

Abstract—This report is the continuation and extension of our previous works and results [1], [2], [3]. Hippocampal field potentials for network state detection and medial septum (MS) unit activities were recorded concurrently in anaesthetized rats (a. rat), anaesthetized mice (a. mouse) and freely moving mice (f.m. mouse). Here we present some key differences between datasets. Furthermore, we show a methodological tool to recognize duplicate cells after action potential clustering.

In our previous work rhythmicity groups were defined in the MS based on the rhythmic behaviours during hippocampal delta and theta dominant segments (pacemakers, tonic, delta, follower, theta-follower) [3]. Rhythmic relations between groups were mapped with cross-correlation analysis [2]. The pacemaker group were found to be the source of synchrony in the network. Here we report further confirmation of this idea.

When we analyzed pacemaker synchronization during theta we found that their rhythmicity frequencies tend to converge to a general frequency [2]. To better understand this mechanism, we implemented a pacemaker model network. Parameter space search revealed a set of optimal values for theta generation. Simulations with these parameters reproduced frequency synchronization seen in vivo [1]. While looking for further similarities

we have tested phase relations between model neurons. In vivo pacemakers shown to fire preferentially either at the peak or trough of hippocampal theta [4]. Owing to this, they form two antiphase clusters that can be detected by taking their cross-correlations. Similar quantification of antiphase behavior helped us to explore the model parameter space. Interestingly, we have observed bimodal phase segregation only in a totally different parameter region.

Keywords-neuronal oscillations, theta rhythm, hippocampus, medial septum, pacemaker, frequency synchronization, antiphase clusters, network model

REFERENCES

- [1] B. Kocsis, "A simple model to simulate rhythm generation in the medial septum." 32568558, conference paper, PPKE-ITK, 2020.
- [2] B. Kocsis, "Optogenetic identification of rhythmic neurons in the medial septum." 32568560, conference paper, PPKE-ITK, 2021.
- [3] B. Kocsis and B. Hangya, "Huygens synchronization of medial septal pacemaker neurons generates hippocampal theta oscillation." submitted.
- [4] Z. Borhegyi, V. Varga, N. Szilágyi, D. Fabo, and T. F. Freund, "Phase segregation of medial septal gabaergic neurons during hippocampal theta activity," *Journal of Neuroscience*, vol. 24, no. 39, pp. 8470–8479, 2004.

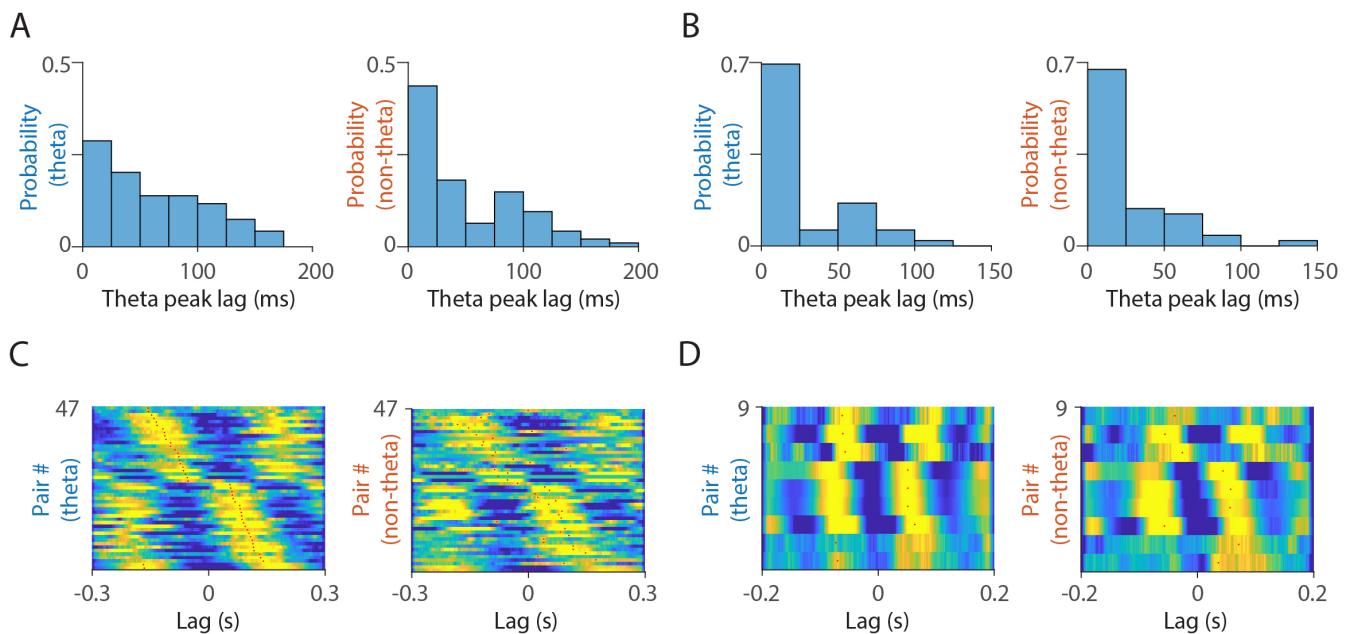


Fig. 1. In-phase versus anti-phase pacemaker synchronization in the mouse MS. A. mouse: (A, C), f.m. mouse: (B, D). (A, B): After calculating all crosscorrelograms of pacemaker pairs from the same recordings, we determined offsets as the lags corresponding to the crosscorrelogram peaks in theta frequency range. Histograms of offsets can be seen during theta (left) and non-theta (right). Interestingly, proportion of antiphase pairs (80-120 ms bin) increased during delta in a. mouse (A), while decreased in f. m. mouse. (C, D): Crosscorrelograms of antiphase pacemaker pairs (offset above 50 ms) during theta (left) and non-theta (right). A state independent, sustained offset was characteristic to both a. mouse and f. m. mouse.

Drug absorption through psoriatic mouse skin

Dorottya KOC SIS

(Supervisor: Franciska ERDŐ)

Pázmány Péter Catholic University, Faculty of Information Technology and Bionics

50/a Práter street, 1083 Budapest, Hungary

kocsis.dorottya@itk.ppke.hu

Abstract—Psoriasis is a common, immune-mediated disease, representing a significant health care challenge around the world. During the development of topical medications, skin permeability is an important aspect, however little data are available on checking this parameter at different stages of psoriasiform dermatitis. Contributing to this knowledge, we investigated the changes in drug absorption at different time points in imiquimod-induced psoriatic mice using a "skin-on-a-chip" microfluidic device. Our results show, that higher skin permeability is present in the psoriatic group compared to the control animals, however the permeability decreased with the progression of the disease, suggesting that a topical cream formulation as a medication can be more effective at the early phase.

Keywords—psoriasis; imiquimod; skin permeability; skin-on-a-chip diffusion chamber

I. SUMMARY

Psoriasiform dermatitis is a chronic inflammatory skin condition, affecting more than 125 million people worldwide [1]. Though it does not occur naturally in laboratory animals, in order to describe its pathophysiology and to determine the potential therapeutic targets, several animal models have been developed using genetic modifications, xenotransplantation or chemical induction. The imiquimod (IMQ)-induced mouse model is proven to represent several psoriasis-like symptoms at the epidermal, dermal and immunological levels [2].

Transient Receptor Potential Ankyrin 1 (TRPA1) is a nonselective cation channel, which shows a protective role in psoriasis, therefore, blocking or knocking out (KO) TRPA1 enhances the IMQ-induced dermatitis [3]. A further nonselective cation channel, Transient Receptor Potential Vanilloid 1 (TRPV1) enhances the development of the disease, which means that blocking or knocking out TRPV1 leads to severely impaired inflammation [3].

There are different approaches in therapy, however, the topical delivery route plays one of the most important roles, thus investigating the changes of the epidermal barrier function during the development is crucial [4].

In our study, the drug delivery through the psoriatic epidermal barrier was examined at different phases of the IMQ-induced psoriasis in wild type (WT), TRPA1 KO and TRPV1 KO mice. In all cases, vaseline (VAS)-treated mice were used as control.

The permeability experiments were performed in a "skin-on-a-chip" microfluidic device using a topically widely applied hydrophilic model drug, caffeine [4]. Based on the results, it can be concluded that the drug permeability increased with the progression of psoriasiform dermatitis in wild type animals [4]. The same could be found in the case of TRPA1 KO and TRPV1 KO animals, which suggests that the deletion of these ion channels has no effect on the transdermal drug delivery [4]. Interestingly, the drug permeability showed a moderate decrease between the 24 and 96 h observation time points,

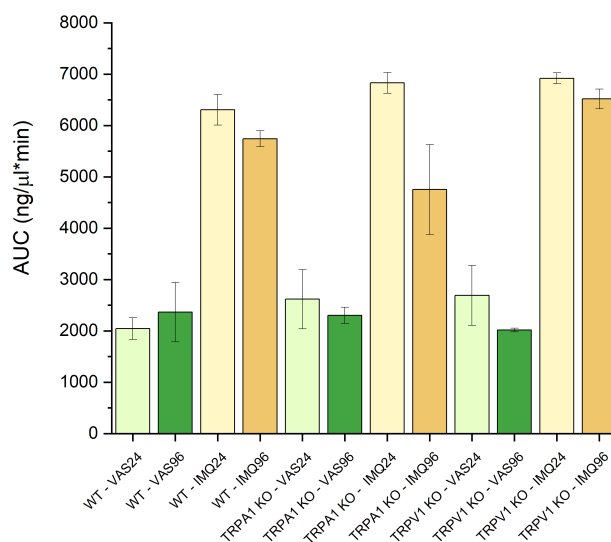


Fig. 1. Area under the curve values calculated from the concentration-time profiles of caffeine absorption.

which might be a consequence of the higher level keratinocyte proliferation, the plaque formation, and therefore the partial closure of the hair follicles, which are crucial in the absorption of caffeine [4].

In summary, these data suggest that the topically applied drugs have a greater chance to relieve the symptoms at an early stage of the disease.

ACKNOWLEDGEMENTS

The author thanks Dr Franciska Erdő (Pázmány Péter Catholic University), Dr Rolland Gyulai, Dr Ágnes Kemény, Dr Erika Pintér and Dr Szabina Horváth (University of Pécs) for the help in understanding the theoretical background and providing the animals for the research.

REFERENCES

- [1] K. Srivastava, T. C. Yadav, H. K. Khera, P. Mishra, N. Raghuvanshi, V. Pruthi, R. Prasad, "Insights into interplay of immunopathophysiological events and molecular mechanistic cascades in psoriasis and its associated comorbidities", *J Autoimmun*, vol. 118, no. 102614, 2021.
- [2] M. P. Schön, V. Manzke, L. Erpenbeck, "Animal Models of Psoriasis-Highlights and Drawbacks", *J Allergy Clin Immunol*, vol. 147, pp. 439-455, 2021.
- [3] Á. Kemény, X. Kodji, S. Horváth, R. Komlódi, É. Szőke, Z. Sándor, A. Perkecz, C. Gyömörei, G. Sétáló, B. Kelemen, T. Bíró, B. I. Tóth, S. D. Brain, E. Pintér, R. Gyulai, "TRPA1 Acts in a Protective Manner in Imiquimod-Induced Psoriasiform Dermatitis in Mice", *J Invest Dermatol*, vol. 138, no. 8, pp. 1774-1784, 2018.
- [4] D. Kocsis, S. Horváth, Á. Kemény, Z. Varga-Medveczky, C. Pongor, R. Molnár, A. Mihály, D. Farkas, M. B. Naszlady, A. Fülöp, A. Horváth, B. Rózsa, E. Pintér, R. Gyulai, F. Erdő, "Drug Delivery through the Psoriatic Epidermal Barrier—A "Skin-On-A-Chip" Permeability Study and Ex Vivo Optical Imaging", *Int J Mol Sci*, vol. 23, no. 4237, 2022.

Parameter space investigation for SVM based Brain-Computer Interfaces

Csaba Márton KÖLLŐD

(Supervisor: István ULBERT)

Pázmány Péter Catholic University, Faculty of Information Technology and Bionics

50/a Práter street, 1083 Budapest, Hungary

kollod.csaba@itk.ppke.hu

Abstract—This report present the effect of different EEG bands with respect the classification accuracy of a Support Vector Machine based BCI System. With the used prototype BCI system realtime gameplays were also conducted where the tetraplegic subject had to control an avatar on a virtual track to reach the finish line.

I. INTRODUCTION

Brain-Computer Interfaces (BCI) are integrated software and hardware systems which record the bio-electrical signals of the brain. And by classifying the signals it controls an external device. (Fig. 1.)

Our research team, lead by István ULBERT, aims to create a BCI system, which will be challenged by other BCI devices of other research groups, in 2024 at the international Cybathlon competition. [1], [2]

II. DATASETS

Next to the online available motor imaginary dataset on PhysioNet [3] we recorded our own dataset with the help of 2 tetraplegic subjects. For signal recording, 64 channeled ActiChamp+ EEG system were used, which is produced by Brain Products. On both datasets we made parameter space investigation with respect to the EEG bands. We focused on the effect of different EEG bands with respect the classification accuracy of our classifier.

III. METHODS

For searching the parameter space the High Performance Cluster (HPC) machine were used. The original BCI code were uploaded to the server with the databases. Many different preprocessing configurations were created and submitted as jobs to calculate the Accuracy results on the whole databases.

Raw EEG data is recorded and send to the Signal Processing part of the BCI System. With a given window length data is cut and for each window the absolute of the complex Fast-Fourier Transformation of the EEG signals were calculated as a Source Feature (SF). Two different methods are created for feature extraction and classification. One of them is the SF AVERAGE method, where the average SF of a well known EEG band was calculated for each channel. This resulted a *number of channel x 1* feature vector which is used as train and test data for a Support Vector Machine (SVM). The other is the SF RANGE method, which further utilizes the SF Average method, by creating feature vectors form distinct 2 Hz wide parts of the SF. These features are fed to separate SVMs with respect to the frequency range. The final classification result is calculated as the max vote of the individual SVMs.

Next to the parameter space investigation of EEG bands we also conducted real-time game-play experiments, where

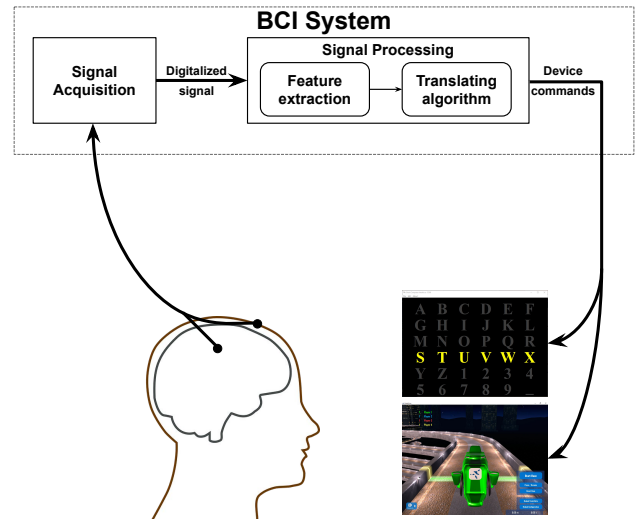


Fig. 1: BCI System workflow, based on J. R. Wolpaw et al. [4]

the time required to reach the finish-line was recorded and measured.

IV. RESULTS

The Range40 method clearly outperformed the rest of the EEG bands and the Range30 method. With respect to the real-time experimtns we conducted 59 gameplays in total from which 27 were under the 240 second time limitation, which was defined by the organizers of the Cybathlon.

REFERENCES

- [1] R. Riener and L. J. Seward, "Cybathlon 2016," in *2014 IEEE International Conference on Systems, Man, and Cybernetics (SMC)*, 2014, pp. 2792–2794.
- [2] S. Perdakis, L. Tonin, S. Saeedi, C. Schneider, and J. d. R. Millán, "The Cybathlon BCI race: Successful longitudinal mutual learning with two tetraplegic users," in *PLOS Biology*, vol. 16, no. 5, e2003787, 2018.
- [3] Goldberger Ary L., Amaral Luis A. N., Glass Leon, et al., "PhysioBank, PhysioToolkit, and PhysioNet," *Circulation*, vol. 101, no. 23, e215–e220, 2000.
- [4] J. R. Wolpaw, N. Birbaumer, D. J. McFarland, G. Pfurtscheller, and T. M. Vaughan, "Brain-computer interfaces for communication and control," *Clinical Neurophysiology*, vol. 113, no. 6, pp. 767–791, 2002.

Optical characterization of a flexible, transparent micro-ECoG device for multimodal neuroimaging

Zsófia LANTOS

(Supervisor: Zoltán FEKETE)

Pázmány Péter Catholic University, Faculty of Information Technology and Bionics

50/a Práter street, 1083 Budapest, Hungary

lantos.zsafia@itk.ppke.hu

Abstract—The hippocampus has a significant role in memory formation and spatial navigation. The observation of these brain processes increasingly relies on the combination of multiple neuroimaging methods, like electrophysiology and two-photon microscopy imaging. During these experiments, the electrophysiological device is placed in the beam path of the two-photon microscope. It is therefore necessary that these devices are transparent. Since the images are taken through these devices during imaging it is necessary to investigate their optical properties.

In this paper, the spatial resolution of fluorescent two-photon imaging through the micro-electrocorticography (microECoG) device is presented in fluorescent microbeads, transgenic hippocampal slices, and in the change of relative intensity in *in vivo* images under the long-term (155 days) implanted device. During the 22 weeks *in vivo* measurements, the fluorescent activity remained stable and Ca²⁺ signals were captured. Based on the results our device is suitable for multimodal imaging.

Keywords—microECoG; electrophysiology; two-photon microscopy; optical characterization

I. INTRODUCTION

The hippocampus is one of the most investigated structures in the brain. It is responsible for the formation of memory through long-term potentiation [1]. Although the hippocampus plays a significant role in the function of the brain, research mainly relies on single modalities, like electrical recordings and optical imaging. Multimodal techniques, like the combination of electrophysiological recording and two-photon microscopy, take advantage of the temporal resolution of electrophysiology recording and spatial resolution of neuroimaging techniques [2]. However, the conventional microelectrodes track electrical activity from only a few neurons. To have a better spatial resolution, microECoGs can be used instead of penetrating microelectrodes. Because the microECoG is placed in the light path of the two-photon microscope, and the images are taken through it, it is important to investigate the optical properties of the device.

II. METHODS

The microECoG with shape memory polymer on both sides was made in the collaboration of the University of Texas at Dallas, Femtonics Ltd. and Pázmány Péter Catholic University. The design and electrical properties of the device were presented previously [3]. The electrode grid has a custom thiolene-acrylate softening thermoset polymer presented on both sides. To investigate the optical characteristics of the device, Two-photon Ca²⁺ images were taken of fluorescent microbeads and brain slices. To determine the long-term effects of the implanted device, *in vivo* measurements were made over 155 days. The images were analyzed with custom

made MATLAB scripts and algorithms.

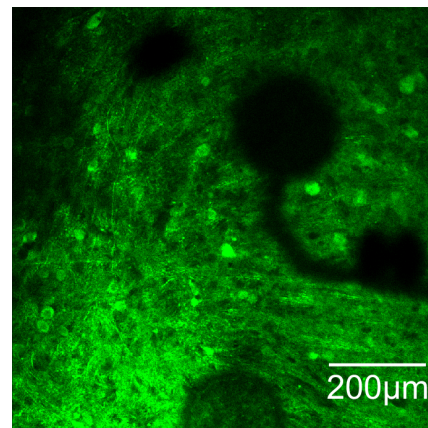


Fig. 1. Image taken with the device placed in the light path. The shadows of the recording sites are visible.

III. DISCUSSION

In this project, our goal was to determine the optical properties of a thiolene-acrylate based microECoG device for multimodal hippocampal recordings. To investigate the optical properties of the device, multiple *in vitro* Ca²⁺ images were recorded with and without the fully fabricated device from fluorescent microbeads and hippocampal brain slices. For the investigation of the long-term effects of the implanted device, the change in relative fluorescence was measured over 155 days after implantation. Based on these results we can say, that the thiolene-acrylate based microECoG device is suitable for the use of multimodal neuroimaging of the hippocampus, even after 155 days.

ACKNOWLEDGEMENT

This research was supported by the National Research, Development and Innovation Office through the grant TKP2021-EGA-42.

REFERENCES

- [1] J. J. Knierim, “The hippocampus,” *Current Biology*, vol. 25, no. 23, pp. R1116–R1121, 2015.
- [2] A. Zátanyi, M. Madarász, Á. Szabó, T. Lőrincz, R. Hodován, B. Rózsa, and Z. Fekete, “Transparent, low-autofluorescence microecog device for simultaneous ca2+ imaging and cortical electrophysiology *in vivo*,” *Journal of Neural Engineering*, vol. 17, no. 1, p. 016062, 2020.
- [3] F. Z. Fedor, M. Madarász, A. Zátanyi, Á. Szabó, T. Lőrincz, V. Danda, L. Spurgin, C. Manz, B. Rózsa, and Z. Fekete, “Soft, thiol-ene/acrylate-based electrode array for long-term recording of intracranial eeg signals with improved biocompatibility in mice,” *Advanced Materials Technologies*, p. 2100942, 2021.

Examination of the distribution and structure of postsynaptic protein complexes by extended simulations

Marcell MISKI

(Supervisor: Attila CSIKÁSZ-NAGY)

Pázmány Péter Catholic University, Faculty of Information Technology and Bionics

50/a Práter street, 1083 Budapest, Hungary

miski.marcell@itk.ppke.hu

Abstract—The postsynaptic protein complexes are capable of dynamic redistribution in different timescales. These structural changes of the complexes can affect the behaviour of the synapse therefore the changes are the molecular mechanisms behind learning and memory, as well as several neurological conditions like autism. I am using Gillespie-based computer simulations and integrative modeling of the three dimensional structures of the complexes arising in the postsynaptic density (PSD) as a function of the abundance of individual proteins translated. I am investigating further the already published simulations [1] by the effects of different binding and unbinding rates on the complex formation which may simulate how mutations can change the synapse.

Methods: The Gillespie-based simulations are performed with Cytocast. Structural data for the individual proteins were obtained from the Protein Data Bank (PDB) database. The abundances are generated from mRNA expression levels as described in [1]. For comparison several dimension reduction methods and metrics were used such as principal component analyses (PCA) and cluster distances.

Results: I have made further 3D modeling of complexes using the previously created protein models, but to conclude the integrative modeling platform (IMP) were not able to deal with flexible C-terminal binding sites due to too much freedom by long linker region, the main domains did not changed positions accurately. I have considered several methods of mutation analyses to use or alter for predicting binding rates but all of them proved to be lacking in some respect.

Keywords—keyword; postsynaptic density; Cytocast; Synaptic Theory; PeProb; disordered regions; protein models; mutational analyses

I. INTRODUCTION

The Synaptic Theory [2] postulates that the neuron's behaviour is largely determined by the postsynaptic complexes created by its constituent proteins available in different abundances. In our simulations using only protein abundances the results would be purely based on random diffusion, however other parameters may change the complex formations. One of the main parameters in addition are the binding and unbinding rates which tells the probability of two proteins who already met whether they will be bound together. These binding rates can be altered by mutations and other factors such as the flexibility of the domains and their interference upon binding. The main difficulty of considering mutations is lack of experimental data and prediction methods. The widely used predictions of binding rate changes by mutations are focusing on the mutations which has a very low chance to change the binding rates as in industry its more important. These results unfortunately the complement of what we would like

to accomplish in our simulations considering the binding rate changes.

II. METHODS AND VALIDATION

My simulations run by Cytocast uses Gillespie-algorithm conclusions were created by mathematical methods. The principal component analyses can show outlier regions that need further examinations to find out the cause of outlying. Considering different binding rates the region mapped on a plane can be compared by simulations made by uniform binding rates. I use relative distances as a comparison measure.

HoTMuSiC [3], CAD-Score [4], PredictSNP [5], NeEMO [6] are available methods to predict protein and binding stability.

III. DISCUSSION

I conclude that nevertheless the methods mentioned above are focusing on different aspects and none of them are easily converted for our cause.

ACKNOWLEDGEMENTS

The authors acknowledge the support of the National Research, Development and Innovation Office – NKFIH through grant no. NN124363. The research was funded by the European Union and co-financed by the European Social Fund under grant number EFOP-3.6.2-162017-00013. Molecular graphics and analyses performed with UCSF Chimera, developed by the Resource for Biocomputing, Visualization, and Informatics at the University of California, San Francisco, with support from NIH P41-GM103311.

REFERENCES

- [1] M. Miski, B. M. Keömley-Horváth, D. R. Megyeriné, A. Csikász-Nagy, and Z. Gáspári, "Diversity of synaptic protein complexes as a function of the abundance of their constituent proteins: A modeling approach," *PLOS Computational Biology*, vol. 18, p. e1009758, Jan. 2022.
- [2] S. G. Grant, "The synaptic theory of behavior and brain disease," *Cold Spring Harbor Symposia on Quantitative Biology*, vol. 83, pp. 45–56, 2018.
- [3] F. Pucci, J. M. Kwasigroch, and M. Rooman, "Protein thermal stability engineering using HoTMuSiC," in *Methods in Molecular Biology*, pp. 59–73, Springer US, 2020.
- [4] K. Olechnovič and Č. Venclovás, "Contact area-based structural analysis of proteins and their complexes using CAD-score," in *Methods in Molecular Biology*, pp. 75–90, Springer US, 2020.
- [5] J. Bendl, J. Stourac, O. Salanda, A. Pavelka, E. D. Wieben, J. Zendulka, J. Brezovsky, and J. Damborsky, "PredictSNP: Robust and accurate consensus classifier for prediction of disease-related mutations," *PLoS Computational Biology*, vol. 10, p. e1003440, Jan. 2014.
- [6] M. Giollo, A. J. Martin, I. Walsh, C. Ferrari, and S. C. Tosatto, "NeEMO: a method using residue interaction networks to improve prediction of protein stability upon mutation," *BMC Genomics*, vol. 15, May 2014.

Closed Neural Spike Sorting System Using FPGA

Obada MUHAMMAD

(Supervisor: István ULBERT)

Pázmány Péter Catholic University, Faculty of Information Technology and Bionics

50/a Práter street, 1083 Budapest, Hungary

muhammad.obada@itk.ppke.hu

Abstract—Recent advances in high-density neural probe technology have made it possible for scientists to record in vitro neural action potentials (spikes) from a large number of neurons all at once. The goal of this project is to design and build a closed loop system that can do record and process brain spikes in real time with the utmost accuracy. A Field Programmable Gate Arrays (FPGAs) board with Neuropixels high density probes and Tensor Processing Unit (TPU) chip with deep-learning algorithms will be used to build and create a system.

Keywords-neural activity; action potential; spike sorting; FPGA ; deep learning

I. DISCUSSION

For decades, researchers have investigated the process of assigning neuronal action potentials (spikes) to a group of neurons (clusters) [1]. A high-density probe with a large number of recording channels is used to measure these spikes by implant it in the brain to record action potential (AP) and local field potential (LFP) data from the neural space where extracellular neuronal activity can be measured in this manner[1]. The extracellular recordings reveal a different number of neurons than what would be expected based on the location and anatomical structure of the brain where this discrepancy may lead to the recording of distinct brain activity in response to different stimuli. Understanding the patterns of neural firing can be accomplished in part by the detection and clustering of neuronal action potentials (Neural Spikes). Spike sorting algorithms is used to improve this procedure, which can lead to better understand how neurons communicate [2]. Neuropixels has produced new state-of-the-art probes with 384 recording channels and a probe base capable of analog pre-processing and digitalization of brain data (5x9mm²) [3]. The Neuropixels probe is used in this study to create a closed-loop system with 384 recording channels that can be used simultaneously. Data will be received and pre-processed on an FPGA board before being transferred to a TPU chip equipped with a deep-learning algorithm for sorting and classifying neural spikes, and finally, real-time results will be sent to the user via wireless transmissions as it is shown in Fig. 1.

ACKNOWLEDGMENTS

This research was supported by the National Research, Development and Innovation Office through the grant TKP2021-NKTA-66. I would like to thank János Rokai for his contribution to the project by handling the spike sorting task on a TPU chip.

REFERENCES

- [1] M. S. Lewicki, "A review of methods for spike sorting: the detection and classification of neural action potentials," *Network: Computation in Neural Systems*, vol. 9, no. 4, pp. R53–R78, 1998.

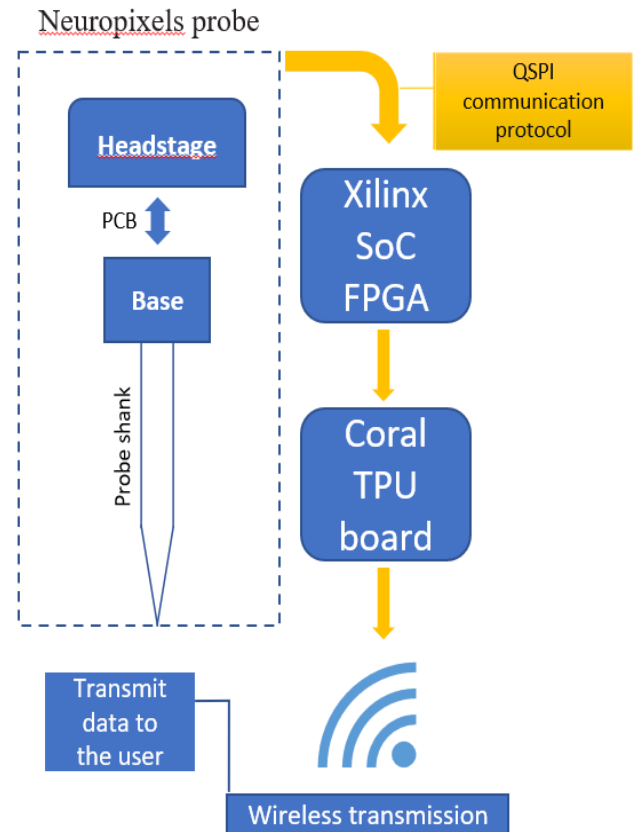


Fig. 1. Block diagram of the close-loop system design. Data acquisition starts from the probe shank sending the data to the FPGA board, then it is transferred to the TPU chip where the spike sorting algorithm, finally the results are transmitted to the user via wireless communication.

- [2] H. G. Rey, C. Pedreira, and R. Q. Quiroga, "Past, present and future of spike sorting techniques," *Brain research bulletin*, vol. 119, pp. 106–117, 2015.
- [3] C. M. Lopez, S. Mitra, J. Putzeys, B. Raducanu, M. Ballini, A. Andrei, S. Severi, M. Welkenhuysen, C. Van Hoof, S. Musa, and R. F. Yazicioglu, "22.7 a 966-electrode neural probe with 384 configurable channels in 0.13 μ m soi cmos," in *2016 IEEE International Solid-State Circuits Conference (ISSCC)*, pp. 392–393, 2016.

Isolation methods and storage stability of extracellular vesicles

Afrodité NÉMETH

(Supervisor: Tamás Márton GARAY)

Pázmány Péter Catholic University, Faculty of Information Technology and Bionics

50/a Práter street, 1083 Budapest, Hungary

nemeth.afrodite@itk.ppke.hu

Abstract—Extracellular vesicles (EVs) are present in all types of body fluids and they are harboring the characteristics of their origin. However, the isolation of EVs is challenging researchers all over the world. Our group aim to find a method that can not only isolate, but separate intact EVs from different types of bio-fluids, a technique which is repeatable and easy to carry out in clinical practice. Our first step toward this goal is to try out and compare the available methods as well as study their obstructions to develop an appropriate procedure. On the other hand, for experiments conducted simultaneously, storage stability of EVs needs to be widely studied. Therefore, we examined the vesicle’s characteristics after a freezing-thawing process.

Keywords—extracellular vesicles, ultracentrifugation, size-exclusion chromatography, precipitation, storage stability

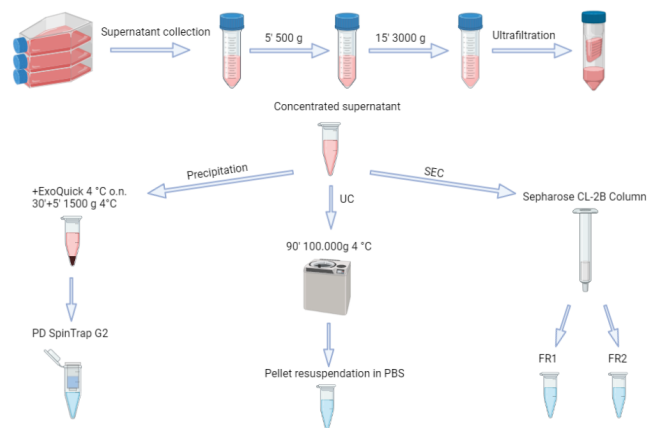


Fig. 1. Schematic representation of the different types of extracellular vesicles isolation’s process

I. INTRODUCTION

Extracellular vesicles are lipid bilayer bound particles with heterogeneous cargo, which represent their cell of origin. Cancer cells produce significantly more EVs than healthy cells, and the fact that they can be found in every body fluid, makes them promising progressive and predictive biomarkers for cancer [1]. EVs are commonly isolated by density-, size- or precipitation-based methods, however, due to the size and density overlap of the contaminants, these isolates might be spoiled. As a matter of fact, these contaminants are present in the body fluids on larger scales, so accurate information could be buried under them [2]. Moreover extracellular vesicle features are changing during storage, therefore for comparable studies, storage conditions need to have minimal impacts on EVs [3].

II. METHODS

The used EV isolation methods and it’s steps are represented in Fig. 1. Before EVs were isolated with one of the three evaluated methods, the collected supernatant was ultrafiltered. Then we used the concentrated supernatants to isolate vesicles either with size-exclusion chromatography (SEC), ultracentrifugation or ExoQuick precipitation reagent. The extracellular vesicle’s characteristics were investigated with Qubit protein assay, transmission electron microscopy (TEM) and dynamic light scattering.

III. SUMMARY

The extracellular vesicles isolation was successful with ultracentrifugation (UC), size-exclusion chromatography (SEC) and ExoQuick precipitation reagent. The isolated fraction’s mean particle size was in a range of supernatant-isolated EVs. We were able to visualize the lipid-bilayered compartments in the UC-isolated fractions with TEM. The total protein content of the isolates was variable among the compared methods. However, every method has it’s disadvantages, so for appropriate EV isolation we should combine different types of techniques.

ACKNOWLEDGEMENT

This research was supported by the National Research, Development and Innovation Office through the grant TKP2021-EGA-42.

REFERENCES

- [1] A. J. et al, “Inside(sight) of tiny communicator: exosome biogenesis, secretion, and uptake,” pp. 77–94, 2020.
- [2] R. H. Nicolas and G. Goodwin, “Overview of extracellular vesicles, their origin, composition, purpose, and methods for exosome isolation and analysis,” *Cells*, pp. 41–68, 2019.
- [3] L. . et al, “Effect of storage on physical and functional properties of extracellular vesicles derived from neutrophilic granulocytes,” *Journal of Extracellular Vesicles*, 2014.

Link prediction in the protein–protein interaction network using generative adversarial networks

Bence NÉMETH

(Supervisor: András HORVÁTH) or

Pázmány Péter Catholic University, Faculty of Information Technology and Bionics

50/a Práter street, 1083 Budapest, Hungary

nemeth.bencze@itk.ppke.hu

Abstract—Representing the proteins as nodes of a network and the interactions as edges, allows us to leverage network analyzing tools to discover new links and interactions. Image-to-image translation inspired conditional generative adversarial network (cGAN) model utilizing Wasserstein distance-based loss improved with gradient penalty was used, taking the combined representation from the data processing as input, and training the generator to predict the probable unknown edges in the provided induced subgraphs.

Keywords—Conditional GAN, Edge prediction, Protein interaction prediction, Interactome

I. INTRODUCTION

Comprehensive understanding of the human protein-protein interaction (PPI) network (interactome) could offer insights into cellular organization, genome function, and genotype–phenotype relationships. The human interactome map is still sparse and incomplete where computational methods can facilitate the exploitation of missing undiscovered interactions. [1]

II. METHODS

The available data processing framework created by Balogh et al. [2] was adapted in its original form which allows to a use modified breadth-first search algorithm to traverse the network and extract induced subgraphs on an updated newly preprocessed database in the following steps:

A. Database

In order to quantitatively assess the performance of different predictive models, STRING (Search Tool for the Retrieval of Interacting Genes/Proteins) database was used to benchmark different algorithms through standardized performance metrics, which is a biological database of known and predicted protein–protein interactions [3].

B. Preprocessing

In the preprocessing step the original(N100) PPI network will be downscaled to multiple versions with decreased number of edges, and will be stored in an adjacency list, generated by the node2vec algorithm [4] with a set of adjacency matrices of induced subgraphs, serving as input for the training and evaluation of the machine learning part. cGAN architecture was selected to train an edge predictor model. The model consists of a discriminator and a generator trained by an adversarial learning method [5]. The input for the generator are the embedding of the truncated networks and adjacency matrices. By 10-fold cross-validation ten N90 subgraphs have been generated, which will be truncated once again with 10-fold cross-validation into ten different N81 networks keeping 81% of the edges of the original network.

C. Model training

cGAN architecture was selected to train an edge predictor model. The model consists of a discriminator and a generator trained by an adversarial learning method [5]. For the generator, an encoder-decoder style network with skipping concatenations as short-cuts was implemented, based on the pix2pix GAN, where convolutional layers first encode, compress the input into increasingly smaller feature maps, following by a decoder pathway to decode them into increasingly larger ones. The input for the generator are the embedding of the truncated networks and adjacency matrices [6], [5].

III. SUMMARY

During the first semester of my PhD work I continued a PPI project of the Cardiometabolic and MTA-SE System Pharmacology Research Group (Olivér Balogh, Bettina Benczik, Mátyás Pétervári) led by Bence Ágg in the Department of Pharmacology and Pharmacotherapy led by Péter Ferdinandy, MD, PhD, MBA at Semmelweis University, Budapest. The first semester was spent getting to know the literature, learning the complete workflow, interpreting codes, preparation of the updated database and training of new neural networks (GAN) on the new dataset. I have generated learned and performed pre- and postprocessing- and GAN training steps of the whole workflow and applied on the updated STRING database in order to evaluate their performance and compare with other known networks. I have identified several interactome databases (e.g. UniHI, BioGRID, MINT, ADAN, PDZBase, PARPs) for further evaluation and new possible neural network types to train different predictor models in the next semester.

REFERENCES

- [1] X.-W. Wang, L. Madeddu, K. Spirohn, L. Martini, A. Fazzone, L. Becchetti, T. P. Wytock, I. A. Kovács, O. M. Balogh, B. Benczik, et al., “Assessment of community efforts to advance computational prediction of protein-protein interactions,” *BioRxiv*, 2021.
- [2] O. M. Balogh, B. Benczik, A. Horváth, M. Pétervári, P. Csermely, P. Ferdinandy, and B. Ágg, “Efficient link prediction in the protein–protein interaction network using topological information in a generative adversarial network machine learning model,” *BMC bioinformatics*, vol. 23, no. 1, pp. 1–19, 2022.
- [3] L. J. Jensen, M. Kuhn, M. Stark, S. Chaffron, C. Creevey, J. Muller, T. Doerks, P. Julien, A. Roth, M. Simonovic, et al., “String 8—a global view on proteins and their functional interactions in 630 organisms,” *Nucleic acids research*, vol. 37, no. suppl_1, pp. D412–D416, 2009.
- [4] A. Grover and J. Leskovec, “node2vec: Scalable feature learning for networks,” in *Proceedings of the 22nd ACM SIGKDD international conference on Knowledge discovery and data mining*, pp. 855–864, 2016.
- [5] G. I. P.-A. J. Mirza, “M. xu b. warde-farley d. ozair s. courville a. bengio y,” *Commun. ACM*, vol. 63, pp. 139–144, 2020.
- [6] P. Isola, J.-Y. Zhu, T. Zhou, and A. A. Efros, “Image-to-image translation with conditional adversarial networks,” in *Proceedings of the IEEE conference on computer vision and pattern recognition*, pp. 1125–1134, 2017.

Investigation of toxin producing yeast strains

Bíborka PILLÉR

(Supervisor: Attila CSIKÁSZ-NAGY)

Pázmány Péter Catholic University, Faculty of Information Technology and Bionics

50/a Práter street, 1083 Budapest, Hungary

pillér.biborka@itk.ppke.hu

Abstract—In the last few decades the knowledge about intracellular processes increased dramatically. However, we still do not have enough information about the interactions occurring between cells, because most laboratory experiments of microbial growth are focusing on individual strains. In nature, microbial populations form complex communities including more strains. These strains have the ability, to affect each other, and these arising interactions can influence the fate and the future of the growth of the population. In these mixed colonies both cooperation and competition can arise between the strains, so it is possible that some of the strains will thrive while others might be suppressed. Our goal is to study these interactions between different strains of *Saccharomyces cerevisiae* and to gain better understanding of the importance of coexistence and competition.

Keywords—yeast strains; yeast growth; toxin production

I. INTRODUCTION

Saccharomyces cerevisiae, commonly known as Baker's yeast is an important research and industrial microorganism [1]. It played a role in many discoveries regarding cellular and evolutionary processes.

Some interactions have already been observed between yeast strains in the 1970s [1]. These experiments mainly included the investigation of the effect of mixed colonies on the fermentation process [2]. While cooperation appears in many populations to produce the appropriate substances for survival, the most common interactions occurring between strains is the competition for nutrients [3]. One form of competition between strains can be caused by toxin production [4]. In this case one of the strains in a mixed colony is able to produce a toxin gaining an advantage over the other strain. This toxin production was proved to be important in fermentation of food and beverages and even in medical research [4]. Our goal is to extend this knowledge by examining the effect of different toxin producing strains on the growth of other laboratory strains with the help of a fluorescence-based approach.

II. DISCUSSION

A. Liquid culture experiments

1) *Growth of individual strains*: First to determine the unique growth characteristics of the strains they were tested in different liquid media: in SD containing 2% and 10% of glucose in SD with 2% ethanol concentration and in grape juice (15% glucose). For most of the previously mentioned strains it can be said that the most suitable environment for their growth is the SD containing the 2% or 10% glucose and they also grow well in grape juice.

2) *Co-culture experiments*: Between Sgu165 and Y55 there was no observable interaction, Sgu165 did not affect the growth of Y55 negatively, despite the fact that on solid media Y55 clearly showed a sensitivity to its toxin. However there can be many reasons why their behaviour is different in liquid

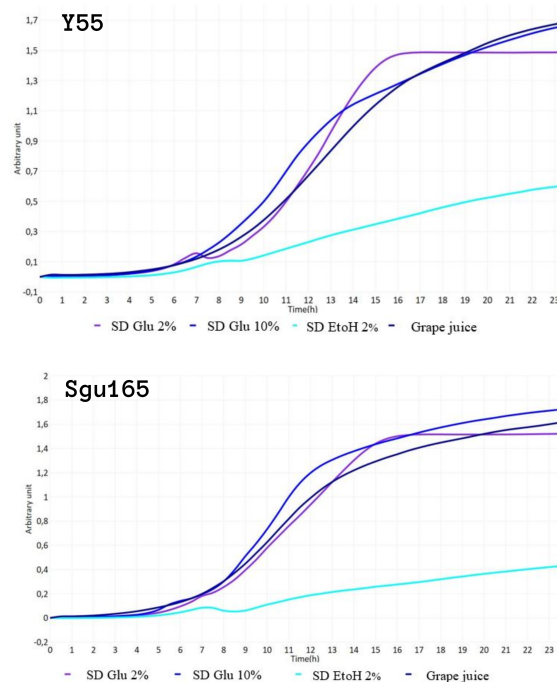


Fig. 1. The growth of Y55 and Sgu165 in different liquid media

culture compared to the solid medium. One of them being the glucose concentration which was 20% on solid medium, much higher than in the liquid culture. Also the length of the experiments differ from each other, while in liquid they can be observed for about 24 hours, on solid medium it took 3 days to see the effect of the toxin.

ACKNOWLEDGEMENTS

The research was supported by the Hungarian National Research, Development and Innovation Office (NKFI/NRDI) through the Hungarian Scientific Research Fund (OTKA-K20-134489) and the Thematic Excellence Programme (TKP2021-EGA-42).

REFERENCES

- [1] M. Cavaliere, S. Feng, O. S. Soyer, and J. I. Jiménez, "Cooperation in microbial communities and their biotechnological applications," *Environmental Microbiology*, vol. 19, no. 8, pp. 2949–2963, 2017.
- [2] B. C. Viljoen, "4.1 Introduction Yeast Ecological Interactions. Yeast–Yeast, Yeast–Bacteria, Yeast–Fungi Interactions and Yeasts as Biocontrol Agents 4.2 Ecological Interaction Between Microorganisms 4.2.1 The Secretion of Antifungal or Antibacterial Compounds," 2006.
- [3] J. Friedman and J. Gore, "Ecological systems biology: The dynamics of interacting populations," *Current Opinion in Systems Biology*, vol. 1, pp. 114–121, 2017.
- [4] V. Palpacelli, M. Ciani, and G. Rosini, "Activity of different 'killer' yeasts on strains of yeast species undesirable in the food industry," *FEMS Microbiology Letters*, vol. 84, no. 1, pp. 75–78, 1991.

Human movement analysis to improve control algorithms

Balázs RADELECZKI
(Supervisor: József LACZKÓ)

Pázmány Péter Catholic University, Faculty of Information Technology and Bionics
50/a Práter street, 1083 Budapest, Hungary
radeleczki.balazs@itk.ppke.hu

Abstract—In human movement analysis, we would like to quantitatively investigate how the human body is able to perform the given tasks in different environments and physiological conditions. Beside the proper physical and health assessment, this knowledge is useful to mimic human-like movements and inspire neuromorphic movement controls.

In our research group, we measure kinematic and electromyogram (EMG) data. With these two components, we are able to monitor the role of distinguished muscles in predefined movement tasks. Based on this data, we can create descriptive and control models for predefined tasks.

I studied the simultaneous arm and leg (hybrid) cycling and pendulum test. Both of them are widely used exercises in rehabilitation. The hybrid cycling with functional electrical stimulation (FES) is used to attenuate the side effects of paraplegia and in some cases to improve gait rehabilitation by a device, so-called hybrid ergometer. Meanwhile, the pendulum test is one of the simplest and most transparent way to monitor and detect reflex and muscular disorders [1]. These two methods support each other well in clinical applications.

The detailed model construction and simulation results of hybrid FES cycling control are displayed in our recent paper which is accepted by The Anatomical Records [2]. In this work, we introduce a model to control the lower limbs cycling with the EMG signals from the arms. This control is performed by a nonlinear auto-regressive recurrent neural network [3].

The neural network was able to learn similar patterns like the base line activity but their precision did not satisfy the accuracy

criteria. We explained these results with the artifacts of the measurements and the absence of the appropriate amount of data.

In case of pendulum test, we measured two paraplegic patients who had muscle stiffness in their lower limbs. From this data, I calculated the knee angle changes during the tasks. I also determined the beginning and endpoints of the kinematic data and EMG activity in time. These results are going to be compared with healthy participants records.

Our recorded data of human motion are also useful to test and develop a principle component analysis-related method with the cooperation of Wigner Research Center for Physics [4]. This research is hopefully able to describe natural laws in human movement.

Keywords-neural networks; dimension reduction

REFERENCES

- [1] G. Leslie, C. Muir, N. Part, and R. Roberts, "A comparison of the assessment of spasticity by the wartenberg pendulum test and the ashworth grading scale in patients with multiple sclerosis," *Clinical Rehabilitation*, vol. 6, no. 1, pp. 41–48, 1992.
- [2] B. Radeleczi, M. Mravcsik, L. Bozheim, and J. Laczko, "Prediction of leg muscle activities from arm muscle activities in arm & leg cycling,"
- [3] P. Xia, J. Hu, and Y. Peng, "Emg-based estimation of limb movement using deep learning with recurrent convolutional neural networks," *Artificial organs*, vol. 42, no. 5, pp. E67–E77, 2018.
- [4] A. Jakovac, "Time series analysis with dynamic law exploration," *arXiv preprint arXiv:2104.10970*, 2021.

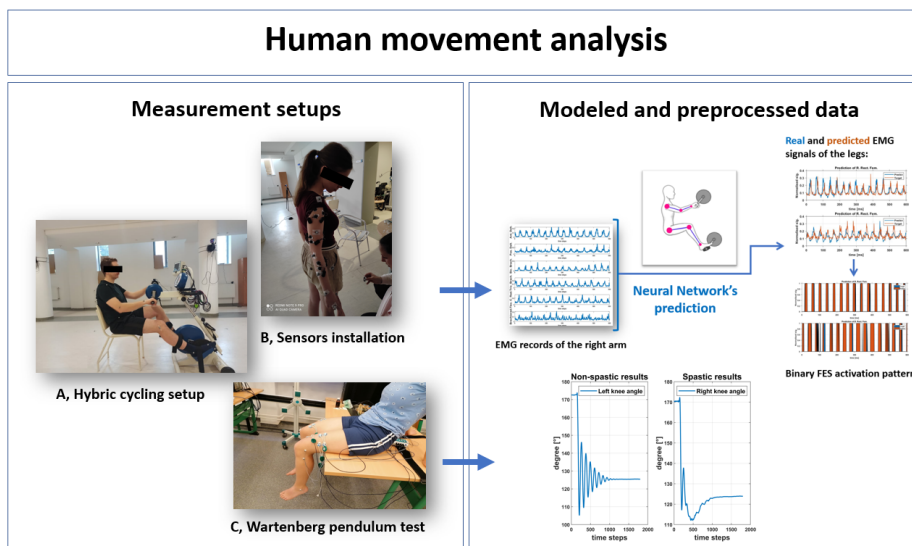


Fig. 1. Two measurement setups for human movement analysis; **Left**: A: measurement setup for hybrid cycling, B: arrangement of EMG and kinematic markers, C: Wartenberg pendulum test. **Upper right**: hybrid cycling-based FES control. Prediction of right thigh muscle EMG from right upper limb EMG signals; simulated FES control signals with thresholding. Lower right: transient changes in knee angle (left: healthy, right: spinal cord injury).

Mutations affecting the binding site of the Shank PDZ domain

Anna SÁNTA

(Supervisor: Zoltán GÁSPÁRI)

Pázmány Péter Catholic University, Faculty of Information Technology and Bionics

50/a Práter street, 1083 Budapest, Hungary

santa.anna@itk.ppke.hu

Abstract—Shank proteins are important scaffolding proteins found in the postsynaptic density (PSD), the phase separated structure responsible for the processing of incoming signals in glutamatergic synapses. In the course of this study, disease associated binding site mutations of the PDZ domain of Shank1 were investigated experimentally.

Keywords—postsynaptic density; protein interaction; colorectal cancer; oncogene; PDZ

I. INTRODUCTION

The postsynaptic density (PSD) is a disk-shaped, phase separated organelle located in glutamatergic synapses in the central nervous system. Shank proteins are a family of scaffolding proteins with a crucial role in holding this system together, participating in the series of interactions connecting membrane-embedded receptors with the cytoskeleton. [1] All members of the Shank family contain a conserved PDZ domain that is also found in all splice variant isoforms. The domain is highly promiscuous, but its main interaction partner, the C-terminal of GKAP, binds it with an over 10-fold stronger affinity than others. [2] While the Shank family mostly associated with autism spectrum disorders, expression abnormalities, and some point mutations of the PDZ had been found in various types of cancers. [3] [4] Besides the PSD, some isoforms of Shank proteins are expressed ubiquitously. There is also an SH3 domain, another common protein-protein interaction domain located adjacent to the PDZ, which is likely to be cooperating during the GKAP interaction. A shifting of preferences between different binding partners of the PDZ domain therefore might contribute to the disruption of signaling pathways and through that, cancer development. For this study, three point mutations of the binding site of Shank1-PDZ were picked from the COSMIC database. [5] These mutations are among the most common missense mutations of this domain.

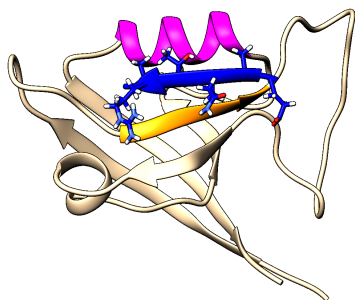


Fig. 1. Structure of the Shank1 PDZ. The GKAP C-terminal binding motif is drawn in blue. β B and α B are highlighted with yellow and magenta respectively. The image was created in Chimera.

II. MATERIALS AND METHODS

Proteins were produced and purified as described earlier. [6] In vitro mutagenesis of the cDNA containing plasmid was used to produce the mutant constructs. The TECAN Spark 20M plate reader was used for fluorescence polarization (FP) experiments. Results were analyzed in Microsoft Excel. Biolayer interferometry (BLI) was performed on a Fortebio BLItz device, using NTA coated probes. Peptides labelled with fluorescein were synthesized by BioBasic.

III. RESULTS

BLI on the WT construct and the three point mutants was performed, and relative binding affinities were calculated. All three mutants were found to have decreased binding affinity compared to WT. With FP, two dilution series were measured for each mutant. Results align with those measured with BLI. The K_d value obtained for WT is in the same order of magnitude as seen in literature previously, and measured with ITC in a previous study.

IV. DISCUSSION

It was confirmed that the mutations change binding affinity, as expected. More studies with different methods and binding partners are in progress.

ACKNOWLEDGEMENTS

The author thanks Bálint Péterfia for initiating the point mutant studies, and supervisor Zoltán Gáspári for guidance.

REFERENCES

- [1] C. Verpelli, C. Heise, and C. Sala, "Structural and functional organization of the postsynaptic density," *The Synapse: Structure and Function*, pp. 129–153, 12 2013.
- [2] M. Zeng, Y. Shang, T. Guo, Q. He, W. H. Yung, K. Liu, and M. Zhang, "A binding site outside the canonical PDZ domain determines the specific interaction between Shank and SAPAP and their function," *Proc. Natl. Acad. Sci. U.S.A.*, vol. 113, pp. E3081–3090, May 2016.
- [3] C. S. Leblond, C. Nava, A. Polge, J. Gauthier, G. Huguet, R. Delorme, T. Bourgeron, *et al.*, "Meta-analysis of SHANK Mutations in Autism Spectrum Disorders: a gradient of severity in cognitive impairments," *PLoS Genet.*, vol. 10, p. e1004580, Sep 2014.
- [4] L. Wang, Y. Lv, and G. Liu, "The roles of SHANK1 in the development of colon cancer," *Cell Biochemistry and Function*, vol. 38, pp. 669–675, July 2020.
- [5] J. G. Tate, S. Bamford, H. C. Jubb, Z. Sondka, D. M. Beare, N. Bindal, H. Boutselakis, C. G. Cole, C. Creatore, E. Dawson, P. Fish, B. Harsha, C. Hathaway, S. C. Jupe, C. Y. Kok, K. Noble, L. Ponting, C. C. Ramshaw, C. E. Rye, H. E. Speedy, R. Stefancsik, S. L. Thompson, S. Wang, S. Ward, P. J. Campbell, and S. A. Forbes, "COSMIC: the Catalogue Of Somatic Mutations In Cancer," *Nucleic Acids Research*, vol. 47, pp. D941–D947, 10 2018.
- [6] A. Sánta, "Structural characterization and interactions of Shank, a postsynaptic scaffold protein," *PHD PROCEEDINGS ANNUAL ISSUES OF THE DOCTORAL SCHOOL FACULTY OF INFORMATION TECHNOLOGY AND BIONICS*, vol. 15, p. 101, 2020.

Thermal-based Neuromodulation in a Penicillin-induced acute epilepsy model

Ágnes SZABÓ

(Supervisor: Zoltán FEKETE)

Pázmány Péter Catholic University, Faculty of Information Technology and Bionics

50/a Práter street, 1083 Budapest, Hungary

szabo.agnes@itk.ppke.hu

Abstract—Epilepsy is a heterogeneous neurological disorder, characterized by recurrent unprovoked seizures. During epileptic seizures, the neurons are activated abnormally, with a high level of synchronization. Up to 30% of the patient are not responding to the medical treatment. Some of these cases are inoperable because the epileptic focus is in a vital area of the brain. An alternative solution is a thermal neuromodulation. In this paper, we investigate the effects of infrared light emitted optrode on penicillin-induced rat epilepsy model.

Keywords-Epilepsy; neuromodulation; electrocorticogram

I. INTRODUCTION

During neuromodulation the behavior of the neurons is manipulated, altering their biochemical processes or their electric signals. The optically induced thermal modulation achieves rapid heating through the targeting of near-infrared laser light, therefore the technique is often referred to as infrared neuromodulation (INM). In the case of infrared neuromodulation, the cellular activity is controlled through the elevation of temperature in part of the target tissue[1]. INM uses pulsed or continuous-wave infrared light to generate highly controlled temperature changes in neural tissue, that can lead to excitation or inhibition of the neurons [2].

Based on intracranial pre-surgical studies, epileptic seizures can be separated into five main phases: seizure onset, pre-ictal, ictal, interictal, and post-ictal. In this study, interictal spikes are examined and captured with electrocorticogram during infrared stimulation by optrode. Electrocorticography (ECoG), or intracranial EEG, is a recording method when the electrode array captures the neural activities directly from the external surface of the cerebral cortex. Optrode is an optical stimulation microdevice, mostly with an integrated optical fiber.

II. MATERIALS AND METHODS

ECoG signals are recorded in penicillin induced, anaesthetized rats. Optrode device is used to induce the heat irradiation within neocortex. After preprocessing of the data, interictal spikes are detected and classified. To investigate the impact of thermal-based neuromodulation, the morphological shape and inducing rate of interictal spikes are examined. We test continuous and pulsed-wave stimulations with different frequencies.

III. DISCUSSION

During this project, our goal is to investigate the effects of the neuromodulation on penicillin-induced epilepsy model. The research focuses on the number of interictal spikes, and their length. Our preliminary results suggest that the used infrared neuromodulation has a mitigation effect on interictal spikes.

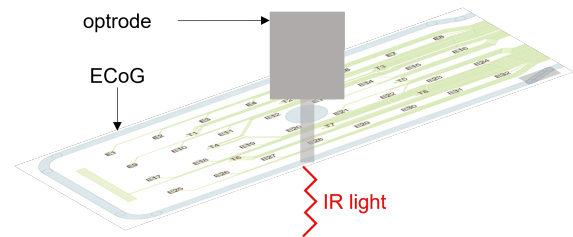


Fig. 1. Experimental setup. The two devices are the optrode, emitting the infrared light and the ECoG, recording the neural activities.

ACKNOWLEDGEMENTS

This research was supported by the ÚNKP-21-3 New National Excellence Program Of The Ministry For Innovation And Technology From The Source Of The National Research, Development And Innovation Fund.

REFERENCES

- [1] Fekete, Z., Horváth, Á. C., Zátanyi, A. , *Infrared neuromodulation: a neuroengineering perspective.*, Journal of Neural Engineering, 17(5), 051003. 2020.
- [2] Horváth, Á. C., Borbély, S., Boros, Ö. C., Komáromi, L., Koppa, P., Barthó, P., Fekete, Z., *Infrared neural stimulation and inhibition using an implantable silicon photonic microdevice.*, Microsystems and nanoengineering, 6(1), 1-12. 2020.

Examination of protein phase separation via experimental and computational methods

András László SZABÓ

(Supervisor: Zoltán GÁSPÁRI)

Pázmány Péter Catholic University, Faculty of Information Technology and Bionics

50/a Práter street, 1083 Budapest, Hungary

szabo.andras.laszlo@itk.ppke.hu

Abstract—Protein phase separation is a complex mediatory mechanism in various cellular processes, resulting in the formation of membrane-less organelles that are essential for the proper function of postsynaptic densities. My studies have so far revealed correlations between liquid-liquid phase separation and certain charged sequence motifs, while my current work set out to develop an experimental procedure to examine the phenomenon via microfluidics and fluorescent microscopy.

Keywords—protein phase separation; charge-dense regions; microfluidics; fluorescent microscopy

I. INTRODUCTION

Synaptic transmissions provide interneural connections that are not just highly versatile but also change continuously. These constant changes in the strength of synaptic transmissions, as well as more permanent alterations such as long-term potentiation and depression, are strongly coupled to the structural organization of the postsynaptic density (PSD). An increasing amount of experimental evidence shows that the internal dynamics of PSDs is heavily influenced by protein phase separation that leads to the formation of membrane-less organelles (MLOs). [1] The computational part of my work investigates the correlations between liquid-liquid phase separation (LLPS) and certain protein regions with charged residues, such as single α -helices (SAHs). The inspiration for the project came from my supervisor who pointed out that RNA-binding proteins exhibit a higher propensity towards LLPS, while they also often contain SAHs. The experimental part of my studies aims to determine the hydrodynamic diameters of fluorescent particles via their diffusion coefficients. This method was utilized by Arosio et al. to differentiate between nanobodies, α -Synuclein fibrils, and nanobodies with α -Synuclein fibrils attached to their surfaces. [2]

II. METHODS

SAHs were detected by the FT-CHARGE algorithm of the CSAH webservice, while other charge-dense regions (CDRs) were investigated with custom MatLAB scripts. [3] Several online databases provided insight into the LLPS-association of human proteins. Correlation between the traits of LLPS and special sequence motifs were examined via Fisher's exact test of independence. The general process for the measurement of diffusion coefficients can be broken down into three steps. First, fluorescent microspheres of various sizes are to be measured in the microfluidic system to gain insight into their diffusion profiles. These profiles would provide benchmarks for the "calibration" of a simulation that mimics the laminar flow within the channel. Second, the appropriately calibrated simulation is used to generate a vast library of diffusion profiles in order to cover most of the particle size compositions

that we may encounter with proteins. Finally, the system is used to measure the profiles of various protein solution and the library is used to determine its approximate composition.

III. RESULTS

A high through-put approach was developed for the recognition of specific sequence motifs, and together with the FT-CHARGE algorithm multiple libraries were assembled from the gathered regions. Their plausible contribution to LLPS was analysed in detail, and an article was published about the results. [4] Preliminary experiments have begun to find an optimal layout for the microfluidic device which should facilitate the focusing of the analyte solution, followed by the diffusion of the particles within.

ACKNOWLEDGEMENT

This research was supported by the National Research, Development and Innovation Office through the grant TKP2021-EGA-42.

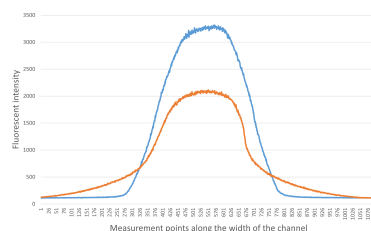


Fig. 1. Distribution of fluorescent microspheres along the width of the channel, as revealed by the fluorescent intensity profiles. The blue diagram shows the intensity profile at the beginning of the channel, while the orange diagram displays fluorescent intensity at the end. It is clearly visible that particle diffusion resulted in a more even, less focused distribution towards the end of the channel.

REFERENCES

- [1] Z. Feng, X. Chen, M. Zeng, and M. Zhang, "Phase separation as a mechanism for assembling dynamic postsynaptic density signalling complexes," *Current Opinion in Neurobiology*, vol. 57, pp. 1–8, Aug. 2019.
- [2] P. Arosio, T. Müller, L. Rajah, E. V. Yates, F. A. Aprile, Y. Zhang, S. I. Cohen, D. A. White, T. W. Herling, E. J. De Genst, and et al., "Microfluidic diffusion analysis of the sizes and interactions of proteins under native solution conditions," *ACS Nano*, vol. 10, no. 1, p. 333–341, 2015.
- [3] Z. Gáspári, D. Süveges, A. Perczel, L. Nyitrai, and G. Tóth, "Charged single alpha-helices in proteomes revealed by a consensus prediction approach," *Biochimica Et Biophysica Acta*, vol. 1824, pp. 637–646, Apr. 2012.
- [4] A. L. Szabó, A. Sánta, R. Pancsa, and Z. Gáspári, "Charged sequence motifs increase the propensity towards liquid-liquid phase separation," *FEBS Letters*, vol. 596, no. 8, p. 1013–1028, 2022.

Prediction of Alzheimer’s disease using magnetic resonance imaging

János SZALMA

(Supervisor: Béla WEISS)

Pázmány Péter Catholic University, Faculty of Information Technology and Bionics

50/a Práter street, 1083 Budapest, Hungary

szalma.janos@itk.ppke.hu

Abstract—Alzheimer’s disease (AD), the most common form of dementia is affecting 44 million people. Early prediction using magnetic resonance imaging (MRI) and suitable intervention could prolong the onset of the disease and improve the quality of life of people affected by it, while the quality control of the MRI records could further improve the prediction. I utilized the TADPOLE challenge dataset consisting of patients with normal cognition, mild cognitive impairment and AD together with a dataset consisting of MRI scans with different amount of motion artefacts. To classify diagnostic labels and image quality a linear support vector machine and an extreme gradient boosting ensemble was considered. While for diagnostic label classification an accuracy of 60 % could be achieved, on the image quality classification the best performing model achieved an 84 % accuracy. In both cases the thickness of the entorhinal cortex was found to be one of the most influential features.

I. INTRODUCTION

Alzheimer’s disease (AD) is a neurodegenerative disease, the most common form of dementia is affecting 44 million people. AD is a non curable, heterogenous disease and as a result, much work has gone into developing early detection strategies using MRI, especially at pre-symptomatic stages, in order to delay or prevent disease progression. When the MRI data is of poor quality, image analysis can lead to incorrect results. Additionally, obtaining very large samples make eye assessment of each image impractical and introduce the risk of site variability. As a result, completely automated, robust, and minimally biased quality control (QC) processes are required.

II. MATERIALS AND METHODS

I utilized the TADPOLE challenge dataset consisting of 1667 patients with cognitive normal (CN), mild cognitive impairment (MCI) and with Alzheimer’s disease (AD). In this study only MRI region of interest (ROI) measures of brain volumes, cortical thicknesses and surface areas were used together with demographic information such as age and gender. For the image quality classification task I utilized 4 databases. Overall this whole dataset contained 2328 MRI records from 1911 participants. In both the diagnostic label and the image quality classification FreeSurfer was utilized to perform the segmentation of all T1w images. Image quality was scored on a scale from 1 to 4 (best to worst), reflecting the amount of noise present before merging labels 1,2 and 3. To predict future diagnosis two classifiers were considered: linear Support Vector Machine (SVM) and an eXtreme Gradient Boosting ensemble (XGBoost), while feature selection was performed using Elastic Net. Both paradigms were evaluated using a 10-fold stratified nested cross-validation. Individual feature contributions were assessed using individual classification accuracy, selection frequency, and the SHAP values.

III. RESULTS AND DISCUSSION

For the diagnostic label classification task a maximal classification accuracy of 60 % was reached using a SVM. While both classifiers can predict patients with stable Alzheimer’s disease more than 83 % accuracy and stable cognitive normal patients with at least 70 % accuracy they fail to detect patients with stable mild cognitive impairment or patients progressing from a cognitively normal state (see Fig. 1). Regarding image

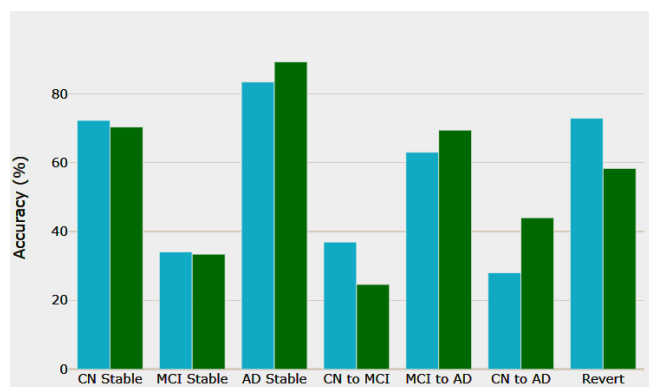


Fig. 1. Classification accuracy of linear SVM (blue) and XGBoost (green) classifiers for stable and progressive disease state changes.

quality, linear SVM with feature selection could achieve the best classification accuracy of 84 %. In both classification tasks, linear SVM outperformed the XGBoost classifier. In the case of the diagnostic classification the most predictive brain areas were the entorhinal cortex, amygdala and hippocampus, while the time passed between the MRI scan and the diagnosis and the age of patient were also among the most important features. Furthermore, the overall most influential area was the hippocampus and individually no feature reached a 50 % classification accuracy. Considering the SHAP values of the best image quality classifier the amount of surface holes present was the most significant predictor together with the entorhinal thickness. The prediction pipeline presented here could be further improved by more complex imputation methods, hyperparameter optimization and the addition of other feature modalities.

REFERENCES

- [1] Castellani, R. J., Rolston, R. K., and Smith, M. A. (2010). Alzheimer disease. *Disease-a-month: DM*, 56(9), 484.
- [2] Marinescu, R. V., Oxtoby, N. P., Young, A. L., Bron, E. E., Toga, A. W., Weiner, M. W., ... and Alexander, D. C. (2018). TADPOLE challenge: Prediction of longitudinal evolution in Alzheimer’s disease. arXiv preprint arXiv:1805.03909.

Mechanisms of burst firing in hippocampal CA1 pyramidal cells

Luca TAR

(Supervisors: Szabolcs KÁLI, Tamás FREUND)

Pázmány Péter Catholic University, Faculty of Information Technology and Bionics

50/a Práter street, 1083 Budapest, Hungary

tar.luca@itk.ppke.hu

Keywords-hippocampus; pyramidal cell; burst firing

I. SUMMARY

The downside of implementing new channels models, that is makes model simulations to run much longer, so the required time for parameter tuning greatly increased. I tried to tune 20 different parameters at once, which would require bigger population and more generations to converge to an acceptable result and to reduce the standard deviation of parameters between runs from different random seeds. To resolve this issue I used the Neuroscience Gateway supercomputer that made our simulations much faster.

There were several different approaches to take the dendritic spines into account, but the most computationally efficient way appeared to be a correction with the F-factor. The F-factor gives us the increase of the membrane area on a unit length, then the leak conductance and the capacity has to be multiplied by it.[1] The spines can also be modelled explicitly. The geometry was taken from Harnett et al.[2].

I got the right algorithms and boundaries for the parameters I got results good enough to test the dendritic integration of this uniquely detailed state of the art CA1 pyramidal cell model, and can predict the mechanisms behind the different dendritic phenomena. It turned out that for burst firing I had to adjust the maximal conductance of the R-type calcium channel by hand tuning, because somatic behavior could not constrain this parameter and with the current state of Neuroptimus we could not simultaneously optimize our model to somatic features and burst-firing. I could create models that performed good on all the HippoUnit[3] tests (except the Depolarization Block test).

I found that the sigmoid R-type distribution with a very steep slope was the most promising. I managed to create burst firing with little or no influence on the somatic response to current step protocols. Biologically a sigmoid distribution would make sense, but it is also hypothesised from Yasuda et al.[4] that R-type calcium channels are only present on the dendritic spines. It seemed more biologically realistic, if the increment in the maximal conductance of these channels were dendrite-type specific. When I increased the amount of the R-type calcium channels only on the tuft dendrites and let it be uniform everywhere else I could also make the model burst without influencing the somatic behavior. I multiplied the initial amount with many different multipliers and based on the validation the amount of the R-type calcium channels of the tuft should be 5-6 times higher than everywhere else. This way we also got satisfying results on the new Pathway interaction test, without spoiling other behaviors.

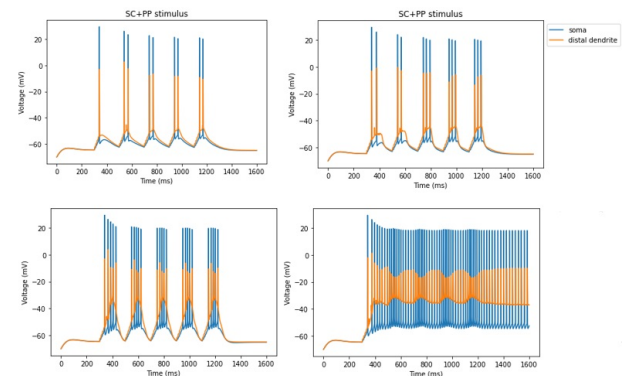


Fig. 1. We chose a model that performed well on most of the HippoUnit tests, however it did not capture the burst behavior during the Pathway interaction test due to the low amount of initial R-type calcium channels. We increased the R-type calcium channel only on the tuft dendrites of the model (original response, 5x, 10x and 15x on the figures) to see if we can make the model burst without altering the somatic behavior to standard square current step protocols.

II. ACKNOWLEDGEMENT

I thank my supervisor Szabolcs Káli and Sára Sára for their support and contribution.

REFERENCES

- [1] M. Rapp, Y. Yarom, and I. Segev, "The impact of parallel fiber background activity on the cable properties of cerebellar purkinje cells," *Neural Computation*, vol. 4, no. 4, pp. 518–533, 1992. [Online]. Available: <https://doi.org/10.1162/neco.1992.4.4.518>
- [2] M. T. Harnett, J. K. Makara, N. Spruston, W. L. Kath, and J. C. Magee, "Synaptic amplification by dendritic spines enhances input cooperativity," *Nature*, vol. 491, p. 599–602, 2012.
- [3] S. Sára, C. A. Rössert, S. Appukuttan, R. Migliore, P. Vitale, C. A. Lupascu, L. L. Bologna, W. Van Geit, A. Romani, A. P. Davison, E. Muller, T. F. Freund, and S. Káli, "Hippounit: A software tool for the automated testing and systematic comparison of detailed models of hippocampal neurons based on electrophysiological data," *PLoS Computational Biology*, vol. 17, no. 1, pp. 1–38, 01 2021. [Online]. Available: <https://doi.org/10.1371/journal.pcbi.1008114>
- [4] R. Yasuda, B. Sabatini, and K. Svoboda, "Plasticity of calcium channels in dendritic spines," *Nature Neuroscience*, vol. 6, pp. 948–955, 2003. [Online]. Available: <https://www.nature.com/articles/nn1112#citeas>

Qualitative analysis of generalized ribosome flows

Mihály András VÁGHY

(Supervisors: Mihály KOVÁCS, Gábor SZEDERKÉNYI)

Pázmány Péter Catholic University, Faculty of Information Technology and Bionics

50/a Práter street, 1083 Budapest, Hungary

vaghy.mihaly.andras@itk.ppke.hu

This progress report is based on [1]. We study systems consisting of a set of interconnected compartments and objects (e.g. ribosomes, molecules, vehicles etc.) moving between them. These models with strongly connected compartmental topology have a wide variety of advantageous properties such as persistence or ℓ^1 non-expansion [2]. We focus on so-called generalized ribosome flows introduced in [3] where we give a Hamiltonian representation as well. These models can formally be obtained as finite volume discretization of conservation laws [4].

Consider the set $Q = \{q_1, q_2, \dots, q_m\}$ of compartments and the set $A \subset Q \times Q$ of transitions, where $(q_i, q_j) \in A$ represents a transition from compartment q_i into q_j . The directed graph given by $D = (Q, A)$ is the compartmental graph of the model. Let $I_m = \{1, 2, \dots, m\}$. We introduce the sets of donors and receptors for a compartment q_i , respectively, as

$$D_i = \{j \in I_m \mid (q_j, q_i) \in A\}, \quad \mathcal{R}_i = \{j \in I_m \mid (q_i, q_j) \in A\}.$$

For such a compartmental model we can assign a chemical reaction network (CRN). Let n_i and s_i denote the continuous concentration of particles and free spaces in q_i , respectively. Then the dynamics of the system is given by

$$\begin{aligned} \dot{n}_i &= \sum_{j \in D_i} \mathcal{K}_{ji}(n_j, s_i) - \sum_{j \in \mathcal{R}_i} \mathcal{K}_{ij}(n_i, s_j), \\ \dot{s}_i &= - \sum_{j \in D_i} \mathcal{K}_{ji}(n_j, s_i) + \sum_{j \in \mathcal{R}_i} \mathcal{K}_{ij}(n_i, s_j) \end{aligned} \quad (1)$$

where $\mathcal{K}_{ij}(n_i, s_j) = k_{ij} \theta_i(n_i) \nu_j(s_j)$ is the transition rate of $(q_i, q_j) \in A$.

Let $x \in \mathbb{R}^{2m}$ be such that $x_i = n_i$ and $x_{m+i} = s_i$ and define the functions $\gamma_i = \theta_i$ and $\gamma_{m+i} = \nu_i$ for $i = 1, 2, \dots, m$. Let y_i be the stoichiometric coefficient vector of complex C_i for $i = 1, 2, \dots, M$. Using these notations rewrite (1) as follows:

$$\dot{x} = \sum_{i=1}^M \sum_{j=1}^M k_{ij} \gamma^{y_i}(x) (y_j - y_i). \quad (2)$$

In this paper we consider the following entropy-like function [5]:

$$V(x, \bar{x}) = \sum_{i=1}^{2m} \int_{\bar{x}_i}^{x_i} (\log \gamma_i(s) - \log \gamma_i(\bar{x}_i)) ds \quad (3)$$

and proceed by showing that it is a Lyapunov function for (2).

As a small example, consider a compartmental model with $Q = \{q_1, q_2, q_3\}$ and $A = \{(q_1, q_2), (q_2, q_3), (q_3, q_1)\}$. We assume that $\gamma_i(r) = \frac{r}{k+r}$ with $k = 500$ and we set the capacities as $c_1 = c_2 = c_3 = 100$ and the reaction rate coefficients as $k_{12} = 80$, $k_{23} = 40$ and $k_{31} = 20$.

Figure 1 shows orbits on the level set of the first integral $H(n) = \sum_{i=1}^m n_i$ with the level curves of (3). Figure 2 shows the level curves and the vector field of the system with the unique equilibrium.

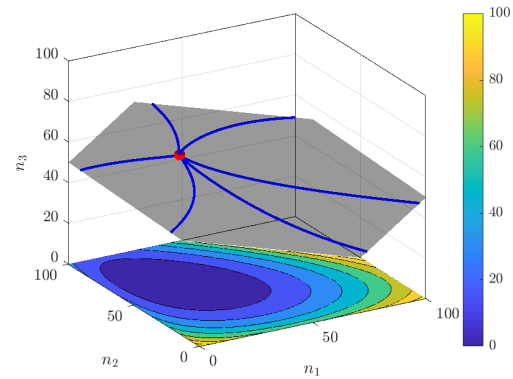


Fig. 1. Phase portrait of a compartmental model with fractional kinetics

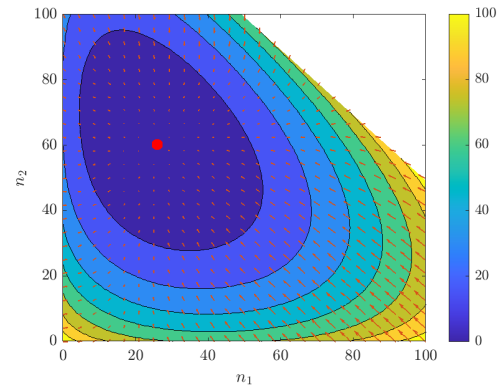


Fig. 2. Level curves of (3) for a compartmental model with fractional kinetics

REFERENCES

- [1] M. A. Vághy and G. Szederkényi, “Lyapunov stability of generalized ribosome flows,” in *4th IFAC Workshop on Thermodynamic Foundations of Mathematical Systems Theory*, 2022. Submitted.
- [2] G. Szederkényi, B. Ács, G. Liptak, and M. A. Vághy, “Persistence and stability of a class of kinetic compartmental models,” *Journal of Mathematical Chemistry*, DOI: 10.1007/s10910-022-01338-7, 2022.
- [3] M. A. Vághy and G. Szederkényi, “Hamiltonian representation of generalized ribosome flow models,” in *European Control Conference - ECC*, 2022. Accepted, to appear.
- [4] M. A. Vághy, M. Kovács, and G. Szederkényi, “Kinetic discretization of one-dimensional nonlocal flow models,” in *10th Vienna International Conference on Mathematical Modelling - MATHMOD*, 2022. Accepted, to appear.
- [5] M. Chaves, “Input-to-state stability of rate-controlled biochemical networks,” *SIAM Journal on Control and Optimization*, vol. 44, pp. 704–727, 2005.

Structural characterization of the postsynaptic Drebrin protein

Soma VARGA

(Supervisor: Bálint Ferenc PÉTERFIA)

Pázmány Péter Catholic University, Faculty of Information Technology and Bionics

50/a Práter street, 1083 Budapest, Hungary

varga.soma@itk.ppke.hu

Abstract—The postsynaptic density (PSD) of excitatory synapses is a complex network of nervous system proteins involved in postsynaptic signaling. Our research group focuses on the function of proteins in PSD organization. Drebrin is a cytoskeleton-organizing protein of the PSD and its detailed structural and functional characterization is yet to be revealed. Our aim is to use several biophysical and spectroscopic methods for obtaining atomic level information of the protein which can lead to a better understanding of Drebrin's biological role.

Keywords—PSD, Drebrin, SAH domain, Circular dichroism spectroscopy, solution NMR, protein structure, protein-protein interaction

I. INTRODUCTION

Drebrin modulates and regulates several functions of the nervous system, thereby responsible for a few molecular mechanisms involved in learning and memory [1]. The Drebrin protein is an essential component of the cytoskeleton, and its presence is required for actin polymerization of synapses and recruitment of CXCR4 chemokine receptors [2], as well as for the morphogenesis of the dendritic spine. Drebrin also plays an important role in synaptic plasticity associated with hippocampal memory and establishes several key interactions with other proteins present in PSD [3].

In this work we aim to characterize the structure of three different Drebrin regions, namely the ADFH (Actin-Depolymerizing Factor Homology) domain at the N-terminal, the SAH (Single Alpha Helix) domain which was earlier predicted with bioinformatic methods [4], and the HBMs (Homer Binding Motifs) near the C terminus.

II. METHODS

We performed the molecular cloning with pEV vectors and the expression of the corresponding constructs with our competent DH5 alpha and BL21 E. coli bacteria cells. Purification of the proteins were done by several chromatography methods, namely: IMAC (Immobilized Metal Affinity Chromatography), IEC (Ion Exchange Chromatography), and SEC (Size Exclusion Chromatography). We started the initial characterization of the successfully purified constructs with CD (Circular Dichroism) and NMR (Nuclear Magnetic Resonance) spectroscopy. Molecular interactions with other PSD proteins (mostly the Homer), will also be investigated with BLI (Biolayer Interferometry) and ITC (Isothermal Titration Calorimetry) measurements.

III. RESULTS

The preparation of the pEV plasmids for all 3 constructions was successfully accomplished. The results were checked by Sanger DNA sequencing. The expression and purification

protocols of the ADFH and SAH domains has been experimentally optimized and monitored by SDS-PAGE (Sodium Dodecyl Sulfate-Polyacrylamide Gel Electrophoresis). For characterizing the secondary protein structure of the ADFH and SAH domains, CD measurements were performed. These results were also confirmed by initial NMR measurements of unlabeled protein samples .

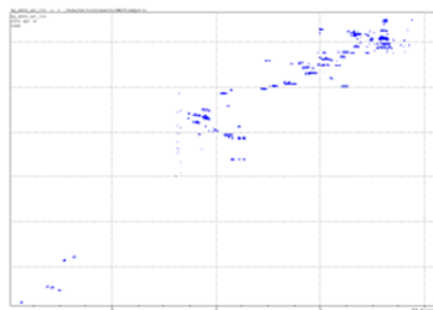


Fig. 1. HSQC NMR spectra of ADFH domain, refer to a properly folded protein with a globular structure.

ACKNOWLEDGEMENTS

I would like to thank my supervisor Dr. Bálint Ferenc Péterfia for his help and guidance with my laboratory work and to Dr. Zoltán Gáspári for his comprehensive help with my research and to Dr. Gyula Batta for performing the NMR measurements and to Dr. Viktor Farkas for helping with the CD measurements. This research was supported by the National Research, Development and Innovation Office through the grant TKP2021-EGA-42.

REFERENCES

- [1] V. M. Ho, J.-A. Lee, and K. C. Martin, "The Cell Biology of Synaptic Plasticity," *Science*, vol. 334, pp. 623–628, Nov. 2011.
- [2] M. Pérez-Martínez, M. Gordón-Alonso, J. R. Cabrero, M. Barrero-Villar, M. Rey, M. Mittelbrunn, A. Lamana, G. Morlino, C. Calabia, H. Yamazaki, T. Shirao, J. Vázquez, R. González-Amaro, E. Veiga, and F. Sánchez-Madrid, "F-actin-binding protein drebrin regulates CXCR4 recruitment to the immune synapse," *Journal of Cell Science*, vol. 123, pp. 1160–1170, Apr. 2010.
- [3] Y. Hayashi, "Drebrin-Homer Interaction at An Atomic Scale," *Structure*, vol. 27, pp. 3–5, Jan. 2019.
- [4] Á. Kovács, D. Dudola, L. Nyitray, G. Tóth, Z. Nagy, and Z. Gáspári, "Detection of single alpha-helices in large protein sequence sets using hardware acceleration," *Journal of Structural Biology*, vol. 204, pp. 109–116, Oct. 2018.

Comparative evaluation of permeability properties of a human skin equivalent and *ex vivo* human skin tissue in skin-on-a-chip microfluidic device

Zsófia VARGA-MEDVECZKY

(Supervisor: Franciska ERDŐ)

Pázmány Péter Catholic University, Faculty of Information Technology and Bionics

50/a Práter street, 1083 Budapest, Hungary

varga-medveczky.zsafia@itk.ppke.hu

Abstract—Both in the pharmaceutical and cosmetic industries, there is a growing need to develop and produce a variety of skin substituents that can properly mimic the structure and the biochemical milieu of the skin [1], furthermore, the physical and pathological processes that take place in this organ [2]. All these processes are greatly encouraged by the fact that the experimental use of animals is increasingly restricted by law for ethical reasons. As a result, various *in vitro* testing approaches are receiving increasing emphasis in the field of dermal research [1].

In this work, we developed a human skin substituent based on an electrospun membrane. Keratinocyte cells were cultured on the surface of the membrane, the confluent layer of which corresponded well to the outermost layer of the skin, the epidermis. To evaluate our human skin equivalent, we compared its permeability properties with excised human abdominal skin samples. Permeability studies were performed with topically applied caffeine cream in a skin-on-a-chip microfluidic device, the result of which revealed that caffeine shows a similar transport kinetics for the two diffusion samples. Our results confirm that the human skin equivalent developed in the present work, although a substantially simplified model, is suitable for modelling the epidermis, and its further development can be used to create additional models that have even more similar structure to the human skin [3].

Keywords—skin equivalent; 3D printed device; skin-on-a-chip; microfluidics; skin permeability; topical drug diffusion

I. INTRODUCTION

Topical drug administration offers an alternative, non-invasive drug delivery route of different active compounds through the dermal barrier to treat a variety of dermatological problems. In addition, a number of other uses, cosmetic purposes [4], [5], and therapeutic indications targeting the central nervous system are also known [3], [6].

The mapping of the physical properties, safety (irritancy, toxicity) and efficacy of the drug molecules required extensive testing [1], [3]. Testing of drugs for dermatological use is widespread in diffusion cells, the size of which has been significantly reduced due to technical advances. More and more microfluidic devices have appeared on the market in which different samples can be tested cost-effectively [7]. In parallel, the experimental use of animals is becoming increasingly stringent by law, in fact the experimental use of animals for cosmetic purposes was banned in 2013 in the European Union for ethical reasons [1], [3], which greatly accelerated the development of *in vitro* assays and various artificial skin substituents, which correspond well to the structure and the properties of the skin.



Fig. 1. A measuring system designed to investigate the permeability properties of the artificial skin equivalent [3].

During the experimental work, we systematically investigated the diffusion properties of cell-free membranes, human skin substituent and human abdominal skin tissue by examining the penetration pattern of a hydrophilic model drug molecule, caffeine in a skin-on-a-chip device. By comparing the caffeine content of perfusion samples flowing through a microfluidic diffusion chamber, we found that our human skin equivalent shows comparable caffeine transport kinetics to human skin tissue [3].

REFERENCES

- [1] I. Risueño, L. Valencia, J. L. Jorcano, and D. Velasco, "Skin-on-a-chip models: General overview and future perspectives," *APL Bioengineering*, vol. 5, p. 030901, Sept. 2021. Publisher: American Institute of Physics.
- [2] S. Moon, D. H. Kim, and J. U. Shin, "In Vitro Models Mimicking Immune Response in the Skin," *Yonsei Medical Journal*, vol. 62, no. 11, pp. 969–980, 2021.
- [3] J. Tárnoki-Zách, E. Mehes, Z. Varga-Medveczky, D. G. Isai, N. Barany, E. Bugyik, Z. Revesz, S. Paku, F. Erdo, and A. Czirok, "Development and Evaluation of a Human Skin Equivalent in a Semiautomatic Microfluidic Diffusion Chamber," *Pharmaceutics*, vol. 13, p. 910, June 2021.
- [4] F. Erdo, "3D Skin Bioprinting: A Novel Tool for Dermato-Pharmacology, -Toxicology and Drug Development," vol. 7, no. 2, pp. 76–78, 2019.
- [5] F. Farner, L. Bors, G. Bajza, G. Karvaly, I. Antal, and F. Erdő, "Validation of an In vitro-in vivo Assay System for Evaluation of Transdermal Delivery of Caffeine," *Drug Delivery Letters*, vol. 9, pp. 15–20, Feb. 2019.
- [6] Z. Varga-Medveczky, D. Kocsis, M. B. Naszladly, K. Fónagy, and F. Erdő, "Skin-on-a-Chip Technology for Testing Transdermal Drug Delivery-Starting Points and Recent Developments," *Pharmaceutics*, vol. 13, no. 11, p. 1852, 2021.
- [7] J. Pomozhi, S. Dhinakaran, Z. Varga-Medveczky, K. Fónagy, L. A. Bors, K. Iván, and F. Erdő, "Development of Skin-On-A-Chip Platforms for Different Utilizations: Factors to Be Considered," *Micromachines*, vol. 12, p. 294, Mar. 2021.

Complexomic simulations of neurodegenerative diseases

Áron WEBER

(Supervisor: Attila CSIKÁSZ-NAGY)

Pázmány Péter Catholic University, Faculty of Information Technology and Bionics

50/a Práter street, 1083 Budapest, Hungary

weber.aron@itk.ppke.hu

Abstract—Neurodegenerative diseases incur a significant reduction on one’s quality of life, and in turn, provide a significant burden on both the individual and society. Many of these are characterised by misfolding and aggregation of specific proteins, however, to this point, no surefire treatment has been established for such illnesses. Throughout my research project, I aim to run computational simulations of cells affected by these conditions, in an attempt to elucidate possible pathways that can be exploited in the treatment of such diseases. In the first part of this research, I have investigated an *in vitro* approach to model these diseases in yeast, and analysed the proteomic data coming from it. In the near future, I will also try to replicate these experiments *in-silico*, using the Cytocast Cell Simulator algorithm.

Keywords-neurodegenerative diseases; complexomics; computational simulation

SUMMARY

Neurodegenerative diseases pose a significant burden on both individual and society, especially in aging populations, with prevalence rates estimated to be as high as 20-50% of those aged 80 or older in the case of Alzheimer’s disease. Despite of this, to this date, no effective treatment options are available. It is well-known however, that a handful of these diseases exhibit the misfolding and build-up into aggregates of so-called aggregation-prone proteins, APPs. The malfunctioning APPs themselves are indicative of the disease, so for example amyloid beta is associated with Alzheimer’s disease, while the product of the huntingtin gene is involved in Huntington’s. Therefore, examining the cellular responses to the presence of these malfunctioning proteins can help us illuminate the exact mechanisms between these illnesses, potentially leading the way to new treatment options.

The main goal of this work was to attempt an *in-silico* reproduction of the experiment described in the paper of Melnik and colleagues [1], in which the researchers have expressed five different human aggregation-prone proteins in budding yeast cells, and then performed proteomics analyses 6, 12, 18 and 24 hours after the expression of these APPs. A brief graphical summary of the project’s intended workflow can be seen on Figure 1

During my work, I have collected the experimental data from [1] and converted the relative protein expression changes into absolute measures of protein abundance, to be used for the complexomic simulations. I have also examined three methods aimed at predicting which yeast proteins the aforementioned APPs may be able to interact with. Furthermore, I have performed some rudimentary analysis of the proteomics data of the aforementioned article using the Gene Ontology (GO) resource - first, I have performed GO enrichment analysis, to

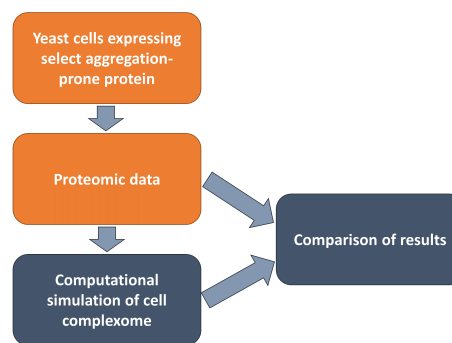


Fig. 1. Graphical representation of the major steps of the research project.

see which GO terms associated to proteins with an altered expression may be over- or underrepresented in these experiments. As the second part of this, I have queried which protein complexes these under-/overexpressed proteins may be able to form - this is to aid the selection of protein complexes of interest as soon as complexomic simulation data is available. While the analyses were performed were rather rudimentary, they were still able to uncover some pathways and protein complexes that may play a role in the pathophysiology of these diseases.

ACKNOWLEDGEMENTS

This work was done using the resources of Cytocast Hungary Kft.

REFERENCES

- [1] A. Melnik, V. Cappelletti, F. Vaggi, I. Piazza, M. Tognetti, C. Schwarz, G. Cereghetti, M. A. Ahmed, M. Soste, K. Matlack, N. de Souza, A. Csikasz-Nagy, and P. Picotti, “Comparative analysis of the intracellular responses to disease-related aggregation-prone proteins,” *Journal of Proteomics*, vol. 225, p. 103862, Aug 2020.
- [2] H. Yang and H. Hu, “Sequestration of cellular interacting partners by protein aggregates: implication in a loss-of-function pathology,” *The FEBS Journal*, vol. 283, p. 3705–3717, Oct 2016.
- [3] M. G. Erkkinen, M.-O. Kim, and M. D. Geschwind, “Clinical neurology and epidemiology of the major neurodegenerative diseases,” *Cold Spring Harbor Perspectives in Biology*, vol. 10, p. a033118, Apr 2018.
- [4] C. Hetz and S. Saxena, “Er stress and the unfolded protein response in neurodegeneration,” *Nature Reviews Neurology*, vol. 13, p. 477–491, Aug 2017.
- [5] S.-A. Lee, C.-h. Chan, C.-H. Tsai, J.-M. Lai, F.-S. Wang, C.-Y. Kao, and C.-Y. F. Huang, “Ortholog-based protein-protein interaction prediction and its application to inter-species interactions,” *BMC Bioinformatics*, vol. 9, p. S11, Dec 2008.

PROGRAM 2
COMPUTER TECHNOLOGY BASED ON
MANY-CORE PROCESSOR CHIPS, VIRTUAL
CELLULAR COMPUTERS, SENSORY AND
MOTORIC ANALOG COMPUTERS

Head: Péter SZOLGAY

Fiber Photometry: a way to look inside the brain

Boldizsár Zsolt BALOG

(Supervisors: Gábor NYIRI, György CSEREY)

Pázmány Péter Catholic University, Faculty of Information Technology and Bionics

50/a Práter street, 1083 Budapest, Hungary

balog.boldizsar.zsolt@itk.ppke.hu

Abstract—Experiments in neuroscience have a crucial role in understanding brain physiology and pathology. An emerging technique, fiber photometry allows researchers to measure the activity of specific nuclei, neurons, or neural pathways during behavioral experiments. This article describes fiber photometry data acquisition, data processing, use cases and the most recent developments in the field.

Keywords—fiber photometry; survey

I. INTRODUCTION

In the PhD proceedings journal of last year, I wrote about the behavior analysis of laboratory mice [1]. This year, I write about a technique that researchers can use to determine, how and when neuronal activity is correlated with the movement and the behavior of the animals, typically in mice. Genetic tools can alter neurons, so that they can create a fluorescence signal exactly when they are active. Fiber photometry allows measuring this fluorescence through an optic fiber.

II. FIBER PHOTOMETRY TECHNOLOGY

The usual procedure to do a fiber photometry experiment is as follows. Genetically engineered, harmless viruses are injected into the correct anatomical location to express an inducible fluorophore in the neurons of interest. This surgery is followed by a few weeks long rest that lets the virus express the key proteins and helps the recovery of mice. Then a second surgery is done that aims implanting an optic fiber above the infected cells. After a second recovery period, mice are ready for the measurements.

The purpose of fiber photometry is analyzing neural activity. When cells are active, the intracellular Ca^{2+} concentration increases. The injected viruses express normally not fluorescent proteins, that become fluorescent at high Ca^{2+} concentrations. When we activate these proteins with their excitation wavelength, the fluorescence response can be measured, and it will be possible to obtain information about cell activity.

These measurements suffer from movement artifacts, so a control signal is necessary. This signal is Ca^{2+} concentration independent (also termed isosbestic). In practice, researchers can use a simple fluorescent protein (e. g. mCherry), but measurements using a GCaMP protein (green fluorescent protein, calmodulin, M13 peptide) do not need a second protein. GCaMP's fluorescence is Ca^{2+} concentration dependent at the 465 nm wavelength excitation light, however, with excitation at 405 nm, its fluorescence is Ca^{2+} concentration independent.

A typical fiber photometry setup using GCaMP is illustrated in Figure 1. The data acquisition controller unit creates the driver signals for the light sources of both the Ca^{2+} dependent and the independent light sources. Using dichroic mirrors and a single optic fiber the excitation and the emission light are

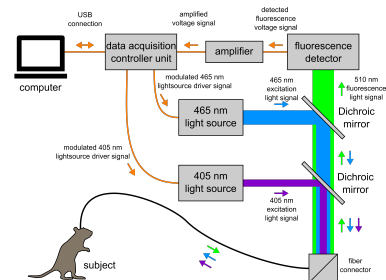


Fig. 1. Fiber photometry system setup.

directed to the mouse and back to the fluorescence detector. The light sensor converts the emission light to a voltage signal, that is amplified, digitized, and recorded for post hoc analysis. The Ca^{2+} ion concentration is usually estimated by linearly fitting (shifting and scaling the isosbestic to the Ca^{2+} dependent signal and then using Equation 1.

$$\frac{\Delta F}{F_0} = \frac{\text{Ca}^{2+} \text{ dependent signal} - \text{fitted isosbestic signal}}{\text{mean}(\text{Ca}^{2+} \text{ dependent signal})} \quad [2] \quad (1)$$

III. FURTHER DEVELOPMENTS IN FIBER PHOTOMETRY

As the methodology of fiber photometry had been more widely recognized, research groups and companies developed a wireless fiber photometry device [3], technologies to measure more, than one location via a single fiber (depth resolved technique) [4] and a lot of effort was put into developing a wide variety of sensors to detect not only Ca^{2+} signals, but neurotransmitters as well [5].

ACKNOWLEDGEMENTS

This research was supported by the National Research, Development and Innovation Office through the grant TKP2021-NVA-27.

REFERENCES

- [1] B. Z. Balog, G. Nyiri, and G. Cserey, "Survey of motion analysis in neuroscience mouse experiments," *PhD Proceedings, Faculty of Information Technology and Bionics*, p. 41, 2021.
- [2] C. Seo, A. Guru, and A. Et, "Intense threat switches dorsal raphe serotonin neurons to a paradoxical operational mode," *Science*, vol. 363, no. 6426, pp. 538–542, 2019.
- [3] Amuza Inc, "The Wireless Way: Fiber Photometry," 2021.
- [4] F. Pisano, M. Pisanello, S. J. Lee, and A. Et, "Depth-resolved fiber photometry with a single tapered optical fiber implant," *Nature Methods*, vol. 16, no. 11, pp. 1185–1192, 2019.
- [5] A. V. Leopold, D. M. Shcherbakova, and V. V. Verkhusha, "Fluorescent Biosensors for Neurotransmission and Neuromodulation: Engineering and Applications," *Frontiers in Cellular Neuroscience*, vol. 13, p. 474, oct 2019.

Tridsolver: a scalable building block for ADI applications

Gábor Dániel BALOGH

(Supervisor: István REGULY)

Pázmány Péter Catholic University, Faculty of Information Technology and Bionics

50/a Práter street, 1083 Budapest, Hungary

balogh.gabor.daniel@itk.ppke.hu

Abstract—In this work we showcase some advantages of the Tridsolver library compared to the state-of-the-art with special focus on Alternating Direction Implicit (ADI) applications. Tridsolver is a Batch-Tridiagonal solver library, targeting large-scale systems supporting both CPU and GPU architecture. The library support fast approximate algorithms with excellent scaling and The library uses methods based on both approximate and exact algorithms. Performance comparisons with the state-of-the-art show good performance, using a large GPU cluster. We demonstrate performance in all uses that would appear in an ADI context.

Keywords—linear solvers; high performance computing

I. INTRODUCTION

Tridiagonal systems of equations arise in numerous fields, particularly as part of the numerical approximation of multidimensional Partial Differential Equation (PDEs). Many industrial and research problems use the Alternating Direction Implicit (ADI) [1] method in these fields. Tridiagonal systems are formed in these applications by solving along one of the coordinate axes - and there will be as many *independent* systems as there are discretization points along the other axes. In ADI the coefficients are calculated for each grid point, in a way that matches the underlying data structure of the application; data for the diagonals are stored contiguously in either a row-major (Z is contiguous, Y, X are strided) or more commonly a column-major (X is contiguous, Y and Z are strided) format.

To the best of our knowledge, there are no distributed batch tridiagonal solver libraries for GPUs. The cuSPARSE library provides efficient algorithms for batch tridiagonal problems in continuous and interleaved format for a single GPU. Despite supporting two memory layouts in a 3D problem, the library still requires transposition or multiple calls in some dimensions to solve the batch along some axis.

With the advent of such hardware, recent work [2] re-examined the choice between different tridiagonal solution algorithms (Thomas [3], PCR [4] and Hybrid). However, many real-world problems require such algorithms to work efficiently over multiple CPU/GPU devices due to the need for compute and memory resources beyond a single node.

In this work, we aim to extend the single node Tridsolver library to support both multi-node CPU and GPU clusters. The additional advantage of Tridsolver is that it supports solutions along all dimensions of the problem, eliminating the need for multiple library or transpose calls for the solution of a single batch.

II. CONCLUSIONS

In this report we show the performance of our new distributed memory solver library on a GPU cluster. For a

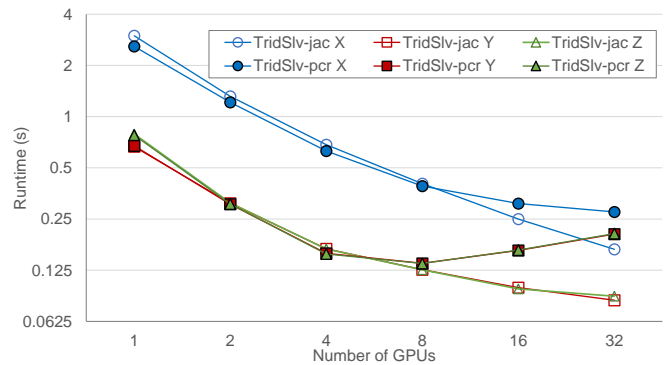


Fig. 1: Tridsolver (TridSlv), strong scaling in X,Y and Z-dims

3D ADI application tridiagonal systems would arise along each dimension in different memory layout. In this work we demonstrated performance along all three dimension of such application without the need for transpose operations.

Figure 1 shows the performance on a GPU cluster. The performance demonstrates that the Jacobi and PCR solvers (for the reduced system solve) scaled with 93% efficiency up to 4 GPUs due to the high bandwidth single node interconnect. However efficiency reduced to 55-66% for Jacobi and 39-57% for PCR beyond this point. Further optimizations with a modified Thomas-PCR forward pass algorithm improved performance with a speedup of 1.8 \times . The new tridiagonal solver library is currently available as open source software¹.

ACKNOWLEDGEMENTS

This work was supported by the ÚNKP-21-3 New National Excellence Program and the grant TKP2021-NVA-27 of the Ministry for Innovation and Technology from the source of the National Research, Development and Innovation Fund.

REFERENCES

- [1] D. W. Peaceman and H. H. Rachford, Jr, “The numerical solution of parabolic and elliptic differential equations,” *Journal of the Society for industrial and Applied Mathematics*, vol. 3, no. 1, pp. 28–41, 1955.
- [2] E. Laszlo, M. Giles, and J. Appleyard, “Manycore algorithms for batch scalar and block tridiagonal solvers,” *ACM Transactions on Mathematical Software (TOMS)*, vol. 42, no. 4, pp. 1–36, 2016.
- [3] L. Thomas, “Elliptic problems in linear differential equations over a network: Watson scientific computing laboratory,” *Columbia Univ., NY*, 1949.
- [4] W. Gander and G. H. Golub, “Cyclic reduction—history and applications,” *Scientific computing (Hong Kong, 1997)*, vol. 7385, pp. 73–86, 1997.

¹<https://github.com/OP-DSL/tridsolver/>
10.5281/zenodo.5564551

doi:

Progress report on epidemic model inversion using feedback linearization

Balázs CSUTAK

(Supervisor: Gábor SZEDERKÉNYI)

Pázmány Péter Catholic University, Faculty of Information Technology and Bionics

50/a Práter street, 1083 Budapest, Hungary

csutak.balazs@itk.ppke.hu

Abstract—In this progress report, I outline our recent results regarding the reconstruction and prediction of epidemiological data, using well known and novel estimation and control techniques from the mathematical toolbox of nonlinear dynamic systems. Using a previously published and validated nonlinear model, we transform the reconstruction into a control problem, which is solved using feedback linearization and asymptotic output tracking. The results are compared with a reconstruction created by an optimization based estimation method using stochastic model predictive control.

Keywords—epidemic, reconstruction, feedback linearization

I. INTRODUCTION

The COVID-19 pandemic is a problem we have been living with for more than two years, being a significant challenge for the economy and healthcare system of all countries around the globe. Without proper medication and vaccine available in the first months, decision-makers opted for restrictive measures aimed to slow down the transmission of the disease. To support well funded decision-making, the construction of accurate epidemic models is needed.

In this report, a new method for the estimation of the epidemic's reproduction number β is presented, which using the official hospitalization data as the only reference, transforms the computation into a nonlinear control problem. By applying a feedback linearization to the model, and setting the poles of the resulting linear system such that we achieve asymptotic output tracking, effectively an inverse of the whole nonlinear system is created.

II. NONLINEAR MODEL OF TRANSMISSION DYNAMICS

A. Model description

To incorporate the key properties of COVID-19 dynamics, I use an eight-compartment compartmental model already published in [1], and used in [2], [3] and [4]. The population of N individuals is divided into eight classes, representing the different stages of the illness, discussed in detail in the original article. The possible transitions between the compartments are illustrated in Fig. 1.

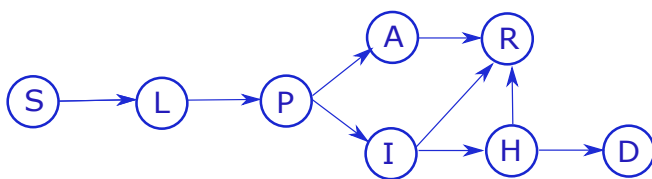


Fig. 1. Transition diagram of the disease spreading model. Characters represent compartments as explained in section II-A, arrows show direction of possible transitions.

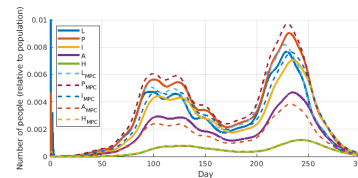


Fig. 2. Estimated trajectories

III. ESTIMATION BY CONTROL

A. Feedback linearization

Following the method described in [5], chapter 4.3, our aim is changing the variables of the nonlinear single input single output system given in the form of

$$\dot{x}(t) = f(x(t)) + g(x(t)) \cdot u(t) \quad (1a)$$

$$y(t) = h(x(t)) \quad (1b)$$

in such a way, that it takes the form of a linear, controllable system. More precisely, we are looking for a transformation $z = \Phi(x)$ and an input mapping $u(t) = a(x(t)) + b(x(t)) \cdot v(t)$, using which the dynamics of $x(t)$ in the new coordinates can be expressed as $\dot{z}(t) = Az(t) + B \cdot v(t)$. Afterwards, we can apply any closed loop control strategy suitable for a linear system to achieve the desired operation.

IV. RESULTS

For the sake of simplicity the estimation is carried out on wave 2 and 3 of Hungary, ie. the period between 1st of September, 2020 and 1st of June, 2021. The estimated trajectories can be seen in Figure 2.

ACKNOWLEDGEMENT

This research was supported by the National Research, Development and Innovation Office through the grant TKP2021-NVA-27.

REFERENCES

- [1] T. Péni, B. Csutak, G. Szederkényi, and G. Röst, “Nonlinear model predictive control with logic constraints for covid-19 management,” *Nonlinear Dynamics*, vol. 102, no. 4, pp. 1965–1986, 2020.
- [2] B. Csutak, P. Polcz, and G. Szederkényi, “Computation of covid-19 epidemiological data in hungary using dynamic model inversion,” in *2021 IEEE 15th International Symposium on Applied Computational Intelligence and Informatics (SACI)*, pp. 91–96, 2021.
- [3] B. Csutak, P. Polcz, and G. Szederkényi, “Magyarországi járványadatok elemzése rendszerelméleti megközelítéssel,” *XXXIV. Neumann Kolokvium*, 2021.
- [4] P. Polcz, B. Csutak, and G. Szederkényi, “Reconstruction of epidemiological data in hungary using stochastic model predictive control,” *Applied Sciences*, vol. 12, no. 3, 2022.
- [5] A. Isidori, *Nonlinear control systems: an introduction*. Springer, 1985.

Approaches to OpenSet Algorithms

Lóránt DAUBNER

(Supervisors: Kálmán TORNAI, Péter SZOLGAY)

Pázmány Péter Catholic University, Faculty of Information Technology and Bionics

50/a Práter street, 1083 Budapest, Hungary

daubner.lorant.szabolcs@itk.ppke.hu

Nowadays recognition algorithms based on machine learning are mainly "closed set" algorithms, which means that all testing classes should be known at training time and the set of categories should remain the same during testing phase. This could lead to false positive detection, because unknown classes are forced into any of the known categories. A more realistic scenario for object recognition is an "open set" approach, where incomplete knowledge of the world is present. [1]

If we consider locating an object of interest in an image, a negative detection is anything other than the class of interest, and in this manner the problem is much more open than closed. As a result binary classifiers should be trained with a large sampling of negative classes, if a good sampling of negative classes is possible at all.

Classifying data is a crucial task in both machine learning and object recognition. Support-vector machines (originally invented by Vladimir N. Vapnik) are linear classifiers which can be used to solve this task. SVM maps training examples to points in space and constructs a hyperplane which represents the largest separation between the two classes. [2] The familiar SVM methodology was adapted to the open set recognition problem by Schölkopf et al. [3] known as 1-class SVM. The application of 1-class SVM to problems in computer vision followed then by Chen et al. [4]

A new variant of SVM was introduced by Scheirer et al. [1] called 1-vs-Set Machine. The aim was to minimize the risk in two ways: a minimization of the positive labeled region to address open space risk (reflecting overgeneralization) combined with margin constraints to minimize empirical risk (reflecting overspecialization). [1]

The formalization of Open-set recognition inspired a number subsequent work in computer vision, thus more and more algorithms are published and available nowadays. With the development of open-set algorithms an additional question arose: whether a closed-set algorithm with stronger classifiers could perform as good as OSR. It was proven by S. Vaze et al. [5] that the closed-set and open-set performance of classifiers are strongly correlated, so the best solution could be a combination of both.

The main goal in this semester was identifying the OSR state of the art and gather knowledge about the available algorithms considering the possible improvements.

ACKNOWLEDGEMENT

This research was supported by the National Research, Development and Innovation Office through the grant TKP2021-NVA-26.

REFERENCES

- [1] W. J. Scheirer, A. Rocha, A. Sapkota, and T. E. Boulton. Towards open set recognition. *IEEE Transactions on Pattern Analysis and Machine Intelligence (T-PAMI)*, 35, July 2013.

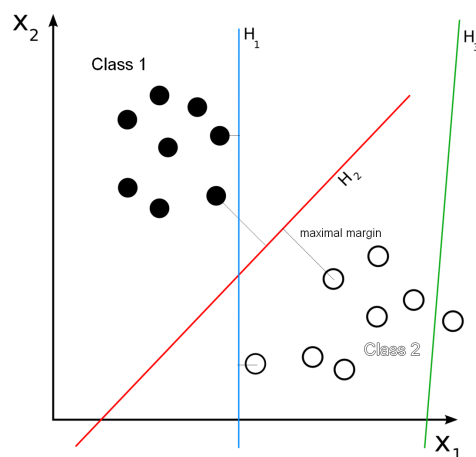


Fig. 1.
Hyperplanes constructed by SVM to separate the classes
 H_1 separates the classes but with small margin only
 H_2 separates the classes with maximal margin

- [2] James, Gareth; Witten, Daniela; Hastie, Trevor; Tibshirani, Robert. *An Introduction to Statistical Learning : with Applications in R*. New York Springer 2013. pp. 337–372.
- [3] B. Schölkopf, J. Platt, J. Shawe-Taylor, A. Smola, and R. Williamson. "Estimating the Support of a High-dimensional Distribution". *Microsoft Research, Tech. Rep. MSR-TR-99-87* 1999.
- [4] Y. Chen, X. Zhou, and T. Huang, "One-class SVM For Learning in Image Retrieval," in *IEEE Conf. on Image Processing*, 2001, pp. 34–37.
- [5] Sagar Vaze, Kai Han, Andrea Vedaldi, Andrew Zisserman. Open-Set Recognition: a Good Closed-Set Classifier is All You Need? *International Conference on Learning Representations*, 2022.

Recognition object to grasp by using a hybrid system

Attila FEJÉR

(Supervisor: Péter SZOLGAY)

Pázmány Péter Catholic University, Faculty of Information Technology and Bionics

50/a Práter street, 1083 Budapest, Hungary

fejér.attila@itk.ppke.hu

Abstract—The present paper proposes an implementation of a hybrid hardware–software system for the visual servoing of prosthetic arms. We focus on the most critical vision analysis part of the system. The prosthetic system comprises a glass-worn eye tracker and a video camera, and the task is to recognize the object to grasp. The lightweight architecture for gaze-driven object recognition has to be implemented as a wearable device with low power consumption (less than 5.6 W). The algorithmic chain comprises gaze fixations estimation and filtering, generation of candidates, and recognition, with two backbone convolutional neural networks (CNN). The time-consuming parts of the system, such as SIFT (Scale Invariant Feature Transform) detector and the backbone CNN feature extractor, are implemented in FPGA, and a new reduction layer is introduced in the object-recognition CNN to reduce the computational burden. The proposed implementation is compatible with the real-time control of the prosthetic arm.

Keywords—FPGA; computer vision; image processing

I. INTRODUCTION

The vision analysis part, which is the most critical in the whole chain of prosthesis servoing, is presented in Figure 1. The underlying hypothesis for the functioning of vision-guided neuroprostheses is that the upper limb amputee wearing the neuroprosthesis is first looking at the object they wish to grasp.

The subject is wearing a Tobii glasses device, which acquires an ego-visual scene and records gaze fixations of the subject in their coordinate system—see the left-most block in Figure 1. The recorded gaze fixations allow for roughly localizing the object of interest in video frames.

Nevertheless, visual saccades to the distractors in a visual scene, microsaccades, and initial scene exploration before the subject finds the object make these measurements noisy. Hence, two blocks of the system—gaze point alignment and gaze point noise reduction—serve to estimate the position of the gaze fixation on the object in the current ego-video frame.

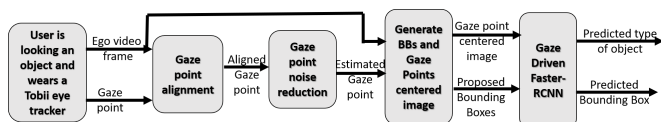


Fig. 1. The prosthetic arm visually guided system.

The gaze point alignment module aims to estimate and compensate for the ego-motion between the past frames and the current frame. For more details, see [1] and for the Scale Invariant Feature Transform algorithm see [2], [3].

The goal of the gaze point noise reduction module is to reduce the noise in the current frame. This noise can be a head motion, or a product of the user being distracted and

looking at another object for a moment. For more details, see [1], [4].

Then, the video frame is cropped around the estimated gaze point to limit the area of the object search. Finally, different object proposal bounding boxes (BBs) at different scales are generated around the point for object localization. The gaze point-centred image and the set of BB coordinates are then submitted to the gaze-driven CNN—see the right-most block in Figure 1.

The gaze-driven CNN is pre-trained on the taxonomy of objects to detect. It outputs the best score for the object class and the best-scored bounding box. When the object is localized in a video frame, the 3D position of it for prosthesis servoing can be estimated from eye tracker depth measures of gaze fixation and the coordinates of the centre of the best-scored bounding box.

The resolution of the Tobii first-person view camera is full HD (1920 × 1080 p), with a frame rate of 25 frames per second (fps).

The real-time requirement for the system in our case means that each processing step of the localization of the object of interest in the glasses-mounted camera in a current video frame has to be lower than 40 ms (the video acquisition rate), and the latency of the whole system should be lower than 100 ms to allow for mechanical servoing of the prosthetic arm [5].

In this work, we do not consider depth estimation, which is a simple regression from eye tracker gaze fixation measures—our focus is on object detection.

II. ACKNOWLEDGEMENT

External supervision by Ms Jenny Benois-Pineau is gratefully acknowledged.

REFERENCES

- [1] A. Fejér, Z. Nagy, J. Benois-Pineau, P. Szolgay, A. de Rugy, and J.-P. Domenger, “Hybrid fpga-cpu-based architecture for object recognition in visual servoing of arm prosthesis,” *Journal of Imaging*, vol. 8, no. 2, 2022.
- [2] A. Fejér, Z. Nagy, J. Benois-Pineau, P. Szolgay, A. de Rugy, and J.-P. Domenger, “Implementation of scale invariant feature transform detector on fpga for low-power wearable devices for prostheses control,” *Int J Circ Theor Appl*, vol. 49, p. 2255 – 2273, 2021.
- [3] A. Fejér, Z. Nagy, J. Benois-Pineau, P. Szolgay, A. de Rugy, and J.-P. Domenger, “Fpga-based sift implementation for wearable computing,” in *2019 IEEE 22nd International Symposium on Design and Diagnostics of Electronic Circuits Systems (DDECS)*, pp. 1–4, 2019.
- [4] A. Fejér, Z. Nagy, J. Benois-Pineau, P. Szolgay, A. de Rugy, and J.-P. Domenger, “Array computing based system for visual servoing of neuroprosthesis of upper limbs,” in *2021 17th International Workshop on Cellular Nanoscale Networks and their Applications (CNNA)*, pp. 1–5, 2021.
- [5] S. Mick, M. Lapeyre, P. Rouanet, C. Halgand, J. Benois-Pineau, F. Paquet, D. Cattaert, P.-Y. Oudeyer, and A. de Rugy, “Reachy, a 3d-printed human-like robotic arm as a testbed for human-robot control strategies,” *Frontiers in Neurobotics*, vol. 13, p. 65, 2019.

HDR reconstruction techniques for light field images

Mary GUINDY

(Supervisors: Vamsi Kiran ADHIKARLA, Péter SZOLGAY)

Pázmány Péter Catholic University, Faculty of Information Technology and Bionics

50/a Práter street, 1083 Budapest, Hungary

guindy.mary.mohsen.messak@itk.ppke.hu

Abstract—With the rapid advancements in the technological era, new displays with tremendous capabilities have been implemented. Among which are the glasses-free 3D displays called light field displays (LFDs). For these high-capable devices, the need for HDR (High Dynamic Range) images has become more demanding. While LFDs provide a sense of 3D immersion for users, HDR adds more realism to the generated results. Combining both techniques can result in a breakthrough in our technological era, however, not much work has addressed the combined technologies. In our work, we test some of the HDR reconstruction techniques on LF images, as well as, propose some techniques that could be additionally used for a better customized reconstruction process.

Keywords—HDR , LDR, light field images, LF, light fields, CNN

I. INTRODUCTION

Within the last century, two technologies have evolved: Light fields (LFs) and high dynamic range (HDR). Combining both technologies can produce powerful results as the output will provide a sense of immersion in the 3D world, in addition to adding more realism to the produced scenes. Although many techniques were implemented for HDR reconstruction, few attempts were done in the LF field. In this paper, we evaluate and discuss the results of applying conventional HDR techniques on LF images. Moreover, we introduce possible theoretical concepts that can be applied for HDR reconstruction CNNs to better fit LF images.

II. PERFORMANCE EVALUATION OF HDR TECHNIQUES ON LF IMAGES

Many methods were devised for conventional HDR image, as well as, HDR video reconstructions. Among which are the *ExpandNet* [4], *HDRDeepCNN* [3] and *DeepHDRVideo* [5]. In our work [1], we have used the *Teddy* [6] dataset for LF images, on which we tested each of the aforementioned methods. For the *DeepHDRVideo* CNN, we fed the network three images at a time as the network exploits the temporal coherence between the video frames. Among the results, *HDRDeepCNN* proved to produce the best results, while unexpectedly the *DeepHDRVideo* had inconsistencies in both color and texture. Although it was expected for video CNNs to better work for LF images due to the spatial coherence existing between the different LF images – similar to the temporal coherence between video frames–, the results were quite different from expectations. On the other hand, the *DeepHDRVideo* had the best value when using the HDR-VCP-2.2.1 metric. This work needs further investigation with more datasets to be used for testing.

III. COMBINING 2D AND 3D CNNs FOR HDR LF IMAGE RECONSTRUCTION

From the previous section, it is noted that conventional HDR CNNs can produce plausible results when applied to LF images but are still lacking in some areas. Since a single LF scene is composed of multiple LF images, the spatial coherence between these images can be exploited for a better HDR reconstruction. This can be done by applying CNN to LF images simultaneously instead of sequential application. On the other hand, the angularly selective nature of LF images can impose some challenges, however, they can convey some information about objects/ materials the scene such as specular reflections. Accordingly, it is better to create new CNNs solely for HDR LF image reconstruction or apply some modifications to the existing CNNs. Some of the key points that could be taken into account when designing the CNNs are depth maps, key point detection and global illumination [2].

IV. FUTURE WORK

In this work, we introduce the importance of HDR LF image reconstruction that could better fit many applications. Due to the lack of LF images datasets, we intend to create a synthetic dataset for further testing, in addition to applying more CNNs on LF images and modifying some of the existing ones for better output generation.

ACKNOWLEDGMENTS

This project has received funding from the European Union’s Horizon 2020 research and innovation programme under the Marie Skłodowska-Curie grant agreement No 813170 and from the National Research, Development and Innovation Office through the grant TKP2021-NVA-27. Also received funding by 2018-2.1.3-EUREKA-2018-00007 and KFI 16-1-2017-0015, NRDI Fund, Hungary.

REFERENCES

- [1] Guindy, Mary, et al. "Performance evaluation of HDR image reconstruction techniques on light field images." 2021 International Conference on 3D Immersion (IC3D). IEEE, 2021.
- [2] Guindy, Mary, et al. "Towards reconstructing HDR light fields by combining 2D and 3D CNN architectures." (2022).
- [3] Eilertsen, Gabriel, et al. "HDR image reconstruction from a single exposure using deep CNNs." *ACM transactions on graphics (TOG)* 36.6 (2017): 1-15.
- [4] Marnerides, Demetris, et al. "Expandnet: A deep convolutional neural network for high dynamic range expansion from low dynamic range content." *Computer Graphics Forum*. Vol. 37. No. 2. 2018.
- [5] Chen, Guanying, et al. "HDR video reconstruction: A coarse-to-fine network and a real-world benchmark dataset." *Proceedings of the IEEE/CVF International Conference on Computer Vision*. 2021.
- [6] Gul, M. Shahzeb Khan, et al. "A high-resolution high dynamic range light-field dataset with an application to view synthesis and tone-mapping." 2020 IEEE International Conference on Multimedia & Expo Workshops (ICMEW). IEEE, 2020.

Implementation of Memristor Cellular Nonlinear Network with non-linear template

Dániel HAJTÓ

(Supervisor: György CSEREY)

Pázmány Péter Catholic University, Faculty of Information Technology and Bionics

50/a Práter street, 1083 Budapest, Hungary

hajto.daniel@itk.ppke.hu

Abstract—Memristor Cellular Nonlinear Networks (MCNN) are an extension of the previous Cellular Nonlinear Network (CNN) computing paradigm. In this Proceedings an uncoupled, single cell MCNN circuit implementation is presented with a specific non-linear template. It is shown through measurements that a non-linear behaviour can be achieved reliably on a single MCNN cell.

Keywords—Memristor; CNN; Neuromorphic Computing

I. INTRODUCTION

The memristor is a resistive passive two-terminal device and its resistance depends on its internal state [1]. The nanoscale production of device and the non-linear, synapse-like behaviour makes the memristor an excellent candidate for neuromorph computing applications [2].

The used memristor is an emulated device using sixteen Ge_2Se_3 based memristors [7]. The memristors are interconnected in a 4-by-4 gridlike structure to make the device more robust to thermal noise. It has been shown [8] that the resulting memristor circuit can be considered a single device with an improved, more continuous characteristics.

The recently introduced Memristor Cellular Nonlinear Network [3], [4], [5] (MCNN) is an extension of the existing Cellular Nonlinear Network (CNN) computing paradigm [6].

II. CIRCUIT SCHEMATICS

The circuit schematics of the implemented single cell MCNN circuit is shown in Fig. 1.

III. RESULTS

The working principle of the non-linear template has two main consideration.

The first one: let us consider that on low voltages the memristor state does not change significantly, only higher voltages do. The threshold is $100mV$ in the case of the memristor used during the measurements. Such assumption is often used, typically in the context of reading the memristor state over a short period of time.

The second one: if a single erase (or write) impulse change the memductance from LRS to HRS (or HRS to LRS), then the MCNN cell capacitor voltage equation can shift from global monostability to bistability (or from bistability to monostability). Therefore the memristor can be used as a switch for two distinct regular CNN macro behaviour.

IV. CONCLUSION

A single cell MCNN hardware architecture design and its implementation are presented. A non-linear template is also presented and measured. The measurements were carried out with consideration for the noise sensitivity of the circuit, to ensure the robustness of the template.

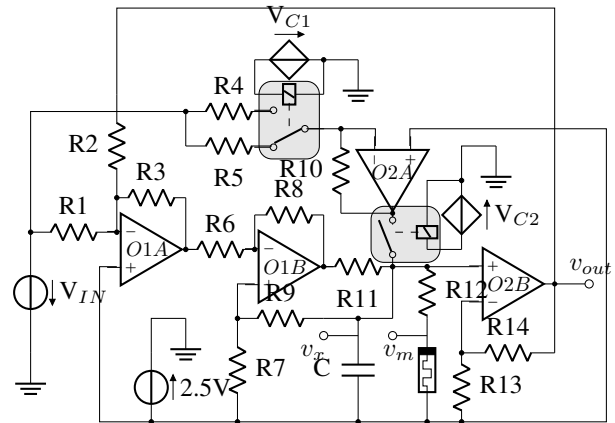


Fig. 1. Implemented MCNN uncoupled cell circuit. The $O1A$ Op. Amp. and resistors $R1 - R3$ implement an analogue voltage adder. The $O1B$ Op. Amp. with $R6 - R9$ and $R11$ resistors are an improved Howland Voltage Controlled Current Source (VCCS). The $O2A$ Op. Amp. with $R4 - R5$ and $R10$ support the setting of the initial value for the MCNN, both the capacitor voltage and the memristor state, has no effect during the MCNN operation. The $O2B$ Op. Amp. with $R13$ and $R14$ resistors implement the standard non-linearity function. $R12$ is used in serial with the memristor to set the memristance dynamics range to a more desired one. The gray devices are relays, controlled by the V_{C1} - V_{C2} voltages through the relay coils.

ACKNOWLEDGEMENT

This research was supported by the National Research, Development and Innovation Office through the grant TKP2021-NVA-27.

REFERENCES

- [1] Chua, L. O., 'Memristor-the missing circuit element', *IEEE Transactions on Circuit Theory*, 1971, **18**, pp. 507-519
- [2] Wang, S., Wang, W., Yakopcic, C., Shin, E., Subramanyam, G., Taha, T. M., 'Reconfigurable neuromorphic crossbars based on titanium oxide memristors', *IET Electronics Letters*, 2016, **52**, p. 1673-1675
- [3] Tetzlaff, R., Ascoli, A., Messaris, I. and Chua, L. O., 'Theoretical Foundations of Memristor Cellular Nonlinear Networks: Memcomputing With Bistable-Like Memristors', *IEEE Transactions on Circuits and Systems I: Regular Papers*, 2019, **67**, pp. 502-515
- [4] Ascoli, A., Messaris, I., Tetzlaff, R. and Chua, L. O., 'Theoretical Foundations of Memristor Cellular Nonlinear Networks: Stability Analysis With Dynamic Memristors', *IEEE Transactions on Circuits and Systems I: Regular Papers*, 2019, **67**, pp. 1389-1401
- [5] Ascoli, A., Tetzlaff, R., Kang, S. and Chua, L. O., 'Theoretical Foundations of Memristor Cellular Nonlinear Networks: A DRM2-Based Method to Design Memcomputers With Dynamic Memristors', *IEEE Transactions on Circuits and Systems I: Regular Papers*, 2020, **67**, pp. 2753-2766
- [6] Chua, L. O. and Roska, T., 'Cellular neural networks and visual computing: foundations and applications', *Cambridge university press*, 2002.
- [7] Knowm Inc. (Available online: <https://knowm.org/memristor-models-inspice/>, accessed on 4 August 2021)
- [8] Hajtó, D., Rák, Á. and Cserey, G., 'Robust Memristor Networks for Neuromorphic Computation Applications', *MDPI Materials*, 2019, **12**, p. 3573.

Improving the performance of Open-set Recognition with generated inner features

András Pál HALÁSZ

(Supervisors: Kálmán TORNAI, Péter Norbert SZOLGAY)
Pázmány Péter Catholic University, Faculty of Information Technology and Bionics
50/a Práter street, 1083 Budapest, Hungary
halasz.andras@itk.ppke.hu

Abstract—Open-set recognition faces a difficult issue compared to classical closed-set classification: We cannot know during training, what will be the appearing unknown samples be like, and the model has to be trained without this information. One can still prepare the model for them to some extent by using generated inputs labelled as unknown. The most common method to acquire these samples is Generative Adversarial Networks. We are using GAN as well, however, we do not generate samples in the input space, but rather fake features in a hidden layer of a much simpler structure. This solution, apart from giving better performance, is computationally cheaper due to the smaller generative model needed, and due to the fact that the generated samples do not have to be run on the first part of the model. We compared our model to other approaches and to our baseline. Our solution outperformed the baseline in all scenarios, and the other approaches in most of them, especially on datasets considered more difficult, indicating a robust model.

Keywords—Open-set Recognition; Fake sample generation; GAN;

Nowadays, various machine learning methods provide excellent results in different classification and recognition tasks, reaching or even exceeding the human level in numerous cases. The experiments yielding these results were conducted in a closed-set scenario, i.e., the assumption that all classes are known during training. A more realistic situation is the open-set case when new classes can appear during testing, and our model has to reject them, which is a great challenge. The problem of Open Set Recognition was formalized by Scheirer et al [1].

The challenging part of Open-set Recognition is that we do not know what will be the unknown samples be like, yet we have to prepare the model to reject them during testing time. However, we can try to model the space of these future samples by generating inputs for the model. It is hardest for the model to reject unknown, similar inputs to positive samples. It makes it advantageous to use the positive samples to create the fake ones – apart from the fact that these are all we have. Then we can train the model to put the generated samples far away from every positive sample. As a result, the actual unknown samples will also be distinguishable from every class during the test, thus recognized as unknown.

However, creating appropriate fake images is a challenging task: there is a danger hard to evade, that depending on the generative models' complexity, the generated inputs will be either too similar to the real objects – thus, we do not want the model to reject it -, or the inputs will be of very low quality and learning to reject them will not help the model to generalize. Hence, instead of generating fake samples in the input space, we generate inner features using the outputs of a hidden layer. This feature space is of a much simpler structure. Using these fake features leads to better results –as the experiments showed

–, but we also gain on computational complexity: only a much smaller model is needed to create these features than what would be needed to generate fake images of good enough quality. We use Generative Adversarial Networks [2] for the sample generation, with the neural network structures adjusted for the altered task, namely to generate features instead of images.

The backbone of our model is a convolutional neural network, followed by some fully connected layers. The output space is not the usual logit space but a feature space with low dimensions. The goal of the training is to put every sample near a predefined class center in this space. This model without the generated samples also serves as a baseline to test the improvement of using fake features. The layer we generate the samples is the output of the last convolutional layer. After it, only some fully connected layers come. This leads to further gain in terms of time complexity, as generated samples do not have to run through the convolutional layers, which takes the vast majority of computation.

The training of the model has two phases: first, we train the whole network without any fake samples, then we use the real features - the output of the first part of the model - to generate the fake samples. With these fake samples we train now only the second part of the model.

As a baseline, we used the same network structure, however we did not employ generated samples. This way, the training was a longer version of the first phase of the training of our model.

ACKNOWLEDGEMENT

This research was supported by the National Research, Development and Innovation Office through the grant TKP2021-NVA-26.

REFERENCES

- [1] W. J. Scheirer, A. Rocha, A. Sapkota, and T. E. Boult, "Toward open set recognition," *IEEE Transactions on Pattern Analysis and Machine Intelligence*, vol. 35, pp. 1757–1772, 2013.
- [2] I. J. Goodfellow, J. Pouget-Abadie, M. Mirza, B. Xu, D. Warde-Farley, S. Ozair, A. Courville, and Y. Bengio, "Generative adversarial nets," in *Proceedings of the 27th International Conference on Neural Information Processing Systems - Volume 2, NIPS'14*, (Cambridge, MA, USA), p. 2672–2680, MIT Press, 2014.

Identifiability of delayed systems

Gergely HORVÁTH

(Supervisor: Gábor SZEDERKÉNYI)

Pázmány Péter Catholic University, Faculty of Information Technology and Bionics

50/a Práter street, 1083 Budapest, Hungary

horvath.gergely@itk.ppke.hu

Abstract—Delayed systems can be used for multiple purposes, e.g. to take the model uncertainty into account. In reality, it happens a lot – e.g. in biochemical research – that the model has some of its parts missing, therefore the unaccounted parts should be modeled via including delay terms into its structure so the dynamics can be more precise. The models of interest are physical model where the aim is to get an accurate representation of the underlying physical processes, therefore the parameters have strict physical meaning. On the other hand, mathematical models have their weaknesses and necessary simplifications, and this is the reason why, in certain cases, it is possible to construct such models, that can reproduce the desired input-output behaviour with multiple parameter settings. This means that parameters with concrete physical meaning can obtain multiple values while fulfilling the mathematical constraints which is a contradiction to be solved, it is an important requirement to have a unique parameter vector. These delayed systems are no exception, their delayed differential equations must be modeled in the same way. Unfortunately, the delayed terms are more complex in terms of mathematical properties, therefore it is harder to assess parameter identifiability. Here we show it can be possible to assess parametric identifiability with the help of approximations applied on these delayed systems by substituting the delay terms with linear ODE subsystems.

Keywords—delayed systems, identifiability, chain approximation

When modelling, one needs to know the dynamics of the system of interest in order to carry out fully-detailed simulations. The most common way is to use a system of ordinary differential equations to represent the phenomenon:

$$\begin{aligned}\dot{\mathbf{x}}(t) &= f(\mathbf{x}(t), \boldsymbol{\theta}) \\ \mathbf{y}(t) &= h(\mathbf{x}(t), \boldsymbol{\theta})\end{aligned}$$

Where $\mathbf{x}(t) \in \mathbb{R}^n$ is the state vector (n is the number of states), $\mathbf{y}(t) \in \mathbb{R}^m$ is the observed output vector (m is the number of observed measures), $\boldsymbol{\theta} \in \mathbb{R}^p$ is the parameter vector (p is the number of parameters), $f : \mathbb{R}^n \rightarrow \mathbb{R}^n$ is for the dynamics of the system, $h : \mathbb{R}^n \rightarrow \mathbb{R}^m$ is observation process. Unfortunately, on many occasions the entire dynamics is not known, therefore the known part of the system is being modeled with delay terms as well to account for the unknown parts. This gives rise to the notion of delayed differential equations (DDE) (for simplicity we assume that the output dynamics does not contain delay terms):

$$\begin{aligned}\dot{\mathbf{x}}(t) &= f(\mathbf{x}(t), \boldsymbol{\theta}, \boldsymbol{\tau}) \\ \mathbf{y}(t) &= h(\mathbf{x}(t), \boldsymbol{\theta})\end{aligned}$$

Here, the system's internal dynamics now contains the $\boldsymbol{\tau} \in \mathbb{R}^d$ vector, which are the already-mentioned time-delays. In order to preserve causality we also assume that:

$$\tau_i \in \mathbb{R}^+ \quad , \quad i = 1, \dots, p$$

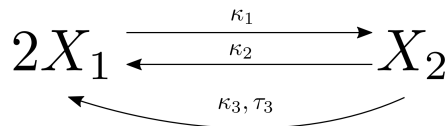


Fig. 1. An example for a delayed system

One such example (Figure 1.) for a system of DDEs is mentioned in [1]. By considering the graph of system, one can write up the dynamics of the delayed system. The general form of a system of DDEs is described by (1) and (2), which will look like the following for this specific example:

$$\dot{x}_1(t) = -2k_1x_1^2(t) + 2k_2x_2(t) + 2k_3x_2(t - \tau_3) \quad (1)$$

$$\dot{x}_2(t) = k_1x_1^2(t) - k_2x_2(t) - k_3x_2(t) \quad (2)$$

After looking at such equations, the first question is how to handle the delayed term(s). Although the mathematical background of handling DDEs is well-founded, it is more difficult than ODEs both in theory and computationally. *E.g.*, in order to be widely usable, one must attain the structural identifiability property of the system, and it turns out the current methods are not well-adjusted for handling DDEs. Fortunately, methods exist that can serve as approximations of such system, which methods are able to rewrite the representation into form of ODEs. One such method is the chain method. The mathematical properties of the chain method approximated systems are well-studied [2], and we built on these results. The can method can be used for rearrange the delayed subsystem into a system of linear ODEs, that will have more desirable mathematical properties, which will result in a more suitable system for the currently existing tools for determining structural identifiability.

REFERENCES

- [1] G. Lipták, K. M. Hangos, and G. Szederkényi, "Approximation of delayed chemical reaction networks," *Reaction Kinetics, Mechanisms and Catalysis*, vol. 123, no. 2, pp. 403–419, 2018.
- [2] B. Krasznai, *A módosított láncmódszer késleltetett differenciálegyenlet-rendszerekre alkalmazásokkal= The modified chain method for systems of delay differential equations with applications*. PhD thesis, Pannon Egyetem, 2016.

A new range-based breast cancer prediction model using the Bayes' theorem and Ensemble learning

Sam KHOZAMA

(Supervisors: Zoltán NAGY, Zoltán GÁSPÁRI)

Pázmány Péter Catholic University, Faculty of Information Technology and Bionics

50/a Práter street, 1083 Budapest, Hungary

khozama.sam@itk.ppke.hu

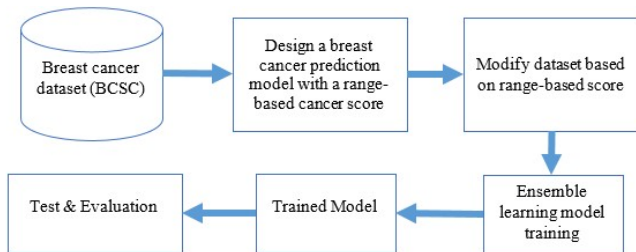


Fig. 1. Proposed system methodology

Abstract—Breast cancer prognosis is critical for cancer prevention and treatment. A novel breast cancer prediction model is presented in this study. Furthermore, instead of binary classification results, this study seeks to produce a range-based cancer score (0 or 1). The BCSC dataset is used and adjusted to provide a range-based cancer score using a proposed probabilistic model. The proposed model looks at a subset of the BCSC dataset, which has 67632 records and 13 risk factors. The weighting mechanism is also used in the model to get the optimal fusion of the BCSC's risk variables. This final prediction is added to the BCSC dataset, which is then used to train an ensemble model using the new version of the BCSC dataset. The new range-based model appears to be accurate and robust. Aside from that, the new BCSC dataset can be used for additional study and analysis.

Keywords—Breast cancer; Cancer Prediction; Machine Learning; Risk factors.

I. INTRODUCTION

Because the number of datasets is growing exponentially every day, data analysis is now one of the most rapidly rising topics of computer science. One of these fields is cancer prediction, which uses data analysis and Machine Learning (ML) algorithms to estimate cancer risk [1]. The estimation accuracy of cancer prognosis has grown dramatically (15 % -20 %) due to the use of the ML algorithm in recent years, thanks to ML approaches. Breast cancer prediction can be used to identify women who are at an increased risk of developing the disease and to advise them on how to change their lifestyle in order to avoid future treatment and expenditures [2].

II. MATERIALS AND METHODS

We recommend utilizing a range-based cancer score value rather than a scalar value (0 or 1) for more precise and effective prediction so that the conclusion is not either cancer or not. Instead, there will be a percentage range between 0% and 100%, representing the risk of breast cancer. The proposed methodology is shown in Figure 1.

III. TRAIN THE ENSEMBLE LEARNING MODEL

Ensemble learning is a technique that combines multiple classifiers (models) to create a large, powerful model. It has the advantage of being able to improve performance by employing many classifiers. In recent years, a marriage of Ensemble learning with hyperparameters optimization has received a lot of attention [3]. Many hyperparameters are chosen for optimization. The maximum number of splits, the number of learners, and the learning rate are the three parameters. The AdaBoost algorithm is utilized as the ensemble method, and the decision trees algorithm is employed as the learner type.

IV. CONCLUSION

One of the most difficult topics of medical engineering is breast cancer prediction. The current study is developing a unique range-based breast cancer prediction algorithm. To get the final prediction value of each case in the BCSC dataset, a probabilistic model is utilized and assessed. The BCSC dataset is updated with this new final score. The Bayesian hyperparameters optimization method is used to train an ensemble learning model using the new version of the dataset. The training process is carried out in two ways: one uses the entire dataset, while the other employs a subset of 67633 samples.

ACKNOWLEDGEMENTS

Data collection and sharing was supported by the National Cancer Institute-funded Breast Cancer Surveillance Consortium (HHSN261201100031C), available at: <http://www.bcs-research.org/>.

This work is done under full supervision by Dr Ali Mayya, a teacher from the Department of Computer Engineering, Tishreen University, Lattakia, Syria.

REFERENCES

- [1] Ahmad AS, Mayya, AM (2020). A new tool to predict lung cancer based on risk factors. *Heliyon*, 6, e03402.
- [2] American Cancer Society (2019). *Breast Cancer Facts & Figures 2019-2020*. Atlanta: American Cancer Society.
- [3] Khozama, S., and Mayya, A. M. (2021). Study the Effect of the Risk Factors in the Estimation of the Breast Cancer Risk Score Using Machine Learning. *Asian Pacific Journal of Cancer Prevention*, 22(11), 3543-3551.

Monitoring Snoring in Sleeping Adults to Detect Respiratory Disorders

Ádám NAGY

(Supervisor: Ákos ZARÁNDY) Pázmány Péter Catholic University, Faculty of Information Technology and Bionics
50/a Práter street, 1083 Budapest, Hungary
nagy.adam@itk.ppke.hu

Abstract—Technological advances and the emergence of new deep learning and machine vision algorithms allow us to diagnose diseases that have been present in a large percentage of the population so far, but their diagnosis requires continuous observation of the patient at night. Examples for that kind of disorders include sleep-time breathing disorders such as asthma, snoring or obstructive sleep apnea (OSA). For the diagnosis of diseases like this, we recommend a neural network-based approach in this work, which focuses on the detection of snoring, which can be an important part of a system for monitoring sleep disorders like the one we mentioned above. The recommended algorithm is an LSTM-CNN that has already provided outstanding results in similar applications.

Keywords-non-contact; snore-detection; deep-learning, recurrent neural network

Currently we build a camera based system with infrared illumination that is able to monitor the respiration and movement of the patient at night. Our basic goal is to be able to analyze records from sleeping adults. Because breathing problems such as apnea can occur during the sleep. Monitoring of sleeping records is to analyze these problems. Snoring detection is important for the detection and analysis of such respiratory problems. This is because of the following: "Snoring is often associated with the sleep disorder called "obstructive sleep apnea".

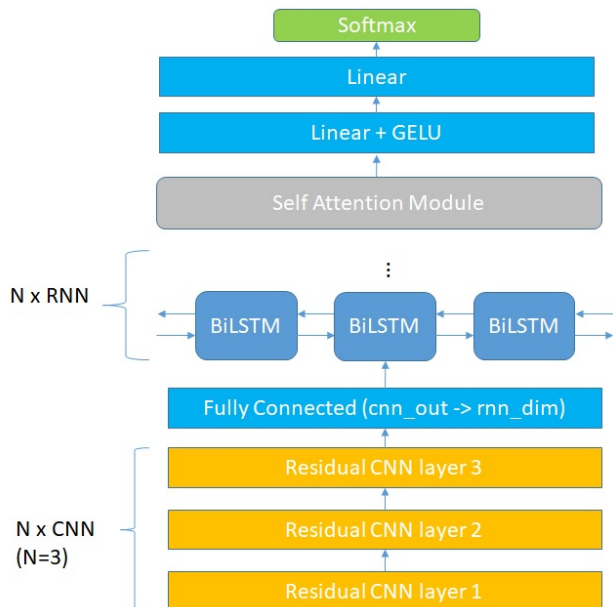


Fig. 1. In this figure we can see a summary of the recommended neural architecture. The architecture includes 3 convolutional layers, a BiLSTM-stack, a self-attention module, two linear layers, and a softmax layer.

The role of snoring in OSA analysis may be as follows: "OSA often is characterized by loud snoring followed by

periods of silence when breathing stops or nearly stops. Eventually, this reduction or pause in breathing may signal you to wake up, and you may awaken with a loud snort or gasping sound." This means, that if we are able to monitor breathing in non-contact way, (we are currently developing for a camera-based solution as mentioned above), then the loudness analysis combined with respiratory monitoring can help diagnose OSA. The first step in this is to be able to detect loud snoring. I will present a possible method for that in this work.

I. METODOLOGY

In this work, I approached snoring detection as a two-dimensional CNN-based spectrum analytical task, similar to speech-to-text applications. I started from the architecture introduced in [2] that was designed to classify the emotions of speakers on audio material. I have made only minor changes on the mentioned article. For example the followings: I applied only 3 convolution layers immediately after generating the spectrogram, with SELU activation functions, as this activation function solves the so called "dying-reLU-problem". In addition we used only 2 layers of LSTM. The summary of the modified architecture can be seen in Figure 1.

II. FUTURE WORKS

In the future, we must first evaluate the trained network on a database that contains recordings of independent individuals. Not only do we need to increase the length of the database, but we also need to pay attention to diversity. We must not ignore gender and racial diversity. If the performance on the independent database is satisfactory, we can move on to integrating the algorithm into our nighttime sleep monitoring system. If the snoring detection algorithm provides adequate performance, it can become an integral part of our sleep monitoring system and greatly aid in the diagnosis of "obstructive sleep apnea" or other sleep disorders.

REFERENCES

- [1] Song, Changyue and Liu, Kaibo and Zhang, Xi and Chen, Lili and Xian, Xiaochen. (2015). An Obstructive Sleep Apnea Detection Approach Using a Discriminative Hidden Markov Model From ECG Signals. *IEEE Transactions on Biomedical Engineering*. 63. 1-1. 10.1109/TBME.2015.2498199.
- [2] Li, Yuanchao and Zhao, Tianyu and Kawahara, Tatsuya, 2019, 09, 2803-2807, *Improved End-to-End Speech Emotion Recognition Using Self Attention Mechanism and Multitask Learning*, doi: 10.21437/Interspeech.2019-2594
- [3] Ephrat, Ariel and Mosseri, Inbar and Lang, Oran and Dekel, Tali and Wilson, Kevin and Hassidim, Avinatan and Freeman, William and Rubinstein, Michael, 2018, 04, Looking to Listen at the Cocktail Party: A Speaker-Independent Audio-Visual Model for Speech Separation, *ACM Transactions on Graphics*, doi: 10.1145/3197517.3201357

Current results and challenges of wrist exoskeleton design

Katalin SCHÄFFER

(Supervisors: György CSEREY, Miklós KOLLER)

Pázmány Péter Catholic University, Faculty of Information Technology and Bionics

50/a Práter street, 1083 Budapest, Hungary

schaffer.katalin@itk.ppke.hu

Abstract—Upper limb wearable assistive devices have the potential to help both healthy and impaired users. One group of these devices aims to restore the movement of the human wrist. There are multiple wrist exoskeletons in the literature which have different design objectives and actuation methods. Recently, exosuits made of soft materials have gained interest, due to their potential for high strength to weight ratio, inherent safety, comfort, and low cost. This paper provides an overview of the existing wrist exoskeletons and also presents the main design principles for building a soft wrist exosuit actuated by fabric pneumatic artificial muscles.

Keywords—wearable devices; exosuits and exoskeletons; soft actuators

I. INTRODUCTION

Upper limb wearable assistive devices can be useful in a variety of scenarios. Healthy people can benefit from physical assistance to avoid fatigue and muscle strain during repetitive tasks or to augment their physical abilities. The physically impaired can benefit from rehabilitation exercises or from assistance for activities of daily living (ADLs).

II. STATE OF THE ART OF WRIST MOVEMENT ASSISTING DEVICES

The wrist movement assisting devices in the literature can be sorted into three main groups based on their mechanism: rigid, compliant and soft devices [1]. The devices in each category have some undesired behaviors or limitations which provides opportunity for further improvements. The first group includes the exoskeletons which consist of rigid links aligned with the wrist. The main source of incorrect behaviour of these devices is the misalignment of the mechanical joint and the human wrist. The second group is for wrist exoskeletons with embedded compliance. They allow less joint misalignment than completely rigid devices, but lacks other benefits of fully soft devices. The third group consists of soft wrist movement assisting devices, also called exosuits which are based on various actuation mechanisms. The cable-driven wrist exosuits are low profile, but the friction buildup in the cables makes control challenging. The shape memory alloy-actuated wrist exosuit is also low profile, but it is limited in its torque and range of motion. The McKibben artificial muscle and the elastomeric pneumatic actuator-based exosuits are lightweight but require somewhat bulky actuators, and the textile pneumatic actuator-based wrist exosuits only consider the pronation-supination degree of freedom.

III. PROPOSED WRIST EXOSUIT DESIGN

Fabric pneumatic artificial muscles (fPAMs) [2] are a recently developed class of linear contractile actuator. They are promising for application in soft exosuits because they

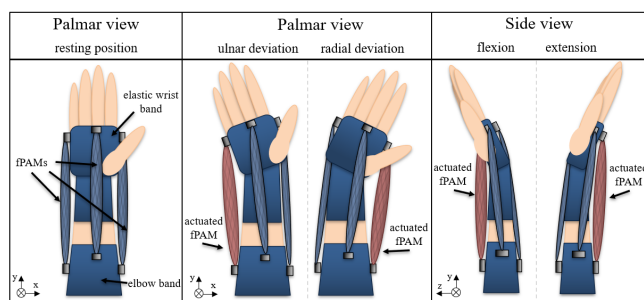


Fig. 1. The proposed wrist exosuit has four fabric pneumatic artificial muscles (fPAMs) as actuators, which are attached to the forearm and the hand through a fabric structural elements. The palmar view shows that the inflated fPAMs promote radial and ulnar deviation. Side view showing that the inflated fPAM at the dorsal side promotes wrist extension and at the palmar side promotes wrist flexion.

are lightweight, fully compressible, and they have a near-linear force-contraction relationship, low hysteresis, and a short response time to dynamic inputs.

This paper introduces a novel soft wrist exosuit design which is based on actuation by fPAMs (Fig. 1). The research work is focused on exploring the applicability of this actuator to move the wrist along a large range of motion in the direction of flexion-extension and radial-ulnar deviation. The proposed antagonistic muscle arrangement and the limited contraction ratio of the fPAMs provide mechanical limits of the wrist movement which makes the device inherently safe. A two dimensional geometric model of the human wrist in the exosuit can help to estimate the torque of the exosuit for different wrist angles. The torque depends on the position of the attachment points of the fPAM on the hand and forearm and it depends on the applied pressure, length, and diameter of the fPAM.

ACKNOWLEDGEMENTS

The research was conducted in the IRIS Lab of the University of Notre Dame. I would like to thank Dr. Margaret Coad and Dr. Yasemin Özkan Aydın for the guidance they provided during the research project. This research was supported by the National Research, Development and Innovation Office through the grant TKP2021-NKTA-66.

REFERENCES

- [1] Chiaradia, D., Tiseni, L., Xiloyannis, M., Solazzi, M., Masia, L. & Frisoli, A. An assistive soft wrist exosuit for flexion movements with an ergonomic reinforced glove. *Frontiers In Robotics And AI*, pp. 182 (2021)
- [2] Naclerio, N. & Hawkes, E. Simple, Low-hysteresis, Foldable, Fabric Pneumatic Artificial Muscle. *IEEE Robotics And Automation Letters*, **5**, 3406-3413 (2020)

Achieving mixed precision computing with the help of domain specific libraries

Bálint SIKLÓSI

(Supervisor: István REGULY)

Pázmány Péter Catholic University, Faculty of Information Technology and Bionics

50/a Práter street, 1083 Budapest, Hungary

siklosi.balint@itk.ppke.hu

In 2008, the Exascale Study Group (ESG) issued a report [1], where they listed four main challenges that had to be solved to reach exascale systems, i.e. a system, which can compute 10^{18} floating point operations in one second. The main challenges: 1) power consumption: using the technology of a system in 2008, would use 600 MW of power for this performance. By today we managed to decrease this need under 20 MW. 2) Speed and energy of data movement: the time needed to move data in the memory, uses more time than the time it takes to execute a floating point operation on that data. 3) Fault tolerance: failures happen faster, than checkpointing a job. 4) extreme parallelism: to compute at a rate of 1 exaflop, it requires 1 billion floating point units performing 1 billion calculations per second each. To overcome several of these challenges, mixed precision computing can be an extremely effective tool. By lowering the precision of the data that we compute on, we also decrease the size that we need to store, we can shrink the overall memory footprint. With less data in size, we can reduce memory and network traffic. With less communication, the previously memory bound application might move closer to become compute bound. Using the full compute power of a system, but by executing more floating point operations per second, we reduce the energy consumption and also the time to compute. However, despite the advantages listed, we need to be very careful when using mixed precision computing. If we lower the precision of some data, then the solution of the overall simulation may fall outside of the expected error range. It is exceptionally important to understand the numerical weaknesses of the application we want to modify. We must carefully choose which data can we reshape in a way, that the overall result's validity is unchanged.

In the last few years, the use of mixed precision computing has become a particularly prominent research direction. Two Gordon Bell Prize winners: a climate simulation [2] and an opioid addiction research [3] partially use decreased precision. The best paper at the ISC'19 conference introduce some algorithms in their GPUMixer project [4], which automatically recognise kernels which might produce performance gain with mixed precision, and they also test the proposed modifications to validate the results. There are plenty of domain fields to use mixed precision computing: from earthquake simulations [5], to Linear solvers and numerical methods [6], [7] through AI and deep learning [8] and mixed precision in-memory computing [9].

The OPS and OP2 (Oxford Parallel libraries) projects are developing open-source frameworks for the execution of structured and unstructured grid applications on clusters of GPUs or multi-core CPUs. Although both DSLs are designed to look

like conventional libraries, the implementations use source-source translation to generate the appropriate back-end code for the different target platforms. Both DSLs can be viewed as instantiations of the *Æcute* programming model, thus allowing the examination of interactions between kernels. In our project, we plan to utilise this additional information, by recognising some additional patterns that might span between kernels. As a baseline test, we hand tuned a CFD mini application to explore the possible performance gain through mixed precision computing in OP2. By halving the size of the most accessed data set, we achieved a 1.13x (1.1x) speedup on CPUs (and GPUs), compared to the speedup of a fully reduced sized execution: 1.76x (1.44x).

REFERENCES

- [1] P. Kogge, S. Borkar, D. Campbell, W. Carlson, W. Dally, M. Denneau, P. Franzon, W. Harrod, J. Hiller, S. Keckler, D. Klein, and R. Lucas, "Exascale computing study: Technology challenges in achieving exascale systems," *Defense Advanced Research Projects Agency Information Processing Techniques Office (DARPA IPTO), Techinal Representative*, vol. 15, 01 2008.
- [2] T. Kurth, S. Treichler, J. Romero, M. Mudigonda, N. Luehr, E. Phillips, A. Mahesh, M. Matheson, J. Deslippe, M. Fatica, Prabhat, and M. Houston, "Exascale deep learning for climate analytics," in *Proceedings of the International Conference for High Performance Computing, Networking, Storage, and Analysis*, SC '18, IEEE Press, 2018.
- [3] W. Joubert, D. Weighill, D. Kainer, S. Climer, A. Justice, K. Fagnan, and D. Jacobson, "Attacking the opioid epidemic: Determining the epistatic and pleiotropic genetic architectures for chronic pain and opioid addiction," in *Proceedings of the International Conference for High Performance Computing, Networking, Storage, and Analysis*, SC '18, IEEE Press, 2018.
- [4] I. Laguna, P. Wood, R. Singh, and S. Bagchi, *GPUMixer: Performance-Driven Floating-Point Tuning for GPU Scientific Applications*, pp. 227–246. 05 2019.
- [5] T. Ichimura, K. Fujita, T. Yamaguchi, A. Naruse, J. C. Wells, T. C. Schulthess, T. P. Straatsma, C. J. Zimmer, M. Martinasso, K. Nakajima, M. Hori, and L. Maddegadara, "A fast scalable implicit solver for nonlinear time-evolution earthquake city problem on low-ordered unstructured finite elements with artificial intelligence and transprecision computing," in *Proceedings of the International Conference for High Performance Computing, Networking, Storage, and Analysis*, SC '18, IEEE Press, 2018.
- [6] A. Abdelfattah, H. Anzt, E. G. Boman, E. Carson, T. Cojane, J. Dongarra, M. Gates, T. Grützmacher, N. J. Higham, S. Li, N. Lindquist, Y. Liu, J. Loe, P. Luszczek, P. Nayak, S. Pranesh, S. Rajamanickam, T. Ribizel, B. Smith, K. Swirydowicz, S. Thomas, S. Tomov, Y. M. Tsai, I. Yamazaki, and U. M. Yang, "A survey of numerical methods utilizing mixed precision arithmetic," 2020.
- [7] A. Haidar, H. Bayraktar, S. Tomov, J. Dongarra, and N. J. Higham, "Mixed-precision iterative refinement using tensor cores on gpus to accelerate solution of linear systems," *Proceedings of the Royal Society A*, vol. 476, 2020-11 2020.
- [8] P. Micikevicius, S. Narang, J. Alben, G. Diamos, E. Elsen, D. Garcia, B. Ginsburg, M. Houston, O. Kuchaiev, G. Venkatesh, and H. Wu, "Mixed precision training," 2018.
- [9] M. Le Gallo, A. Sebastian, R. Mathis, M. Manica, H. Giefers, T. Tuma, C. Bekas, A. Curioni, and E. Eleftheriou, "Mixed-precision in-memory computing," *Nature Electronics*, vol. 1, p. 246–253, Apr 2018.

The effects and mitigation of the object centering bias in common datasets

Gergely SZABÓ

(Supervisor: András HORVÁTH)

Pázmány Péter Catholic University, Faculty of Information Technology and Bionics

50/a Práter street, 1083 Budapest, Hungary

szabo.gergely@itk.ppke.hu

Abstract—Convolutional neural networks are commonly expected to be shift invariant, however multiple studies have shown recently that this expectation is not always realistic. In this progress report we will briefly review based on our currently submitted manuscript to the 2022 ICPR conference[1] the object centering bias present in commonly used datasets and the effects of this bias and the non fully invariant property of the convolutional neural networks combined. We have also investigated semi-novel data augmentation and architectural solutions which you can read about in more detail in the above manuscript[1].

I. INTRODUCTION

During my main research in the PhD program the question arouse whether training a neural network with the purpose of semantic segmentation could be performed on sub-images containing single objects roughly in the center of the sub-image. Motivated by this question and the 2019 paper of R. Zhang "Making convolutional neural networks shift invariant again"[2] we have investigated the phenomenon of object centering bias in a much broader sense, using multiple datasets, neural networks and evaluation approaches. Our concepts and methods are partially based on and motivated by the 2020 results of O. S. Keyhan and J. C. Gemert[3] and the 2021 results of Md. Am. Islam[4], but we believe that some of the evaluation approaches we use and some of the data augmentation and architectural solutions we discovered and validated are novel to the best of our knowledge.

II. THE OBJECT CENTERING BIAS

In the human vision system we have only one location, the fovea centralis in our eye, where the density of the light processing cones is significantly higher than the surrounding regions and this area is responsible for our detailed, central vision as well as main color vision. [9] Since we can focus typically on only one region it is easier for our nervous system to center the important elements in our field of view. It is also more aesthetically pleasing to look at images where the important details and objects are at the center [10]. This evolutionary consequence of human behaviour can introduce a significant bias in all human acquired datasets.

In our measurements we have presented evidence that this bias holds true for popular training and evaluation datasets such as MNIST, CIFAR, ImageNet and MS-COCO. We have also measured the extent of the effects of this bias using a specially designed dataset in which the position of the objects is easily controlled and manipulated as needed and using the popular U-net architecture[5]. These measurements showed that training a convolutional neural network with objects only present near the center of the image — as in case

of many popular datasets — could result in more than 10000 times worse performance with objects at the edges (without any parts of the object leaving the image). We have also made similar measurements using the ImageNet and MS-COCO datasets and various popular architectures such as VGG-16[11], DenseNet121[12], ResNet-50[8] and the Mask R-CNN[6] architecture implemented in the Detectron2[7] environment.

III. MITIGATION OF THE OBJECT CENTERING BIAS

Following the baseline measurements which proved the significance and strong impact of the object centering bias, we designed and validated some data augmentation techniques and simple architectural changes capable of almost completely eliminating the effects of this bias with comparably insignificant drawbacks at worst. For detailed description of these methods and the validation please check the original manuscript this progress report is based on[1]. However if none of these techniques are applicable for a given network we still recommend at least creating some test examples containing objects at the edges and evaluating the network on these samples separately.

REFERENCES

- [1] Szabo, Gergely, and Andras Horvath. "Mitigating the Bias of Centered Objects in Common Datasets." arXiv preprint arXiv:2112.09195 (2021).
- [2] Zhang, Richard. "Making convolutional networks shift-invariant again." International conference on machine learning. PMLR, 2019.
- [3] Kayhan, Osman Semih, and Jan C. van Gemert. "On translation invariance in cnns: Convolutional layers can exploit absolute spatial location." Proceedings of the IEEE/CVF Conference on Computer Vision and Pattern Recognition. 2020.
- [4] Islam, Md Amirul, et al. "Position, padding and predictions: A deeper look at position information in cnns." arXiv preprint arXiv:2101.12322 (2021).
- [5] Ronneberger, Olaf, Philipp Fischer, and Thomas Brox. "U-net: Convolutional networks for biomedical image segmentation." International Conference on Medical image computing and computer-assisted intervention. Springer, Cham, 2015.
- [6] He, Kaiming, et al. "Mask r-cnn." Proceedings of the IEEE international conference on computer vision. 2017.
- [7] Wu, Y., Kirillov, A., Massa, F., Lo, W.-Y., & Girshick, R. (2019). Detectron2. <https://github.com/facebookresearch/detectron2>
- [8] He, Kaiming, et al. "Deep residual learning for image recognition." Proceedings of the IEEE conference on computer vision and pattern recognition. 2016.
- [9] Willmer, Edward Nevill, and William David Wright. "Colour sensitivity of the fovea centralis." Nature 156.3952 (1945): 119-121.
- [10] Chen, Yi-Chia, Clara Colombatto, and Brian J. Scholl. "Looking into the future: An inward bias in aesthetic experience driven only by gaze cues." Cognition 176 (2018): 209-214.
- [11] Simonyan, Karen, and Andrew Zisserman. "Very deep convolutional networks for large-scale image recognition." arXiv preprint arXiv:1409.1556 (2014).
- [12] Huang, Gao, et al. "Densely connected convolutional networks." Proceedings of the IEEE conference on computer vision and pattern recognition. 2017.

PROGRAM 3
FEASIBILITY OF ELECTRONIC AND OPTICAL
DEVICES, MOLECULAR AND
NANOTECHNOLOGIES,
NANO-ARCHITECTURES, NANOBIONIC
DIAGNOSTIC AND THERAPEUTIC TOOLS

Head: Árpád CSURGAY

An optimal retrodirective array

András ESZES

(Supervisor: Zsolt SZABÓ)

Pázmány Péter Catholic University, Faculty of Information Technology and Bionics
50/a Práter street, 1083 Budapest, Hungary
esz.es.andras@itk.ppke.hu

Abstract—Van Atta (VA) arrays are well known for their retrodirective properties. In this paper full wave simulation results are presented of an ongoing research. The engineering of the particular (tightly coupled meander) group delay lines are based on full wave simulation methods and their scattering properties are also presented. The designed array is constitute of 8 aperture coupled Minkowski fractal patch element per row and operating at 10 GHz. The main purpose of this research is to decrease the ripples near to the broadside of the structure without increasing of the overall size. Ripple reduction could be achieved via diffusing the wave at the specular direction. The constructed VA array could be placed on UAV's owing to its compact size compared with other structures with identical RCS. This array could also play an essential role in future validation purposes.

Keywords—Van Atta array, Meandered delay line, Microstrip couplers, Aperture coupled microstrip antenna, Checkerboard metasurface, Polarization rotator, Plane wave diffuser

I. RESULTS

During research HFSS solver were used as a numerical tool for modeling: interconnections, radiator elements, unitcell elements (AMC, polarization rotator).

The components of the overall design were modeled separately, it was critical from optimization point. The separated part were excited with lumped port excitation or floquet port excitation.

The interconnection lines were initially designed based on closed form equations [7]. Ultimately the complete structure was excited with plane wave.

The efficiency of the structure was checked via bistatic RCS patterns, it was turned out that the amplitude of the specular wave and retrodirected wave are at the same power range in the overall incident angle range.

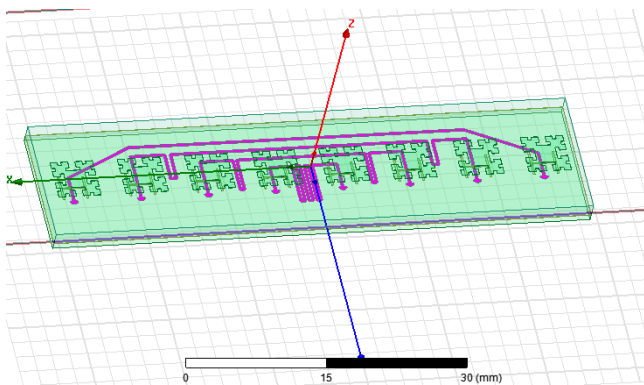


Fig. 1. Van Atta array

II. CONCLUSION

The overall radiation properties of designed Van Atta array is acceptable without the diffuser [7]. To the best of the

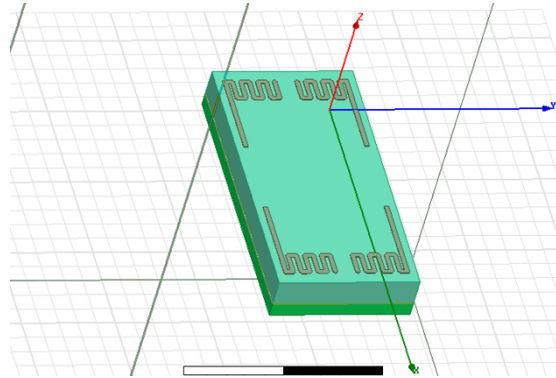


Fig. 2. Diffuser

author's knowledge this structure is the first VA array that deploys polarization rotators for RCS ripple reduction purposes close to the boresight.

ACKNOWLEDGMENT

The authors would like to thank to the Grante Antenna Development and Production Corporation (Esztergom-Kertváros) for providing the ANSYS-HFSS 15 full-wave modeler for the numerical calculations.

REFERENCES

- [1] Atta, L. C. V., "Electromagnetic reflector," U.S. Patent, Vol. 2908, 1959."
- [2] M. Kalaagi and D. Seetharamdoo, "Retrodirective metasurface operating simultaneously at multiple incident angles," 12th European Conference on Antennas and Propagation (EuCAP 2018), London, 2018, pp. 1-5, doi: 10.1049/cp.2018.0545.
- [3] Alharbi, M.; Alyahya, M.A.; Ramalingam, S.; Modi, A.Y.; Balanis, C.A.; Birtcher, C.R. Metasurfaces for Reconfiguration of Multi-Polarization Antennas and Van Atta Reflector Arrays. *Electronics* 2020, 9, 1262. <https://doi.org/10.3390/electronics9081262>
- [4] Nanfang Yu et. al. "Light Propagation with Phase Discontinuities: Generalized Laws of Reflection and Refraction" *Science* 21 Oct 2011: Vol. 334, Issue 6054, pp. 333-337 DOI: 10.1126/science.1210713
- [5] Alharbi, M.; Alyahya, M.A.; Ramalingam, S.; Modi, A.Y.; Balanis, C.A.; Birtcher, C.R. Metasurfaces for Reconfiguration of Multi-Polarization Antennas and Van Atta Reflector Arrays. *Electronics* 2020, 9, 1262. <https://doi.org/10.3390/electronics9081262>
- [6] S. Gupta, A. Parsa, E. Perret, R. V. Snyder, R. J. Wenzel and C. Caloz, "Group-Delay Engineered Noncommensurate Transmission Line All-Pass Network for Analog Signal Processing," in *IEEE Transactions on Microwave Theory and Techniques*, vol. 58, no. 9, pp. 2392-2407, Sept. 2010, doi: 10.1109/TMTT.2010.2058933.
- [7] Y. Liu, K. Li, Y. Jia, Y. Hao, S. Gong and Y. J. Guo, "Wideband RCS Reduction of a Slot Array Antenna Using Polarization Conversion Metasurfaces," in *IEEE Transactions on Antennas and Propagation*, vol. 64, no. 1, pp. 326-331, Jan. 2016, doi: 10.1109/TAP.2015.2497352.

Optimized implementations of neural networks

András FÜLÖP

(Supervisors: András HORVÁTH, György CSABA)

Pázmány Péter Catholic University, Faculty of Information Technology and Bionics
50/a Práter street, 1083 Budapest, Hungary
fulop.andras@itk.ppke.hu

Abstract—Nowadays, various neural networks are used very successfully in solving many practical problems such as medical image processing, facial recognition, stock market prediction, weather forecasting, handwriting analysis (such as signature verification) or self-driving cars. One of the most popular and frequently used neural network is the convolutional neural network, which performs particularly well in image processing tasks. But neural networks can only be trained on huge data sets with a lot of time and energy consumption to work properly. In case of convolutional neural networks the main computation is convolution. In this paper, we show a method, which can optimise the neural networks.

Keywords—neural network; convolution; optimisation

I. INTRODUCTION

The basis of commonly used deep learning methods are similar. The architectures apply a nonlinear transformation on inputs and use what they learn to create statistical models as outputs and the iterations continue until the outputs have reached an acceptable level of accuracy. One of the most commonly used deep learning methods is the convolutional neural network. [1] [2] [3] [4]

II. CONVOLUTIONAL NEURAL NETWORKS

There are four main operations in convolutional neural network:

- 1) convolution
- 2) non-linearity
- 3) pooling
- 4) classification

III. CONVOLUTION

In the case of convolution, we compute an element-wise multiplication between two matrices and add the multiplication outputs to get the final value which forms a single element of the output matrix.

IV. ANALOG SOLUTIONS IN MACHINE LEARNING

The analog solutions in machine learning hardware platforms can be faster and more energy efficient than the digital ones. The wave physics is a candidate for building analog processors for time-varying signals. The physical wave systems can be trained to learn complex features in temporal data, using standard training techniques for neural networks. For example in case of vowel classification on raw audio signals, achieving performance comparable to a standard digital implementation of a recurrent neural network. [5]

Papp et al. demonstrate the design of a neural network hardware, where all neuromorphic computing functions are performed by spin-wave propagation and interference. They envision small-scale, compact and low-power neural networks that perform their entire function in the spin-wave domain. [6]

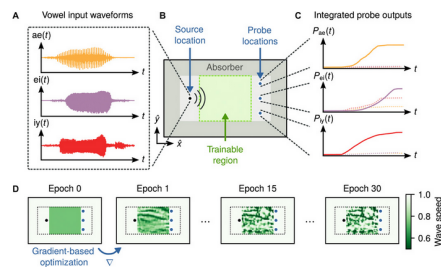


Fig. 1. Schematic setup of Hughes et al. [5]

ACKNOWLEDGEMENTS

I would like to thank my supervisors András Horváth and György Csaba for the continuous support of my work and for their expert advice. Without their precious support it would not be possible to conduct this research.

REFERENCES

- [1] Y. Bengio, A. C. Courville, and P. Vincent, “Unsupervised feature learning and deep learning: A review and new perspectives,” *CoRR, abs/1206.5538*, vol. 1, p. 2012, 2012.
- [2] Y. LeCun, Y. Bengio, and G. Hinton, “Deep learning,” *nature*, vol. 521, no. 7553, p. 436, 2015.
- [3] A. Krizhevsky, I. Sutskever, and G. E. Hinton, “Imagenet classification with deep convolutional neural networks,” pp. 1097–1105, 2012.
- [4] Y. LeCun, B. E. Boser, J. S. Denker, D. Henderson, R. E. Howard, W. E. Hubbard, and L. D. Jackel, “Handwritten digit recognition with a back-propagation network,” in *Advances in neural information processing systems*, pp. 396–404, 1990.
- [5] T. W. Hughes, I. A. Williamson, M. Minkov, and S. Fan, “Wave physics as an analog recurrent neural network,” *Science advances*, vol. 5, no. 12, p. eaay6946, 2019.
- [6] Á. Papp, W. Porod, and G. Csaba, “Nanoscale neural network using non-linear spin-wave interference,” *Nature communications*, vol. 12, no. 1, pp. 1–8, 2021.

Design of oscillatory computing devices by machine learning

Tamás RUDNER

(Supervisor: György CSABA)

Pázmány Péter Catholic University, Faculty of Information Technology and Bionics

50/a Práter street, 1083 Budapest, Hungary

rudner.tamas@itk.ppke.hu

Abstract—In the last decade the need for new types of computing architectures has risen. There are several proposed architectures which are utilising the advantages of physics. Our research is aimed at using coupled oscillators to perform computation. These oscillators can be used as various devices, such as logic gates or even as Hopfield networks. The computation is driven by the couplings between the oscillators but the setting of these couplings is not trivial to solve the tasks, so in order to figuring out these values, we use machine learning to teach the system to make the system converge to desired patterns. In the results section, we show that we can set physical parameters for a coupled oscillator system to solve pattern association tasks by learning parameters of a system of ODE and also we compare it with Hebbian learning to have a quantitative measure of our process against a well-established learning algorithm.

Keywords—coupled oscillators, machine learning, circuit design, ground state computing, pattern association

I. INTRODUCTION

Nowadays the need for alternative computing systems are rising as we are about to hit a wall in terms of physical limitation for CMOS devices.[1] Leveraging physics to perform computations might be a solution to this problem apart from several other methodologies.[2]

II. COUPLED OSCILLATORY SYSTEMS

We can create Ring-oscillators from basic electrical elements and using these, we can create dynamics systems which can make computations based on the relative phase differences of the oscillators to each other.[3] To this, we have a simple system of ODEs as follows:

$$\frac{dV}{dt} = \frac{1}{RC} (f(\mathbf{P}_\pi V) - V) + \frac{1}{R_i C} \mathbf{B}' u + \frac{1}{R_c C} \mathbf{C}' V, \quad (1)$$

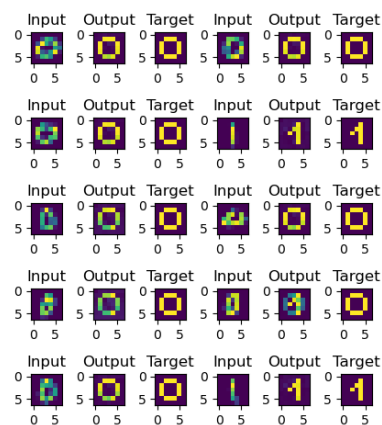
This equation consists three parts in order of the right hands side of the equation:

- Internal dynamics of the Ring-oscillators
- External dynamics of the connected voltage generators
- Dynamics of the coupled oscillators

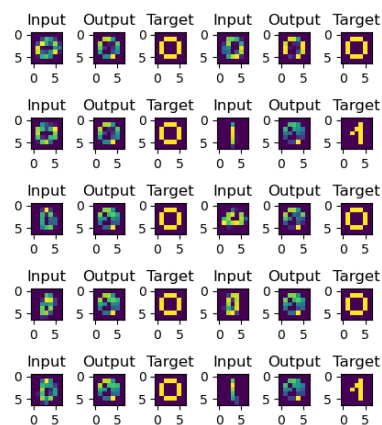
Unfortunately for complex problems setting the couplings parameters is not a trivial task, but it can be learnt using machine learning.

III. MACHINE LEARNING FOR DESIGN

To do that, we created a Python package based on PyTorch, which incorporates both the data handling for a supervised learning and also with the help of another PyTorch package, learn the parameters of the aforementioned ODE to simulate our system.



(a) Proposed fully-connected circuit design by ML



(b) Circuit with existing Hebbian-learning based couplings

Fig. 1: On a) we can see the results of the fully connected network trained by ML, while on b) we can see the results of the system trained by the Hebbian-learning scheme. It is evident, that the former performs better qualitatively, and also, we calculated the mean-squared errors for the set, and for the proposed network, it was 0.020, meanwhile for the Hebbian it was 0.068, so our solution was more than 3 times better.

REFERENCES

- [1] G. E. Moore, “Progress in digital integrated electronics [technical literature, copyright 1975 ieee. reprinted, with permission. technical digest. international electron devices meeting, ieee, 1975, pp. 11-13.],” *IEEE Solid-State Circuits Society Newsletter*, vol. 11, pp. 36–37, 09 2006.
- [2] K. Zuse, “The computing universe,” *Int. J. Theor. Phys.*, vol. 21, pp. 589–600, 1982.
- [3] G. Csaba and W. Porod, “Coupled oscillators for computing: A review and perspective,” *Applied Physics Review*, vol. 7, 2020.

Analysis of the effect of belief reconstruction on POMDP solving

András Attila SÜLYOK

(Supervisors: Kristóf KARACS, Péter SZOLGAY)

Pázmány Péter Catholic University, Faculty of Information Technology and Bionics

50/a Práter street, 1083 Budapest, Hungary

sulyok.andras.attila@itk.ppke.hu

I. INTRODUCTION

Markov Decision Process (MDP) is a general framework that can be used in many practical applications where there is an agent that is in interaction with its environment, and there is a reward function that the agent needs to maximize [1]. Numerous algorithms have been proposed and are in use to effectively solve MDPs (for example, [2]).

Partially Observable Markov Decision Processes (POMDPs, [3]) represent situations when it is either impossible or too costly to collect all information about the environment that would be necessary to make a perfect decision. It has been used in medical and healthcare, educational contexts, but simple robot control and automation problems can be described using its formalism.

It is also a challenging problem, since many possible environment states have to be considered, hence straightforward planning or model-based methods cannot be used.

This work is a preliminary report focusing on a special class of POMDPs inspired by Reconnaissance Blind Chess [4]

Reconnaissance Blind Chess (RBC, [4]) is a variant of chess where neither of the two players can see the other's moves. Instead, before each move, they can choose a 3×3 square that is revealed to them (neither the location, nor the contents of this square is not revealed to the opponent). There is no concept of check, the goal is simply to capture the opponent's king.

This makes it necessary to develop an effective exploration strategy: the agent has to figure out the location of opponent pieces; on the other hand, it has to move in such a way so as to minimize prediction on the opponent's part.

This has obvious applications in any artificial or natural competition where there is a limited window to observe the others' strategies.

We specifically focus on a class of POMDPs where the belief is a multimodal distribution, i.e., it is not enough to keep track of only one state, which is presumed to be a corrupted version of the true underlying state of the environment, but instead there are multiple distinct states with too high probability to be simply ignored (Figure 1).

A. Related work

The traditional approach to solving POMDPs is to transform the problem into belief-MDPs [5], [6], which are MDPs that use the beliefs of the original problem as their state space. Since this means an exponentially large state space, various estimation techniques were developed [6]; however, these are hard to generalize for continuous state spaces.

There are several attempts to solve POMDPs using deep reinforcement learning techniques, by observation aggregation

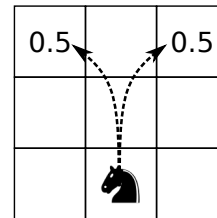


Fig. 1. Illustration of the difference between the representations of marginal and the joint distribution: the knight can move onto either of the two squares with probability 0.5. However, just storing the probabilities for each piece for each cell would imply that there is 0.25 change of the knight being at both places at the same time.

[7] or recurrent models [8], however, these were not specifically designed for tasks involving multimodal belief. This can result in undesired linear combinations of modes, i.e. instead of keeping track of probable states, the model might keep track of states of lower probability instead, corresponding to combinations of two or more modes.

ACKNOWLEDGEMENTS

Supported by the ÚNKP-21-3 New National Excellence Program of the Ministry for Innovation and Technology from the source of the National Research, Development and Innovation Fund.

REFERENCES

- [1] R. S. Sutton and A. G. Barto, *Reinforcement learning: An introduction*. MIT press, 2 ed., 2018.
- [2] A. Abdolmaleki, J. T. Springenberg, Y. Tassa, R. Munos, N. Heess, and M. A. Riedmiller, "Maximum a posteriori policy optimisation," in *6th International Conference on Learning Representations, ICLR 2018, Vancouver, BC, Canada, April 30 - May 3, 2018, Conference Track Proceedings*, OpenReview.net, 2018.
- [3] E. J. Sondik, "The optimal control of partially observable markov processes over the infinite horizon: Discounted costs," *Operations Research*, vol. 26, no. 2, pp. 282–304, 1978.
- [4] J. Markowitz, R. W. Gardner, and A. J. Llorens, "On the complexity of reconnaissance blind chess," *CoRR*, vol. abs/1811.03119, 2018.
- [5] M. Hauskrecht, "Value-function approximations for partially observable markov decision processes," *J. Artif. Intell. Res.*, vol. 13, pp. 33–94, 2000.
- [6] H. Kurniawati, D. Hsu, and W. S. Lee, "SARSOP: efficient point-based POMDP planning by approximating optimally reachable belief spaces," in *Robotics: Science and Systems IV, Eidgenössische Technische Hochschule Zürich, Zurich, Switzerland, June 25-28, 2008* (O. Brock, J. Trinkle, and F. Ramos, eds.), The MIT Press, 2008.
- [7] V. Mnih, K. Kavukcuoglu, D. Silver, A. A. Rusu, J. Veness, M. G. Bellemare, A. Graves, M. Riedmiller, A. K. Fidjeland, G. Ostrovski, et al., "Human-level control through deep reinforcement learning," *Nature*, vol. 518, no. 7540, pp. 529–533, 2015.
- [8] D. Wierstra, A. Förster, J. Peters, and J. Schmidhuber, "Solving deep memory pomdps with recurrent policy gradients," vol. 4668, pp. 697–706, 09 2007.

Wireless sensor network based wildfire monitoring with failure tolerant, event-driven multipath routing protocol

Bálint Áron ÜVEGES

(Supervisor: András OLÁH)

Pázmány Péter Catholic University, Faculty of Information Technology and Bionics
50/a Práter street, 1083 Budapest, Hungary
uveges.balint.aron@itk.ppke.hu

Abstract—In 2021, more than five hundred thousand hectares of land burnt down in the European Union due to wildfires. Enabling authorities to prepare for an efficient firefighting by detecting wildfires relatively early gains special importance due to the negative, burn-invigorating effects of climate change. Satellite based sensors, such as Moderate Resolution Imaging Spectroradiometer or Multispectral Instrument are able to monitor the European countries from wildfire activity point of view, but only via a compromise of spatial or temporal resolution. In case of a natural environment, where such delay or sensitivity is not acceptable, while the monitored area is spatially limited, wireless sensor network based wildfire monitoring is a feasible alternative.

Due to the nature of such physical phenomenon, the network has to meet two extremes: Maintain the network’s consistency and energy during eventless periods, but inform the user about occurring or prevailing events with minimal delay, while mitigating the loss destroyed of nodes.

To fulfill these requirements we propose application-specific extensions of the Heterogeneous Disjoint Multipath Routing Protocol to improve network stability, resiliency and failover, coupled with an application-level protocol to monitor hazardous events with spatial extent. To evaluate the proposed routing protocol, we perform simulations, utilizing a cellular automaton based wildfire model.

Keywords—wireless sensor networks; multi-path routing; wildfire; cellular automaton; event-driven; dependability; failure tolerant

I. WILDFIRE MONITORING WITH WIRELESS SENSOR NETWORKS

Wireless Sensor Networks (WSN) provide feasible alternative for wildfire monitoring, when near real-time sensing is required for a spatially limited area. A WSN consists of battery powered computing, sensing and communicating nodes, that are able to monitor fire activity. Via the wireless communication channel, WSN nodes convey this information via their neighbors to a distinguished node called sink and subsequently to the user.

II. APPLICATION-SPECIFIC ROUTING

The Heterogeneous Disjoint Multipath Routing Protocol (HDMRP) by Hadjid et al. is designed to exploit nodes with unlimited energy to construct multiple paths towards the sink sparing battery powered nodes [1]. To fully utilize HDMRP’s capabilities as the routing protocol for a WSN based wildfire monitoring application, several enhancements are proposed:

- RSSI based path construction message filtering to stabilize links
- Automatic Repeat Request Protocol with hop-by-hop transfer to increase packet delivery

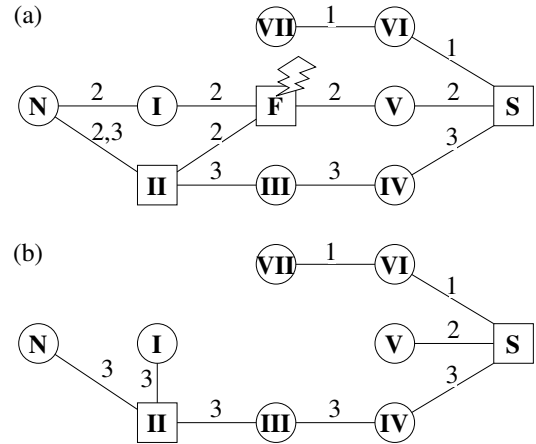


Fig. 1. Partial path reconstruction: (a) Failing node F renders node I disconnected from sink S. (b) Partial path reconstruction re-establishes node I’s connection.

- Established path confirmation to ensure nodes are aware of path-neighbours
- Partial path reconstruction to mitigate path failures caused by node loss

III. SIMULATION

OMNeT++/Castalia was chosen as simulation framework, with a wildfire model proposed by Alexandridis [2] and extended by Freire [3]. Original and enhanced HDMRP variants were compared based on different simulation scenarios.

ACKNOWLEDGEMENTS

The author would like express his gratitude towards Máté Lőrincz, member of the research group and Abdelkrim Hadjidj, the original author of HDMRP. This research was supported by the National Research, Development and Innovation Office through the grant TKP2021-NVA-27.

REFERENCES

- [1] A. Hadjidj, A. Bouabdallah, and Y. Challal, “HDMRP: An efficient fault-tolerant multipath routing protocol for heterogeneous wireless sensor networks,” in *Lecture Notes of the Institute for Computer Sciences, Social Informatics and Telecommunications Engineering*, pp. 469–482, Springer Berlin Heidelberg, 2012.
- [2] A. Alexandridis, D. Vakalis, C. Siettos, and G. Bafas, “A cellular automata model for forest fire spread prediction: The case of the wildfire that swept through spetses island in 1990,” *Applied Mathematics and Computation*, vol. 204, no. 1, pp. 191–201, 2008.
- [3] J. G. Freire and C. C. DaCamara, “Using cellular automata to simulate wildfire propagation and to assist in fire management,” *Natural Hazards and Earth System Sciences*, vol. 19, no. 1, pp. 169–179, 2019.

PROGRAM 4

HUMAN LANGUAGE TECHNOLOGIES, ARTIFICIAL UNDERSTANDING, TELEPRESENCE, COMMUNICATION

Head: Gábor PRÓSZÉKY

Question Answering System Based on Deep Learning Neural Networks for Azerbaijani language

Kamran IBIYEV

(Supervisor: Gábor PRÓSZÉKY)

Pázmány Péter Catholic University, Faculty of Information Technology and Bionics

50/a Práter street, 1083 Budapest, Hungary

ibiyev.kamran@itk.ppke.hu

Abstract—Because of improvements in learning technologies, artificial intelligence communities have focused primarily on question answering. To deal with the huge amount of data available, early question answering models used rule-based approaches before moving on to statistical approaches. Statistical techniques, on the other hand, have been demonstrated to underperform when dealing with the dynamic character and change of language. Our goal is to create a Question Answering dataset for Azerbaijani language, and to train various models on it. The creation of the dataset will be helped by a Question Generation model. We will use a model that is trained on multilingual data, and see how it performs.

Keywords—keyword; Question Answering; M-BERT; Question Generation; Question analysis; Natural language processing

I. INTRODUCTION

Question answering (QA) is a difficult task in natural language understanding. Grasping the question and the environment in which it is formed is one of the most important aspects of QA. The dynamic character of natural languages has made quality assurance difficult [1]. As a result, data-driven methodologies are now being used to answer questions. The aim is to let the data, rather than the methods, do the majority of the work in answering questions. This is owing to the vast number of available text repositories question answering.

II. LITERATURE REVIEW

Since the 2011s [2], QA has been widely researched, following the success of intelligent QA systems, such as Siri and Watson. The QA system, unlike typical information retrieval (IR) systems, receives a user’s inquiry in natural language [3]. The system then provides the best relevant response to the provided inquiry, ideally understanding the user’s true query context and efficiently meeting the user’s information demands [4].

CORPUS ANNOTATION METHOD

In this paper we will use Extractive Question Answering method. For manually annotating the paragraphs we will use Wikipedia Featured articles in Azerbaijani language because it is public and well written. Each paragraph will have at least 5 questions and its answers. We will also cover the option that the paragraph does not contain the answer to the asked question. For annotating I will use the tool implemented by Attila Novák, member of Natural Language Processing Group at Pázmány Péter Catholic University, Faculty of Information Technology and Bionics.

TRAINING THE MODEL

For training our model we will use Multilingual-MiniLM model. Experimental data show that its monolingual model outperforms state-of-the-art baselines. It preserves over 99 percent accuracy on SQuAD 2.0 and various GLUE benchmark problems, while only employing half of the Transformer parameters and calculations of the instructor model. We also get satisfactory performance using multilingual pre-trained models and deep self-attention distillation [5]. This model also can be trained to generate text. Therefore we can use this model to generate questions.

Model	#Layers	#Hidden	Average
mBERT	12	768	57.7 / 41.6
XLM-15	12	1024	61.6 / 43.5
XLM-R _{BASE} [†]	12	768	62.9 / 45.7
XLM-R _{BASE} [‡]	12	768	64.9 / 46.9
MINILM ^a	12	384	63.2 / 44.7
MINILM ^b (w/ TA)	6	384	53.7 / 36.6

Source: Adapted from [5]

Fig. 1: Cross-lingual question answering results on MLQA.

In the figure 1, F1 and EM scores are indicated. Results of mBERT and XLM15 are taken from Lewis [6]. † indicates results taken from Conneau [7]. The fine-tuned results of XLM-R_{BASE} are indicated with symbol ‡. MiniLM team used SQuAD 1.1 as training data. It is indicated on Figure 1 that the 12x384 outperforms mBERT and XLM in terms of performance. MINILM 6-layer also delivers promising results [5].

REFERENCES

- [1] L. Kodra and E. K. Meçe, “Question answering systems: A review on present developments, challenges and trends,” *International Journal of Advanced Computer Science and Applications*, vol. 8, no. 9, 2017.
- [2] L. Yu, K. M. Hermann, P. Blunsom, and S. Pulman, “Deep learning for answer sentence selection,” *arXiv preprint arXiv:1412.1632*, 2014.
- [3] T. Shao, X. Kui, P. Zhang, and H. Chen, “Collaborative learning for answer selection in question answering,” *IEEE Access*, vol. 7, pp. 7337–7347, 2018.
- [4] D. Mollá and J. L. Vicedo, “Question answering in restricted domains: An overview,” *Computational Linguistics*, vol. 33, no. 1, pp. 41–61, 2007.
- [5] W. Wang, F. Wei, L. Dong, H. Bao, N. Yang, and M. Zhou, “Minilm: Deep self-attention distillation for task-agnostic compression of pre-trained transformers,” *Advances in Neural Information Processing Systems*, vol. 33, pp. 5776–5788, 2020.
- [6] P. Lewis, B. Oğuz, R. Rinott, S. Riedel, and H. Schwenk, “Mlqa: Evaluating cross-lingual extractive question answering,” *arXiv preprint arXiv:1910.07475*, 2019.
- [7] A. Conneau, K. Khandelwal, N. Goyal, V. Chaudhary, G. Wenzek, F. Guzmán, E. Grave, M. Ott, L. Zettlemoyer, and V. Stoyanov, “Un-supervised cross-lingual representation learning at scale,” *arXiv preprint arXiv:1911.02116*, 2019.

Progress Report on Building a Corpus for Abstractive Arabic Text Summarization

Mram KAHLA

(Supervisor: Gábor PRÓSZÉKY)

Pázmány Péter Catholic University, Faculty of Information Technology and Bionics

50/a Práter street, 1083 Budapest, Hungary

kahla.mram@itk.ppke.hu

Abstract—The main task of our research is to train various abstractive summarization models for the Arabic language. This study presents the current phase of our research. There has been little research on the Arabic language in the field of abstractive summarization, so the first task in our previous research was to collect data and create a corpus. After data collection, we successfully fine-tuned transformer models with different encoder-decoder architectures. In our experiments, we tested the PreSumm and multilingual BART model. We achieved a “state of the art” result in this area with the PreSumm method. The present study continues this series of research. We extended our corpus and managed to reach up to 50 thousand items, each consisting of an article and its corresponding lead. We pre-trained monolingual and multilingual BART model, in addition, we fine-tuned the mT5 model for abstractive Arabic text summarization. We did the experiments with limited resources and infrastructure, however, most of our models surpassed the XL-Sum which is considered to be state of the art for abstractive Arabic text summarization so far. Our corpus will be released to facilitate future work on abstractive Arabic text summarization.

I. SUMMARY

Abstractive summarization has become one of the key tasks of language technology. Few people have dealt with Arabic text summarization so far, since there was not an available corpus. In our previous research[1], we created the first corpus in the Arabic language for abstractive summarization, based on this corpus, we fine-tuned various transformer models, such as the PreSumm abstractive summarization method and the multilingual mBART-50 model. To improve the performance, we applied cross-lingual transfer. The setups included M-BERT-based summarization models originally trained for Hungarian/English and a similar system based on M-BART-50 originally trained for Russian that were further fine-tuned for Arabic.

In the present research, we extended the corpus for abstractive Arabic summarization to reach more than 50k articles and their corresponding leads. We trained and fine-tuned various abstractive summarization models for the Arabic language. Those models are:

- The BART model [2] is a transformer model with an encoder-decoder architecture developed by Fairseq (Facebook AI Research Sequence-to-Sequence Toolkit)
- The mBART model [3] is a multilingual BART model trained by applying the BART model training algorithm to a large-scale monolingual corpus covering many languages.
- The mT5 model [4] is a multilingual variant of T5 that was pre-trained on the Multilingual Colossal Clean Crawled Corpus (mC4) which covers 101 languages including Arabic.

We evaluated system outputs using stemmed ROUGE-N and ROUGE-L metrics, most of our models surpassed the XL-Sum which is considered to be state of the art for abstractive Arabic text summarization so far.

ACKNOWLEDGEMENTS

I would like to express the deepest gratitude to Professor Gábor Prószéky, main supervisor, Zijian Győző Yang, and Attila Novák for their unrelenting support.

REFERENCES

- [1] M. Kahla, Z. G. Yang, and A. Novák, “Cross-lingual fine-tuning for abstractive Arabic text summarization,” in *Proceedings of the International Conference on Recent Advances in Natural Language Processing (RANLP 2021)*, (Held Online), pp. 655–663, INCOMA Ltd., Sept. 2021.
- [2] M. Lewis, Y. Liu, N. Goyal, M. Ghazvininejad, A. Mohamed, O. Levy, V. Stoyanov, and L. Zettlemoyer, “BART: Denoising sequence-to-sequence pre-training for natural language generation, translation, and comprehension,” in *Proceedings of the 58th Annual Meeting of the Association for Computational Linguistics*, (Online), pp. 7871–7880, Association for Computational Linguistics, July 2020.
- [3] Y. Liu, J. Gu, N. Goyal, X. Li, S. Edunov, M. Ghazvininejad, M. Lewis, and L. Zettlemoyer, “Multilingual denoising pre-training for neural machine translation,” *Transactions of the Association for Computational Linguistics*, vol. 8, pp. 726–742, 2020.
- [4] L. Xue, N. Constant, A. Roberts, M. Kale, R. Al-Rfou, A. Siddhant, A. Barua, and C. Raffel, “mT5: A massively multilingual pre-trained text-to-text transformer,” in *Proceedings of the 2021 Conference of the North American Chapter of the Association for Computational Linguistics: Human Language Technologies*, (Online), pp. 483–498, Association for Computational Linguistics, June 2021.

PROGRAM 5

ON-BOARD ADVANCED DRIVER ASSISTANCE SYSTEMS

Heads: Csaba REKECZKY, Ákos ZARÁNDY

Data Augmentation using Saliency Map

Jalal ALAFANDI

(Supervisor: András HORVÁTH)

Pázmány Péter Catholic University, Faculty of Information Technology and Bionics

50/a Práter street, 1083 Budapest, Hungary

alafandi.mohammad.jalal@itk.ppke.hu

Abstract—Data augmentation is a well-known technique which is used in many machine learning algorithms. Two different advantages are sought when using data augmentation. It can be used to increase the training dataset by generating new samples which can give a better representation of the data distribution. Another advantage can be obtained from using data augmentation is an increase in the invariance of the network against any applied transformation. Feature invariance is only beneficial in an inner class distribution where the features are similar in all samples but many features are used for classification where feature variance is the driving force behind any machine learning classification algorithm. We will discuss a new method which uses saliency map to prevent the invariance of neural networks to certain regions in images enhancing the result of many classification tasks.

Keywords-Neural network; Computer vision; Saliency map

I. INTRODUCTION

The performance of most modern machine learning algorithms relies greatly on the quantity and the quality of the collected dataset. When dealing with complex problems, large datasets are bound to be collected where the samples should cover the expected distribution of the dataset. Data collection and annotation are expensive predispositions hindering the easy usage of machine learning approaches.

Data augmentation transformations are applied to the samples of a dataset and the labels of the new samples are created, in most cases keeping the same class of the original sample. This approach creates new data-points which correlate with the original samples, but might cover unseen situations which can add extra information to our model. In case of any image classification task, we can rotate, scale and shift the images and by this producing new images which can be used as new images in our dataset covering a potentially real data scenario. Class based data augmentation is the process of using data augmentation transformation to create new samples with the same labels.

Another sought advantage of data augmentation is eliminating the strong effect of image transformation over network performance. The transformations of data augmentation, like small shift, rotation, noise and etc, increase data invariance and insure that a small perturbation over the samples won't affect the output of the network.

II. PROBLEM STATEMENT

Unfortunately neural networks are susceptible to small perturbations as was demonstrated in [1], and [2] where they illustrate over many cases that neural network performance is sensitive towards small transformations which can be caused by data augmentation.

In each input image, some regions can be more important than other regions and modifying those pertinent regions can alter the certainty of the output class, while transforming

those regions can enhance the samples which are trying to cover the distributions of the input regime. In the same image, there might be background and unimportant regions which are irrelevant to our model where the neural network should not be affected with any transformation over those regions. Figure 1 illustrates this problem with two samples taken from ImageNet.



Fig. 1: Two selected images from ImageNet representing the problem of feature invariance in general. The left image is labeled as band aid and the right image as space bar. The objects determining the output class in this task occupy only a small area of the input and this can cause a problem in case of invariance based data augmentation. The second image also demonstrates how invariance could be task dependent. For example the orientation of a keyboard and the space bar could be arbitrary, but if the same image is used for letter recognition the orientation of the letters can be important and upside down letters are typically uninterpretable.

Many computer vision approaches use saliency maps to specify regions in the image to create data augmentation transformations [3] or where the augmentation transformations are adapted with the important regions which were extracted from saliency maps [4], all of these approaches only assist with combining two images to create a new image without any explicit restrictions which can impose feature invariance.

REFERENCES

- [1] A. Azulay and Y. Weiss, "Why do deep convolutional networks generalize so poorly to small image transformations?" *arXiv preprint arXiv:1805.12177*, 2018.
- [2] A. Hernández-García, P. König, and T. C. Kietzmann, "Learning robust visual representations using data augmentation invariance," *arXiv preprint arXiv:1906.04547*, 2019.
- [3] C. Gong, D. Wang, M. Li, V. Chandra, and Q. Liu, "Keepaugment: A simple information-preserving data augmentation approach," in *Proceedings of the IEEE/CVF Conference on Computer Vision and Pattern Recognition*, 2021, pp. 1055–1064.
- [4] A. Dabouei, S. Soleymani, F. Taherkhani, and N. M. Nasrabadi, "Supermix: Supervising the mixing data augmentation," in *Proceedings of the IEEE/CVF Conference on Computer Vision and Pattern Recognition*, 2021, pp. 13 794–13 803.

Analysis of Ventricular Function on Echocardiographic Recordings Using Deep Neural Networks

Bálint MAGYAR

(Supervisor: András HORVÁTH)

Pázmány Péter Catholic University, Faculty of Information Technology and Bionics

50/a Práter street, 1083 Budapest, Hungary

magyar.balint@itk.ppke.hu

Abstract—Deep learning algorithms are widely used tools for medical image processing tasks due to their outstanding performance and generalization capabilities. In this work, a deep neural network was applied for the analysis of ventricular function on echocardiographic recordings.

The implemented method significantly outperforms an experienced medical doctor, and achieves comparable results to other existing deep learning based methods for the prediction of ventricular dysfunction.

Keywords—echocardiography, ventricular dysfunction, deep learning

I. SUMMARY

Echocardiography is one of the most important modality for the assessment of cardiac function. A standard measure that can be extracted from echocardiogram recordings and used for the prediction of cardiac dysfunction is the ejection fraction (EF). The accurate prediction of this measure help us to evaluate the patient's condition, the risk of heart failure and to select the right medical treatment [1].

The automatic assessment of EF and cardiac disfunction has been widely researched [2]. Ouyang et al. have developed a method that uses 2D echocardiograms and assess the left ventricular EF by a deep learning based segmentation technique [3]. Shad et al. used a hybrid, neural network, and optical flow based algorithm to predict the future risk of right ventricle failure. In [4] the authors developed a system to classify low- and high-risk groups based on ventricular function using unsupervised clustering methods and neural networks as well.

In our research we trained a deep neural network architecture using 2D echocardiogram recordings and the corresponding right ventricle EF binary labels. The annotations were acquired by medical doctors using 3D echocardiogram recordings from the same patients.

The developed spatiotemporal convolutional neural network is able to extract visual features from each frame as well as the temporal change of the ventricle during a single heart cycle.

Our system significantly outperforms experienced medical doctors in the task of ventricular dysfunction prediction in both sensitivity and specificity. The results are comparable to other state-of-the-art solutions [3], [4] but compare to those, our model was trained on annotations acquired from 3D recordings, not 2D therefore it solves a more complex task.

Beside the quantitative evaluation we applied a visualization technique to explain the decision of the network (Figure 1.).

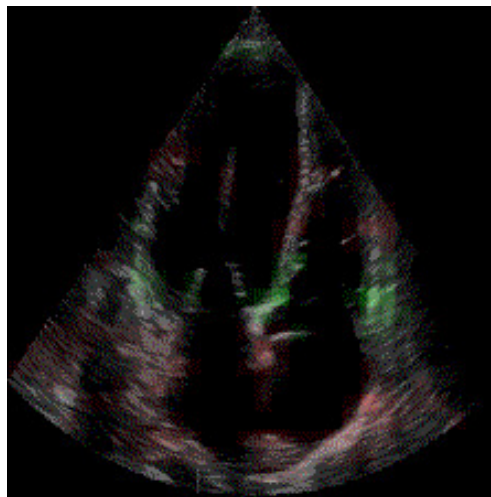


Fig. 1. Visualization of the network's decision. Green regions were used by the network to predict the EF, and red regions were the confusing ones. In this sample the network focused mostly on the area around the tripuscid valve as well as the myocardium of the left and right ventricle.

ACKNOWLEDGEMENTS

The authors would like to acknowledge the use of the Pázmány Péter Catholic University, Faculty of Information Technology and Bionics, High Performance Computing facility in carrying out this work.

REFERENCES

- [1] A. Kovacs, B. Lakatos, M. Tokodi, and B. Merkely, "Right ventricular mechanical pattern in health and disease: Beyond longitudinal shortening," *Heart failure reviews*, vol. 24, no. 4, pp. 511–520, 2019.
- [2] M. Alsharqi, W. Woodward, J. Mumith, D. Markham, R. Upton, and P. Leeson, "Artificial intelligence and echocardiography," *Echo research and practice*, vol. 5, no. 4, R115–R125, 2018.
- [3] D. Ouyang, B. He, A. Ghorbani, *et al.*, "Video-based ai for beat-to-beat assessment of cardiac function," *Nature*, vol. 580, no. 7802, pp. 252–256, 2020.
- [4] A. Pandey, N. Kagiya, N. Yanamala, *et al.*, "Deep-learning models for the echocardiographic assessment of diastolic dysfunction," *Cardiovascular Imaging*, vol. 14, no. 10, pp. 1887–1900, 2021.

Vehicle Pose Tracking in Lidar Point Cloud Maps

Örkény Ádám H. ZOVÁTHI
(Supervisor: Csaba BENEDEK)

Pázmány Péter Catholic University, Faculty of Information Technology and Bionics
50/a Práter street, 1083 Budapest, Hungary
h.zovathi.orkeny.adam@itk.ppke.hu

Abstract—This paper introduces a novel method for estimating and tracking an intelligent vehicle’s (IV) global 3DoF pose – planar position and yaw orientation – by using its sparse 3D measurements captured by a rotating multi-beam (RMB) Lidar sensor and prior high-density 3D maps recorded with a Mobile Laser Scanning (MLS) system. The introduced method consists of two main steps: First, we estimate the vehicle’s global pose by aligning its onboard RMB measurements to the appropriate part of the static MLS map by a novel object based point cloud registration algorithm. Next, we integrate the estimated pose information into a constant velocity model based Kalman filter (KF). By considering the vehicle dynamics in the KF, the accuracy and the reliability of the global pose tracking can be significantly improved, especially in scenarios with temporally heavy occlusions, which is typical in urban environment.

I. INTRODUCTION

Recent scientific and engineering progress in autonomous driving make us believe that cars will be able to drive without human intervention in the near future. State-of-the-art intelligent vehicles (IVs) are often equipped with rotating multi-beam (RMB) Lidar sensors, as they provide accurate 3D geometric information about their environment with high acquisition speed [1]. However, their captured point cloud data is relatively sparse and inhomogeneous. To overcome these limitations, Lidar based perception is often supported by pre-recorded city maps that contain detailed environment and road structure information. Mobile Laser Scanning (MLS) platforms [2] may be effective candidates for this purpose providing dense, accurate and feature rich point clouds precisely registered to a geo-referenced coordinate system.

The main motivation of this research is to improve on the IVs’ often imperfect onboard perception by global MLS city maps [3], [4]. In this context, Lidar-based *localization* and accurate *global pose tracking* of the IVs appears as crucial tasks.

II. THE PROPOSED METHOD

As a first step of our approach, we construct a segmented environment model from the raw MLS point clouds in an offline step. During segmentation, we remove all regions which contain dynamic street parts (such as parking cars) and ghosts caused by independent object motions [2] and keep only point cloud regions belonging to empty street segments. Then, we analyse the RMB Lidar’s measurement flow in real-time, performing the following main steps: First, starting from a poor GPS-based position, we align the actual RMB measurement frame to the static MLS map, using a fast object based registration algorithm [5], and calculate the global 3DoF pose (planar position and yaw orientation) of the vehicle based on the alignment results. Although this method [5] works robustly with a large number of outlier objects, its accuracy is limited in significantly occluded environments where no

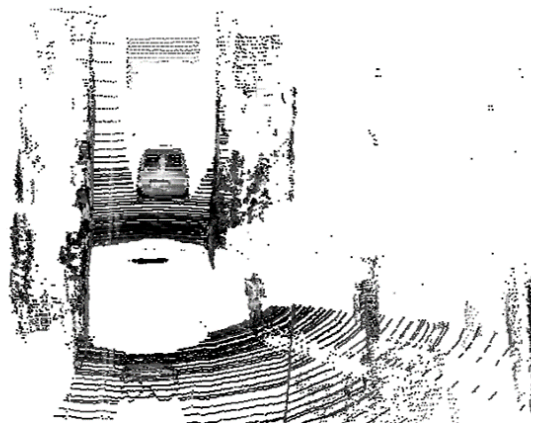


Fig. 1. Limited perception of an RMB Lidar sensor during an urban drive, with extreme temporal occlusions caused by other traffic participants (bus, tram)

alignable static objects are perceived by the IV (see Fig. 1). To deal with these temporal inaccuracies, we integrate the estimated pose information in a Kalman-filter (KF) based dynamic model, and predict the current poses of the IV based on its previous movements and states.

The proposed methods effectively combines the results of the point cloud alignment step with the KF based dynamics, therefore it is able to achieve accurate and reliable global pose tracking for the IVs, even in heavily occluded environments.

ACKNOWLEDGEMENTS

This work was funded by the KDP-2020 Cooperative Doctoral Program (KDP-977852) and the ÚNKP-21-3 New National Excellence Program (ÚNKP-21-3-I-PPKE-14) from the source of the NRD Fund.

REFERENCES

- [1] A. Geiger, P. Lenz, and R. Urtasun, “Are we ready for autonomous driving? The KITTI vision benchmark suite,” in *Conference on Computer Vision and Pattern Recognition (CVPR)*, 2012.
- [2] B. Nagy and C. Benedek, “3D CNN-Based Semantic Labeling Approach for Mobile Laser Scanning Data,” *IEEE Sensors Journal*, vol. 19, no. 21, pp. 10034–10045, 2019.
- [3] Ö. Zováthi, B. Nagy, and C. Benedek, “Exploitation of Dense MLS City Maps for 3D Object Detection,” in *International Conference on Image Analysis and Recognition (ICIAR)*, vol. 12131 of *Lecture Notes in Computer Science*, pp. 393–403, Springer, 2020.
- [4] Ö. Zováthi, L. Kovács, B. Nagy, and C. Benedek, “Multi-object detection in urban scenes utilizing 3D background maps and tracking,” in *2019 International Conference on Control, Artificial Intelligence, Robotics Optimization (ICCAIRO)*, pp. 231–236, 2019.
- [5] Ö. Zováthi, B. Nagy, and C. Benedek, “Point cloud registration and change detection in urban environment using an onboard Lidar sensor and MLS reference data,” *International Journal of Applied Earth Observation and Geoinformation*, vol. 110, p. 102767, 2022.

APPENDIX

PROGRAM 1: Bionics, Bio-inspired Wave Computers, Neuromorphic Models	
Name	Supervisor
András ADOLF	István ULBERT MD DSc
Gréta Lilla BÁNYAI	Tamás GARAY PhD
Camilla CANCRINI	Andrea CILIBERTO PhD
Suchana CHAKRAVARTY	Attila CSIKÁSZ-NAGY DSc
Ward FADEL	István ULBERT MD DSc, Lucia WITTNER MD PhD
Fanni FARKAS	Zoltán GÁSPÁRI PhD
Gábor FARKAS	Szabolcs KÁLI PhD
Tünde Éva GAIZER	Attila CSIKÁSZ-NAGY DSc
István HAJDU	Andor Viktor GÁL PhD, Zoltán VIDNYÁNSZKY DSc
Imre Gergely JÁNOKI	Péter FÖLDESY DSc
Regina KALCSEVSZKI	Sándor PONGOR MHAS
Zsófia Etelka KÁLMÁN	Zoltán GÁSPÁRI PhD
Bence Márk KEÖMLEY-HORVÁTH	Attila CSIKÁSZ-NAGY DSc
Barnabás KOCSIS	István ULBERT MD DSc
Dorottya KOCSIS	Franciska ERDŐ PhD
Csaba Márton KÖLLŐD	István ULBERT MD DSc
Zsófia LANTOS	Zoltán FEKETE PhD
Marcell MISKI	Attila CSIKÁSZ-NAGY DSc
Obada MUHAMMAD	István ULBERT MD DSc
Afrodité NÉMETH	Tamás GARAY PhD
Bence NÉMETH	András HORVÁTH PhD
Bíborka PILLÉR	Attila CSIKÁSZ-NAGY DSc
Balázs RADELECZKI	József LACZKÓ PhD
Anna SÁNTA	Zoltán GÁSPÁRI PhD
Ágnes SZABÓ	Zoltán FEKETE PhD
András László SZABÓ	Zoltán GÁSPÁRI PhD
János SZALMA	Béla WEISS PhD
Luca TAR	Tamás FREUND MHAS, Szabolcs KÁLI PhD
Mihály András VÁGHY	Mihály KOVÁCS DSc, Gábor SZEDERKÉNYI DSc
Soma VARGA	Bálint Ferenc PÉTERFIA PhD
Zsófia VARGA-MEDVECZKY	Franciska ERDŐ PhD
Áron WEBER	Attila CSIKÁSZ-NAGY DSc

PROGRAM 2: Computer Technology Based on Many-core Processor Chips, Virtual Cellular Computers, Sensory and Motoric Analog Computers

Name	Supervisor
Boldizsár Zsolt BALOG	György CSEREY PhD, Gábor NYÍRI PhD
Gábor Dániel BALOGH	István Zoltán REGULY PhD
Balázs CSUTAK	Gábor SZEDERKÉNYI DSc
Lóránt Szabolcs DAUBNER	Péter SZOLGAY DSc, Kálmán TORNAI PhD
Attila FEJÉR	Péter SZOLGAY DSc
Mary GUINDY	Péter SZOLGAY DSc, Vamsi Kiran ADHIKARLA PhD
Dániel HAJTÓ	György CSEREY PhD
András Pál HALÁSZ	Péter SZOLGAY DSc, Kálmán TORNAI PhD
Gergely HORVÁTH	Gábor SZEDERKÉNYI DSc
Sam KHOZAMA	Zoltán GÁSPÁRI PhD, Zoltán NAGY PhD
Ádám NAGY	Ákos ZARÁNDY DSc
Katalin SCHÄFFER	György CSEREY PhD, Miklós KOLLER PhD
Bálint SIKLÓSI	István Zoltán REGULY PhD
Gergely SZABÓ	András HORVÁTH PhD

PROGRAM 3: Feasibility of Electronic and Optical Devices, Molecular and Nanotechnologies, Nano-architectures, Nanobionic Diagnostic and Therapeutic Tools

Name	Supervisor
András ESZES	Zsolt SZABÓ DSc
András FÜLÖP	András HORVÁTH PhD, György CSABA PhD
Tamás RUDNER	György CSABA PhD
András Attila SULYOK	Péter SZOLGAY DSc, Kristóf KARACS PhD
Bálint Áron ÜVEGES	András OLÁH PhD

PROGRAM 4: Human Language Technologies, Artificial Understanding, Telepresence, Communication

Name	Supervisor
Kamran IBIYEV	Gábor PRÓSZÉKY DSc
Mram KAHLA	Gábor PRÓSZÉKY DSc

PROGRAM 5: On-board Advanced Driver Assistance Systems

Name	Supervisor
Mohammad Jalal ALAFANDI	András HORVÁTH PhD
Bálint MAGYAR	András HORVÁTH PhD
Örkény Ádám H. ZOVÁTHI	Csaba BENEDEK PhD
